44

Residential Building Energy Analysis:

Development and Uncertainty Assessment of a Simplified Model

by

Henry C. Spindler

A.B., Chemistry
Dartmouth College, 1992

Submitted to the Department of Architecture
in Partial Fulfillment of the Requirements for the Degree of
Master of Science in Building Technology

at the

Massachusetts Institute of Technology

May 1998

Signature of Author.....
Department of Architecture
May 8, 1998

Certified by.....
Leon R. Glicksman
Professor of Architecture and Mechanical Engineering
Thesis Supervisor

Accepted by.....
Stanford Anderson
Chairman, Department Committee on Graduate Students
Head, Department of Architecture

DISCLAIMER NOTICE

The accompanying media item for this thesis is available in the MIT Libraries or Institute Archives.

Thank you.

Residential Building Energy Analysis:

Development and Uncertainty Assessment of a Simplified Model

by

Henry C. Spindler

Submitted to the Department of Architecture
on May 8, 1998 in Partial Fulfillment of the
Requirements for the Degree of Master of Science in
Building Technology

ABSTRACT

Effective design of energy-efficient buildings requires attention to energy issues during the preliminary stages of design. To aid in the early consideration of a building's future energy usage, a simplified building energy analysis model was developed. Using this model, a new computer program was written in C/C++ to calculate annual heat and cooling loads for residential buildings and to provide information about the relative importance of load contributions from the different building components.

Estimates were made regarding the uncertainties of parameter inputs to the model, such as material properties, heat transfer coefficients and infiltration rates. The new computer program was used to determine the sensitivity of annual heat and cooling loads to model input uncertainties. From the results of these sensitivity studies, it was estimated that the overall uncertainties in the annual sensible heat and cooling load predictions amount to approximately ±30% and ±40%, respectively, for two buildings studied in Boston, Massachusetts.

Further model simplification techniques were implemented that reduced annual load calculation times on a 180 MHz computer to about 8 and 12 seconds for a lightweight and massive building, respectively. The error introduced by these simplifications was approximately 4% and 10% for the annual sensible heat and cooling loads, well below the overall uncertainties in the load predictions.

Comparison studies were performed with this new computer program and Energy-10. Overall, good agreement between the programs' annual load predictions was found.

Thesis Supervisor: Leon R. Glicksman
Title: Professor of Architecture and Mechanical Engineering

Acknowledgments

I would like to express my gratitude to my thesis advisor, Professor Leon Glicksman, for his guidance, encouragement, insight and patience throughout this project.

I am indebted to the National Science Foundation and the M.I.T. Department of Architecture for their financial support of my graduate studies.

Finally, I am especially grateful to my wife, for seeing me (or, more often, not seeing me) through this sustained effort.

TABLE OF CONTENTS

I. Introduction

Extraordinary challenges face the architect seeking to design a building that is both aesthetically pleasing and fully functional. To achieve a successful design, the architect must simultaneously consider many interrelated variables. Unfortunately, one important variable, building energy consumption, is frequently ignored by the architect, especially in the early stages of design. It is often only when the building design is nearly complete that energy requirements are considered.

In this common scenario, an engineer or contractor is given the task of sizing heating and cooling systems based on the specified details of the building plans. At this point, changes to the building that could significantly reduce its energy requirements, such as changes in building orientation or number and placement of windows, are likely to impact seriously the integrity of the building design. In fact, incorporation of these changes could necessitate substantial redesign of the entire building.

This approach to building design is extremely costly: either the architect must completely redesign the building to be more energy-efficient, or the building is built as originally designed at a substantial penalty to society and the environment. Neither alternative is acceptable.

It is the premise of this work that buildings could be more efficiently designed and designed to be more efficient if the architect or designer had available at the earliest stages of design a tool that would allow consideration of such factors as lighting, structural loads, energy consumption, natural ventilation, and air quality. A simple building sketch, which could be entered into the computer and progressively refined, could serve as the basis for calculations by programs targeting each of the factors listed above.

For example, inclusion of a particular window can affect building performance in several ways. After specifying the position of the potential window using this new design tool, the architect could receive rapid feedback regarding the impact of the window on lighting and visual comfort, on cooling and heating energy usage, and also on the potential for natural ventilation.

In order for such a tool to be effective, several requirements must be satisfied. An effective tool includes provisions for:

1) Flexible and simple input of building information. It should be possible to import building plans from a CAD file if desired. Alterations to these plans could be made within the framework of the design tool itself. The tool could also be used for constructing the building plans from the outset.

2) A built-in library of common building materials and components. This would include thermophysical and structural properties of different materials and possibly information regarding cost and embodied energy of the materials.

3) Rapid and reasonably accurate feedback to the designer. If the feedback from the program is not quick enough, the tool will receive limited use, or will be abandoned. If the accuracy is poor, the designer could be misled into incorporating unnecessary or wasteful features into the building.

4) A variety of formats for presenting feedback. Graphical feedback may be most useful, especially if it draws the user's attention to aspects of the building that have the greatest impact on building performance. For example, it might highlight the role of infiltration as being the dominant player in determining the energy consumption of a particular building.

Each of these four areas warrants considerable study. Indeed, a team of architects, engineers and computer scientists should be assembled to integrate successfully the ambitious goals presented above to develop a complete preliminary design tool.

It is within the context of these overall goals that the research described in this thesis has been performed. Specifically, the challenge of providing rapid and accurate estimates of a building's annual heating and cooling energy requirements is addressed in this document.

An integral part of this research has involved the development of a computer program (in C/C++) to calculate annual heat and cooling loads for

residential buildings. The question may arise as to why a need exists for another building energy simulation program. Many such programs are currently available, as attested by a brief survey of the DOE web page [16]. Nevertheless, several reasons do exist for creating a new program.

First, some available programs are very detailed and require extensive training to operate. DOE-2 is an example of such a program. In order to prepare a building description in the format required by DOE-2, several hours are needed for even simple buildings. Once the building is entered into the computer, annual load calculations require about a minute of computer time.[1] It is clear that detailed programs such as DOE-2 do not meet the requirements listed above for the qualities of this new design tool. Furthermore, since many building particulars are unknown at the earliest stages of design, meaningful inputs into such a program would be difficult to obtain.

Second, many simpler building energy simulation programs are available that allow more rapid input of building information and require much less computing time. However, it is not clear what simplifications and assumptions are incorporated into the software. A considerable amount of effort has been devoted to the study of the software package Energy-10. Despite completion of a workshop and extensive contact with the technical support staff, it has not been possible to obtain a clear idea of how the Energy-10 building model was conceived and implemented.

Third, even if the details of a simpler program were available, it would be very difficult to incorporate the program into the framework of the complete design tool without having access to the program source code.

Faced with such obstacles, it was decided to create a new building energy simulation program. Development of this program, which is one of the necessary components of the complete design tool mentioned above, has facilitated research into an area that has received little or no thorough treatment in the literature. This area of research will be introduced in the following paragraphs.

In the simplified programs examined thus far, no mention is made regarding the confidence level associated with such program outputs as heat

[1] On a 200 MHz Pentium machine.

and cooling loads. At most, a disclaimer is provided that absolves the software designers of responsibility for any errors. Unfortunately, the user gains no insight as to how serious those errors might be.

Two principal factors influence the uncertainty associated with the load predictions. The first factor is the uncertainty associated with the parameter inputs to the program. For example, it is difficult or impossible for the designer to specify accurately the convection coefficient for a particular floor, the density of the concrete in the floor and the appropriate heat loss coefficient for the floor perimeter.

The second factor is the uncertainty linked to model simplifications. For example, if an "exact" load prediction may be obtained by incorporating hourly weather data for every day of the year, then what uncertainty in the annual load predictions is introduced when average days for each month are used for calculations? Reducing the full year of weather data to twelve average days leads to a dramatic reduction of the time required for computing annual loads. This time reduction helps to satisfy one of the criteria for an effective design tool–rapid feedback–but it is essential to have an understanding of how the accuracy of the calculations is affected by the program acceleration.

A major component of this thesis is the careful investigation of the sensitivity of annual load predictions to the two factors mentioned above: uncertainties associated with input parameters and modeling simplifications.

Before providing the reader with an outline of what follows in the body of the thesis, a few words are warranted about the building energy simulation program that has been developed as a part of this thesis.

The intent of the program is to provide the designer with information about the annual energy requirements of a potential building. Specifically, the designer learns how much heat must be supplied to the building in the heating season, and how much heat must be removed during the cooling season. No attempt is made to incorporate different HVAC equipment into the model and to calculate how much energy must be consumed to satisfy the cooling and heating requirements.

In addition to information about the overall heat and cooling loads, the designer receives feedback about the relative importance of different building components in determining those loads. For example, the designer may obtain an answer to the question: how important are the heat losses through glazing as compared with the losses via infiltration?

Since the program is tailored to generate rapid feedback about annual building energy requirements, it does not necessarily provide reliable information about the state of the building at any particular instant. For example, this program should not be used if the user is interested in the maximum floor surface temperature on July 21.

As written, the program is intended to aid in the design of residential buildings, buildings whose energy requirements are generally dominated by the weather rather than by internal loads such as from computers and other office equipment. If desired, simple modifications could be made to incorporate internal loads more thoroughly and to broaden the program's range of applicability.

Finally, it is not recommended that the designer use the program for optimization studies of particular building components, such as window size or floor thermal mass. As may well be the case for many other building energy analysis programs, the uncertainties associated with the annual loads predicted by this program may obscure the location of the "true" load minima and render optimization impossible.

The remainder of the main portion of the thesis is composed of six chapters. A brief synopsis follows.

Chapter II is devoted to describing the different components of the building model. Details are given about how weather data is incorporated into the model, how the exterior wall is modeled, how the glazing is modeled, *etc.* Presented along with each model component is an estimate of any related uncertainties.

Chapter III introduces two base-case buildings, one lightweight construction and one massive, which are used throughout the remainder of the thesis as standards for comparison. In order to demonstrate the output

available from the program, simulations for both base-case buildings are performed in two very different environments: Boston, Massachusetts and Phoenix, Arizona.

Chapter IV again steps through each building model component. For each component, parametric studies are performed in order to investigate the sensitivity of the program's load predictions to the uncertainties in each model input. Calculations in this chapter are performed at the Boston site.

Chapter V presents the results of studies pertaining to two different methods of simplifying and accelerating the annual load calculations. The degradation of calculation accuracy introduced by simplifying and accelerating the calculations is investigated.

Chapter VI introduces another simplified building energy analysis program, Energy-10, and compares the results of the program developed in this thesis with those of Energy-10. Ten variations of the two base-case buildings are examined in both the Boston and Phoenix locations.

Finally, Chapter VII summarizes the main results of this work and provides some suggestions for future study.

Two appendices are included at the end of this document. The first contains a brief comparison study of the heat transfer through an infinite slab subject to periodic boundary conditions. The exact time-dependent solution of the temperature distribution within the slab and the finite-difference solution (used in the program to model conduction through the exterior walls of the building) are compared. The second appendix contains a brief program tutorial, a flowchart of the program, a listing of the main program file, and diskettes containing all program files.

II. Development of Building Energy Simulation Model

A. Residential Building Description

This building energy simulation program (henceforth program) is intended to be used during the very early design stages, when interior details of the building (such as the composition and location of interior walls) are not yet specified. Consequently, the building parameter inputs to the program are limited to dimensions and properties of the building envelope, floors and ceilings.

The residential building is divided into an unlimited number of zones, or spaces in the building that share common thermostat setpoints. A two-story building may have one zone, or two zones–one for each floor.

Each zone is further divided into sub-zones, one for every exterior wall of the building zone (**Figure 1**). As discussed further below, the primary reason for introducing this subdivision of zones is the substantial reduction in simulation time that it permits. For simplicity, the internal borders of the sub-zone are modeled as lightweight walls with no thermal mass. Glazing is specified as a percentage of the sub-zone's exterior wall area.

Although the sub-zones belong to a common zone with a single temperature setpoint, it is possible for the sub-zone temperatures to differ from one another at a certain instant. (Air temperature within each sub-zone, however, is assumed to be uniform.) Control of the air temperatures in the sub-zones will be discussed later in a separate section.

Any temperature imbalance between two neighboring sub-zones would result in heat transfer via conduction through the common walls and via convection through any wall openings such as doors. With this program, it is possible to model heat transfer among sub-zones via both pathways.

Again, it must be emphasized that the interior features of the building are undetermined at this point in the design and that the introduction of sub-zones offers a reasonable, general method of modeling the space. Indeed, it allows for the likely possibility of different portions of an entire level of a

building, such as the north-facing portion and south-facing portion, to have different air temperatures.

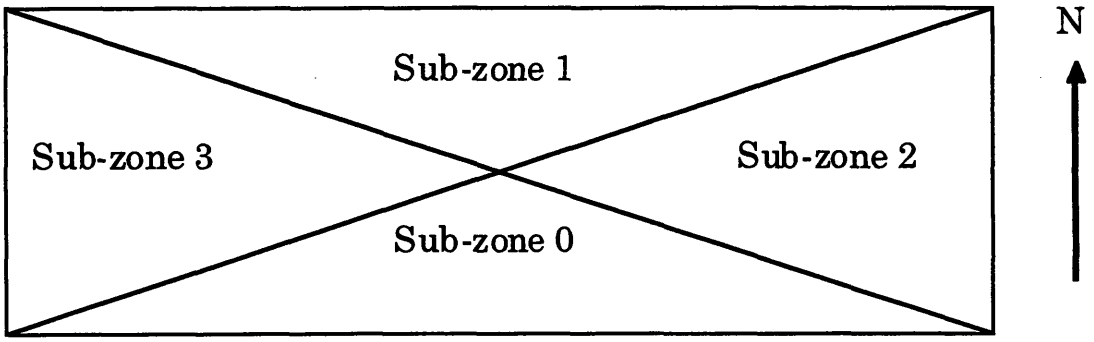

Figure 1. One zone divided into four sub-zones

The thermal behavior of each sub-zone is calculated at hourly intervals throughout the entire year by incorporating the following inputs:

- outside dry-bulb temperature
- outside air humidity ratio
- inside dry-bulb temperature setpoints
- inside humidity ratio setpoint
- dry-bulb temperatures of adjacent sub-zones
- material properties of the floor, ceiling, exterior wall and glazing
- long-wave radiation and convection at all surfaces
- direct, diffuse and reflected solar radiation intercepted by exterior wall and glazing (if any)
- infiltration and ventilation rates

In the following sections, the role of each of these inputs to the thermal model will be described in detail. To illustrate the different heat flow pathways considered in this model, the following figure has been constructed.

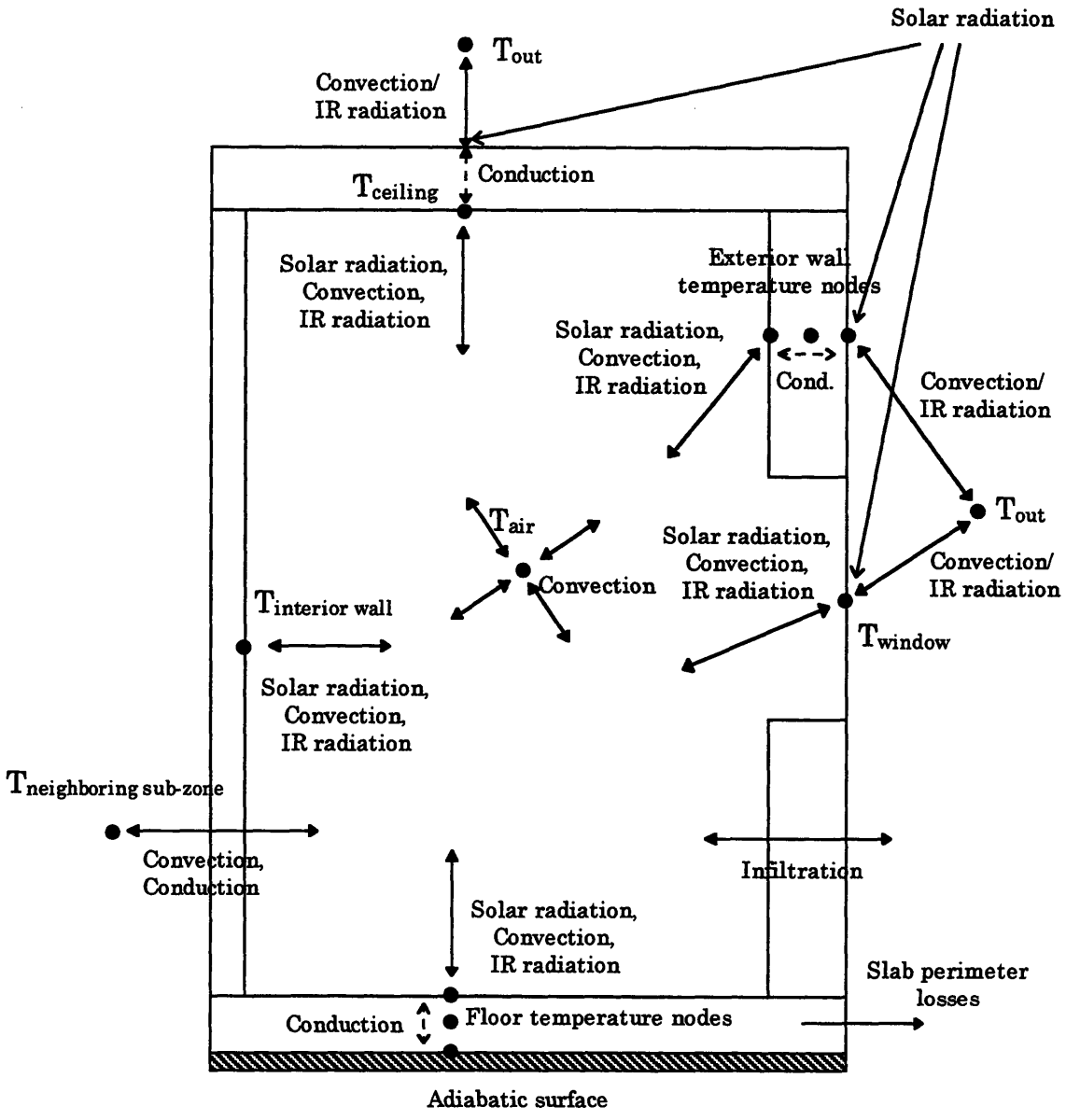

Figure 2. Diagram of sub-zone heat flow pathways (cross-sectional view)

B. Solar Radiation Models and Weather Data

1. Determination of Solar Position

In order to determine the amount of solar radiation striking a certain wall or window, the position of the sun in the sky must first be calculated. The solar position, in conjunction with modeled or measured direct normal and diffuse solar radiation data, can be used to furnish the solar flux impinging on any surface. Much of the information presented in this section was drawn from three especially helpful sources [1,4,25].

The sun's position is determined by two coordinates: the solar altitude, α, the angle the sun makes with the horizon, and the solar azimuth, ϕ, the compass angle one faces when looking directly at the sun (**Figure 3**). More technically, the solar azimuth is the angle between the horizontal projection of the sun's rays and south. The azimuth is reported in degrees relative to due south (angles to the east are negative, angles to the west are positive).

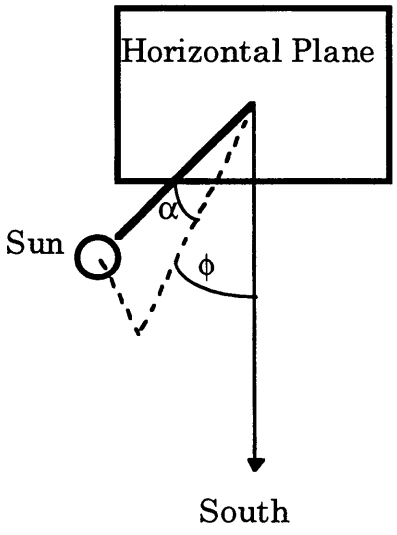

Figure 3. Solar altitude (α) and azimuth (ϕ) angles

To calculate the position of the sun at a certain standard time (the time shared by an entire time zone), the time of day must be converted to local solar time.

Local Solar Time = (Standard Time)
+ 4 × { (Local Standard Meridian) - (Site Longitude) } minutes
+ (Equation of Time) minutes ,

(1)

where the Local Standard Meridian is 75° for Eastern Standard Time, 90° for Central Standard Time, *etc.*

The Equation of Time, introduced to account for the varying speed of the earth in its elliptical orbit, is a function of the day of the year:

$$\text{Equation of Time}(n) = 9.87 \times \sin\left(\frac{4\pi(n-81)}{364}\right) - 7.53 \times \cos\left(\frac{2\pi(n-81)}{364}\right) - 1.50 \times \sin\left(\frac{2\pi(n-81)}{364}\right) \text{ minutes},$$

(2)

where n = 1 to 365.

The solar altitude, α, is given by

$$\sin(\alpha) = \cos(\text{latitude})\cos(\text{hour angle})\cos(\text{declination}) + \sin(\text{latitude})\sin(\text{declination})$$

(3)

and the solar azimuth, ϕ, is given by

$$\cos(\phi) = \left(\frac{\sin(\alpha)\sin(\text{latitude}) - \sin(\text{declination})}{\cos(\alpha)\cos(\text{declination})}\right) \times \frac{\text{hour angle}}{|\text{hour angle}|},$$

(4)

where:

latitude = the latitude at the site (in degrees),

(5)

$$\text{declination}(n) = 23.45 \times \sin\left(\frac{360 \times (n + 284)}{365}\right),$$

n = 1 to 365, corresponding to each day of the year

(6)

and

$$\text{hour angle} = 0.25 \times (\text{local solar time} - 12.0),$$

(7)

where the local solar time is given in hours, *e.g.,* 2:30 p.m. = 14.5.

As an example, the preceding equations were used to calculate the solar altitude at noon (standard time) as a function of the time of year for Boston, MA (**Figure 4**).

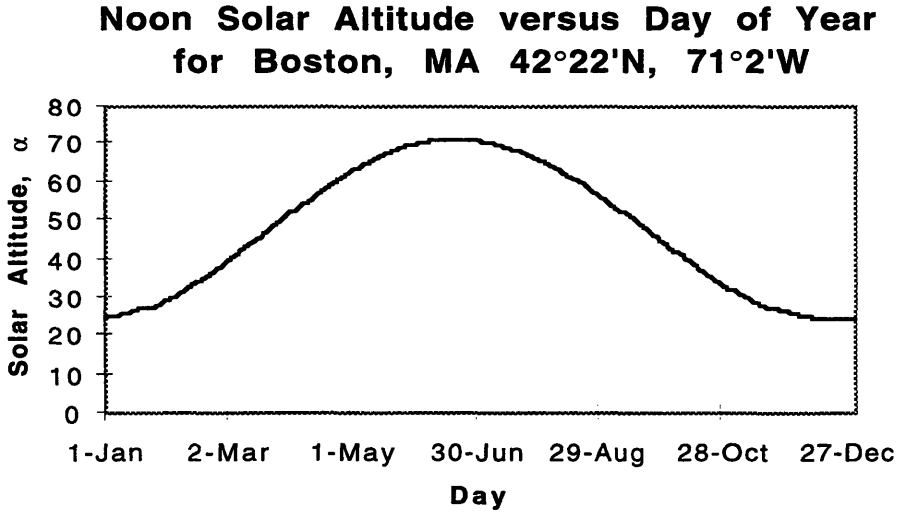

Figure 4. Noon solar altitudes for Boston, MA

Equations (3) and (4) were used to generate the plot in **Figure 5** showing the hourly variation of the solar altitude and azimuth on the summer and winter solstices in Boston, MA.

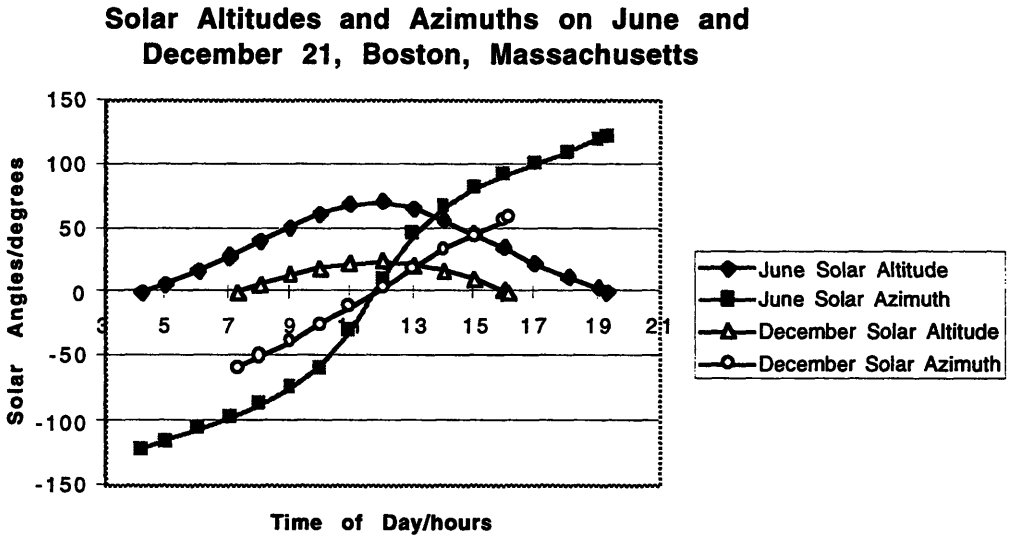

Figure 5. Solar altitudes and azimuths on June and December 21, Boston, MA

Using the relations developed above, it is possible to determine the path of incoming direct solar radiation. Additional geometry shows the designer which surfaces of a building will receive insolation at any given time. However, in order to determine the impact of this radiation on the building energy loads, the amount of energy transported by this radiation must be either modeled or measured.

The following three subsections present different means of determining the radiant energy in beam (direct normal) and diffuse radiation. The first discusses the use of measured weather data (consisting of both radiation and temperature data) to provide this information. The second and third subsections present techniques for calculating the beam and diffuse radiant energies assuming a clear sky. Such techniques can be useful for determining maximum cooling loads in the summer, but are not practical for annual heat load calculations since all cloud cover is ignored. These methods are included

in this report primarily because they offer insight into the large uncertainties associated with calculating properties of solar radiation.

2. Measured Weather Data: TMY2's

The primary source of weather data for use in this energy simulation is the Typical Meteorological Year 2 (TMY2) database [39], which was derived from the 1961-1990 National Solar Radiation Data Base (NSRDB). Contained in this database are temperatures, solar radiation data and other meteorological data for 239 United States weather stations. The data are recorded every hour, using standard time. The database was constructed by concatenating twelve months of actual weather data. For example, the January selected for use in the TMY was chosen from a year whose January was deemed to be a typical January for the thirty-year period covered by the NSRDB. Since the typical January data and February data could be selected from different years, the data were smoothed to ensure a realistic transition between months. Further information about data selection is given in the user's manual for the database [39]. It is important to recognize that the data in the TMY2 are not averaged in any way, but rather are selected for being representative actual data for a particular time of year.

The weather data incorporated into the energy simulation are:

- Global Horizontal Solar Radiation: Given in Wh/m^2. Integrated global radiation hitting a horizontal surface in the previous hour.

- Direct Normal Solar Radiation: Given in Wh/m^2. Integrated direct normal radiation in the previous hour (radiation striking a surface normal to the sunlight).

- Diffuse Horizontal Solar Radiation: Given in Wh/m^2. Integrated diffuse radiation hitting a horizontal surface in the previous hour.

- Dry Bulb Temperature: Given in °C. Dry-bulb temperature at each hour.

- Humidity Ratio: in kg vapor/kg dry air. Derived from given relative humidity, dew point temperature and atmospheric pressure data.

Accompanying each data point in the TMY2 database is an estimate of its associated uncertainty. A survey of the Boston data shows that the three types of radiation data have associated uncertainties of ± 6 to 13%. The dry-bulb temperature has "uncertainty consistent with NWS practices and the instrument or observation used to obtain the data."[2]

Additional uncertainties arise when the building site is not at the immediate location of the weather station. Significant variation in the temperature and solar radiation can occur over short distances due to features of the local geography.

3. ASHRAE Clear-Sky Model

This model implements a correlation[3] to determine the direct normal solar radiation (on dry, cloudless days):

$$\text{Direct Normal Radiation} = C_n \times A \times \exp\left(\frac{-B}{\sin(\alpha)}\right), \tag{8}$$

where A and B are given in tabular form for the twenty-first day of each month. A represents the direct normal solar radiation outside the atmosphere (given in W/m^2) and B (dimensionless) is the atmospheric extinction coefficient, accounting for absorption, reflection and scattering of the incoming light by the atmosphere. C_n is the clearness number [37], which varies from 0.9 to 1.1, depending on the region and season.

[2] [39] pg. 24.
[3] [1] pg. 29.14.

Although modifications have been proposed to the ASHRAE model for calculating diffuse solar radiation incident on a horizontal surface [13], the current model put forth in the ASHRAE Fundamentals Handbook is [1]:

$$\text{Diffuse Horizontal Radiation} = C \times \text{Direct Normal Radiation}\,, \tag{9}$$

where, again, C is given in tabular form for the twenty-first day of each month. C is simply the ratio between the diffuse horizontal and direct normal radiation. This parameter ranges from 6 to 14%. It was found that equation (9) does not adequately predict the diffuse radiation component at low solar altitudes, where the diffuse component can actually exceed the direct normal component of the total radiation [1].

Global horizontal radiation is the sum of direct and diffuse horizontal solar radiation striking a horizontal surface. It is given by:

$$\text{Global Horizontal Radiation} = \left\{C + \cos(\alpha)\right\} \times C_n A \exp\left(\frac{-B}{\sin(\alpha)}\right) \tag{10}$$

The clear-sky solar radiation can be found at any time of day, as long as the appropriate solar altitude for that time is computed. Therefore, if these modeled radiation data are used, care must be taken to implement the resultant values as instantaneous flux, rather than the total hourly solar energy values given by the TMY2 data.

4. Combination of Hottel and Liu-Jordan Models

The following procedure for determining clear-sky direct solar radiation and diffuse horizontal radiation follows Athienitis [4] in his synthesis of models proposed by Hottel [14] (for direct normal radiation) and Liu and Jordan [24] (for horizontal diffuse radiation). As in the ASHRAE Clear-Sky Model, this model calculates instantaneous solar radiation (in W/m^2).

Since the earth-sun distance varies with time due to the earth's elliptical orbit, the amount of direct normal solar radiation outside the

earth's atmosphere varies with the time of year. The earth is closest to the sun on January 3 and farthest from the sun on July 4. The solar constant, I_o, is equal to 1367 W/m^2, although this figure is under constant revision [18]. The variation of the direct normal solar radiation outside the atmosphere as a function of the day of the year is approximated by:

$$I_{DN,out}(n) = I_o \times \left\{1 + 0.033 \cos\left(\frac{2\pi(n-3)}{365}\right)\right\} \quad (11)$$

The fraction of the extraterrestrial beam radiation reaching the earth, is given by the transmittance coefficient, τ_b. Following Hottel,

$$\tau_b = a_0 + a_1 \times \exp(-k \times \sin(\alpha)) \text{ , where} \quad (12)$$

$$a_0 = r_0\left\{0.4237 - 0.00821 \times (6 - A)^2\right\} \quad (13)$$

$$a_1 = r_1\left\{0.5055 + 0.00595 \times (6.5 - A)^2\right\} \quad (14)$$

$$k = r_k\left\{0.2711 + 0.01858 \times (2.5 - A)^2\right\} \quad (15)$$

A is the altitude of the site expressed in kilometers. For mid-latitudes, r_0, r_1 and r_k are 0.97, 0.99, 1.02 for the summer and 1.03, 1.01, 1.00 for the winter.

Once τ_b has been determined by (12), the direct normal solar radiation at the earth's surface can readily be found:

$$I_{DN} = \tau_b \times I_{DN,\,out} \quad (16)$$

The expression for the atmosphere's diffuse transmittance established by Liu and Jordan is:

$$\tau_d = 0.2710 - 0.2939 \times \tau_b \qquad (17)$$

The diffuse solar radiation striking a horizontal surface is given by:

$$I_{d,\,horiz} = I_{DN,\,out} \times \sin(\alpha) \times \tau_d \,, \qquad (18)$$

and the global horizontal radiation is then (combining (16) - (18)):

$$I_{Global,\,horiz} = I_{DN,\,out} \times \sin(\alpha) \times (\tau_b + \tau_d) \qquad (19)$$

5. Determination of Solar Radiation on an Arbitrary Surface

In order to calculate the solar radiation on an arbitrary surface, several additional parameters must be introduced in order to describe the surface orientation. **Figure 6** shows the definition of the surface azimuth, ψ, which is the angle between the horizontal projection of the surface normal and south. ψ is negative when the surface normal points east of south. The surface solar azimuth, γ, is defined:

$$\gamma = \phi - \psi \qquad (20)$$

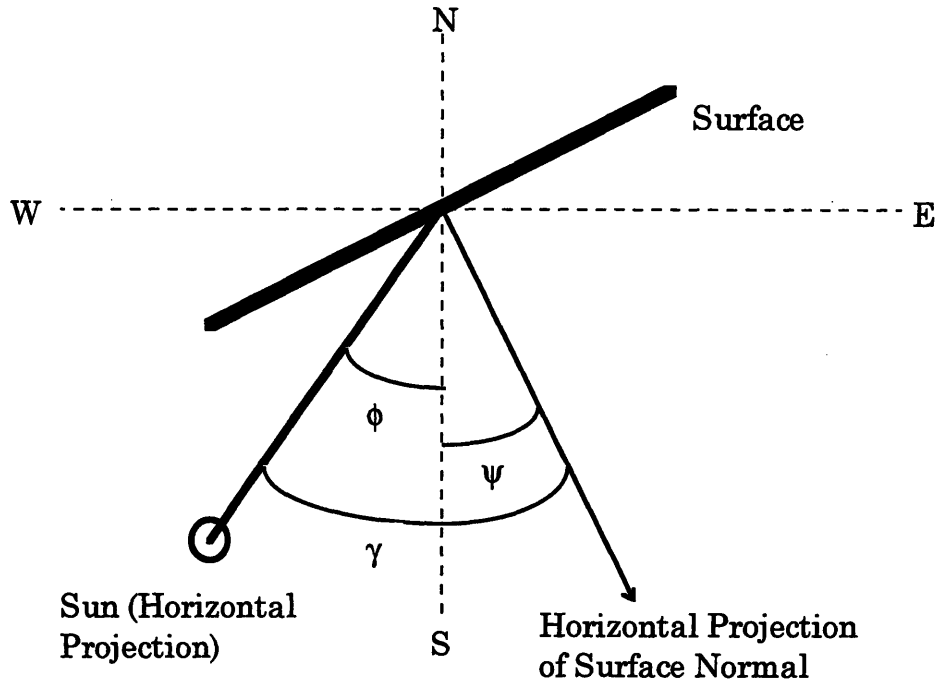

Figure 6. Definition of azimuth angles

The tilt angle of the surface, β, is illustrated in **Figure 7**. The tilt angle is the angle formed between the backside of a surface and the horizontal plane. A horizontal surface has β = 0°, while a vertical surface has β = 90°.

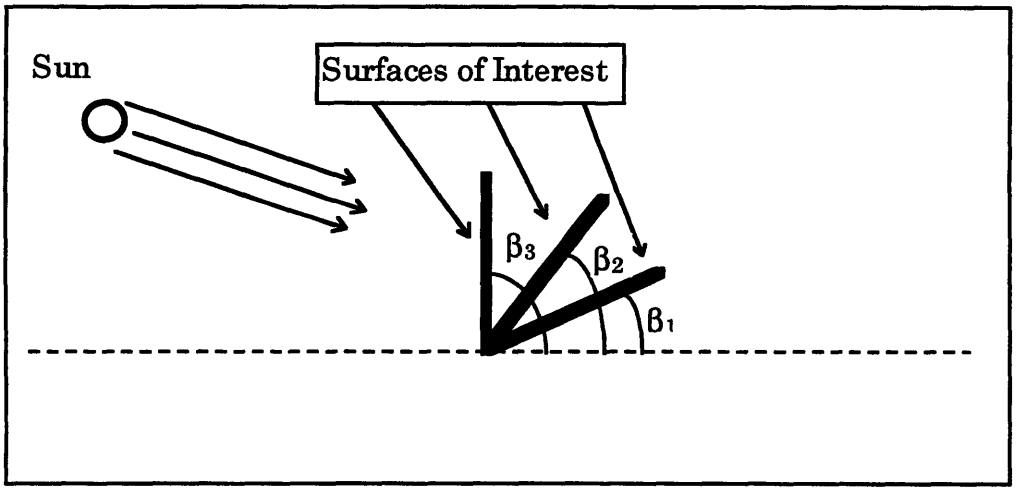

Figure 7. Definition of wall tilt angle

Finally, the angle of incidence, θ, is the angle between the sun's rays and the surface normal.

Given the tilt angle (β) and azimuth (ψ) of a surface in addition to the solar altitude (α) and azimuth (ϕ), it is possible to calculate the angle of incidence of direct solar radiation. First, γ must be determined using equation (20). Then, θ is defined by:

$$\theta = \text{acos}\left\{\cos(\alpha)\times\cos(\gamma)\times\sin(\beta)+\sin(\alpha)\times\cos(\beta)\right\} \qquad (21)$$

Note that if $\theta \geq 90°$, direct solar radiation will not strike the surface.

The direct radiation striking a surface is given by:

$$I_D = I_{DN}\times\cos(\min[\theta,90]) \qquad (22)$$

The diffuse radiation striking a surface has two components. The first component arises from the scattering of beam solar radiation by the atmosphere and the second results from the reflection of global radiation hitting the ground in the neighborhood of the surface of interest. The first component of diffuse radiation is given by [4]:

$$I_{d,sky->surface} = I_{d,\ horiz}\times\frac{1+\cos(\beta)}{2} \qquad (23)$$

Equation (23) incorporates an assumption of an isotropic distribution of the diffuse radiation emanating from the hemisphere of the sky, *i.e.*, all faces of a building (with equal β) will receive the same amount of diffuse radiation.[4] The ASHRAE Fundamentals Handbook recommends using the following relation for $I_{d,sky->surface}$, in which the angle of incidence of the beam radiation affects the amount of diffuse radiation striking a surface.

---

[4] As it is currently written, the program assumes an isotropic distribution of diffuse solar radiation.

For vertical surfaces (only):

$$I_{d,sky->surface} = I_{d,horiz} \times Y(\theta) ,$$

(24)

where Y(θ), the ratio of diffuse radiation striking a vertical surface to that striking a horizontal surface, is given by:

$$\begin{aligned} Y(\theta) &= 0.55 + 0.437\cos(\theta) + 0.313\cos^2(\theta) : \quad \text{for } \cos(\theta) > -0.2 \\ &= 0.45 \qquad\qquad\qquad\qquad\qquad\qquad : \quad \text{for } \cos(\theta) \le -0.2 \end{aligned}$$

(25)

Sowell suggests that use of this expression for Y(θ) may be extended to surfaces of any tilt angle [35].

The diffuse radiation arising from reflection off the ground is given by:

$$I_{d,ground->surface} = I_{Global,\ horiz} \times \rho_{ground} \times \frac{1-\cos(\beta)}{2}$$

(26)

Depending on the nature of the ground surface surrounding the building and the angle of incidence, the ground reflectance, ρ_{ground}, can range from about 0.1 to 0.3 for ground covers such as black parking lots and new concrete, respectively [38]. The default value the program uses for ρ_{ground} is a constant 0.20. For green grass, the reflectance increases 50% as the angle of incidence changes from 20° to 70°. The effect of this parameter on annual loads will be investigated in a later section.

The total solar radiation impinging on an arbitrary surface is calculated using equations (22), (23) or (24), and (26):

$$I_{tot,surface} = I_D + I_{d,total} ,$$

(27)

where

$$I_{d,total} = I_{d,sky->surface} + I_{d,ground->surface} \qquad (28)$$

The following figures illustrate the relative magnitudes of the direct and diffuse radiation striking a south-facing vertical wall on the summer and winter solstices and the fall equinox in Boston. The global horizontal radiation was included for comparison. The model used to generate the direct normal, diffuse and global radiation data for the plots was described in the section entitled "Combination of Hottel and Liu-Jordan Models."

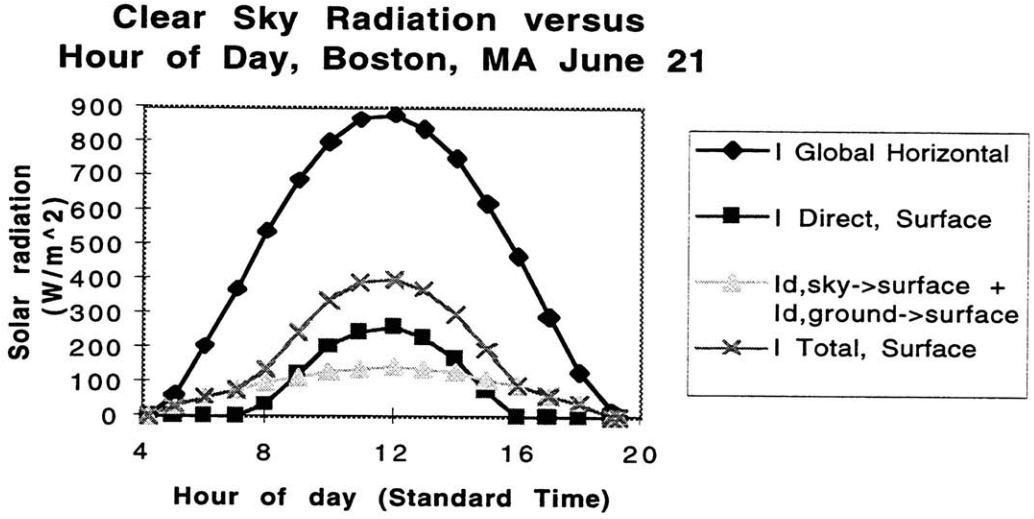

Figure 8. Summer solstice radiation on south-facing wall

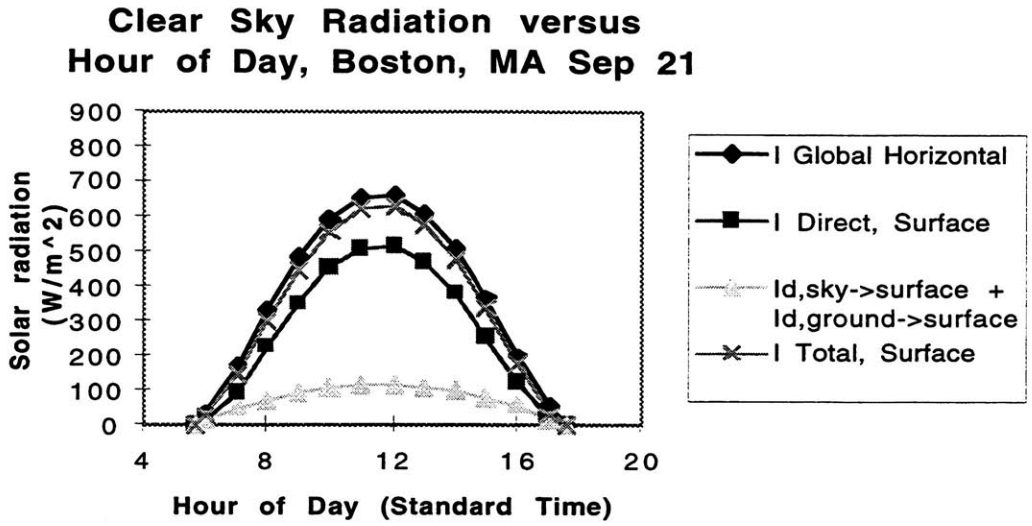

Figure 9. Fall equinox radiation on south-facing wall

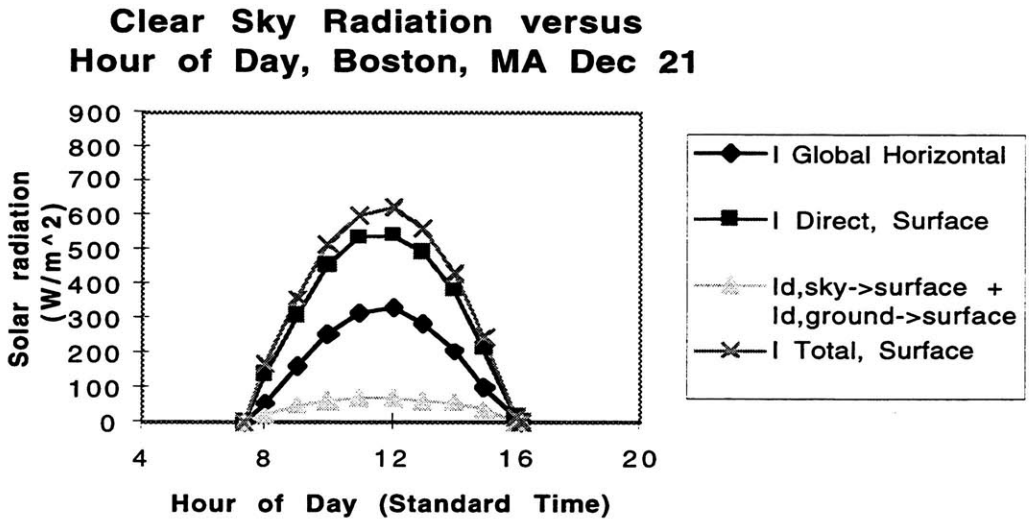

Figure 10. Winter solstice radiation on south-facing wall

6. Discussion of Weather Modeling Errors

Several factors contributed to the decision to use measured weather data rather than the model-derived data described in sections 3 and 4. The primary reason for using the measured weather data provided by the TMY2 database was that several layers of possible error associated with using modeled data were eliminated:

1) Hourly temperatures must be fabricated if a weather database is not used. (The program allows the user to do this, if desired.)

2) Clear-sky radiation alone can be calculated using the models presented in sections 3 and 4. Cloud cover factors (CCF) must be used to estimate actual hourly solar radiation. Further information and references about the use of the CCF are available [35]. Due to the uncertainties associated with the use of these factors, this approach was not pursued. (It is possible to run the program with exclusively model-derived weather input. Since cloud cover is ignored, predicted heat loads may be significantly smaller than actual, and cooling loads significantly greater.)

3) It was discovered that the ASHRAE Clear-Sky Model and the Hottel/Liu-Jordan Model produced very different estimates of clear-sky direct radiation. As estimates for diffuse radiation are based on the direct radiation, all forms of radiation are affected by this modeling discrepancy. Shown in **Figure 11** is a plot comparing the clear-sky direct solar radiation predicted by the ASHRAE model and the Hottel/Liu-Jordan model. The site used was in the mid-latitudes at an elevation of 0.005 km. The solar altitude, α, was 30°.

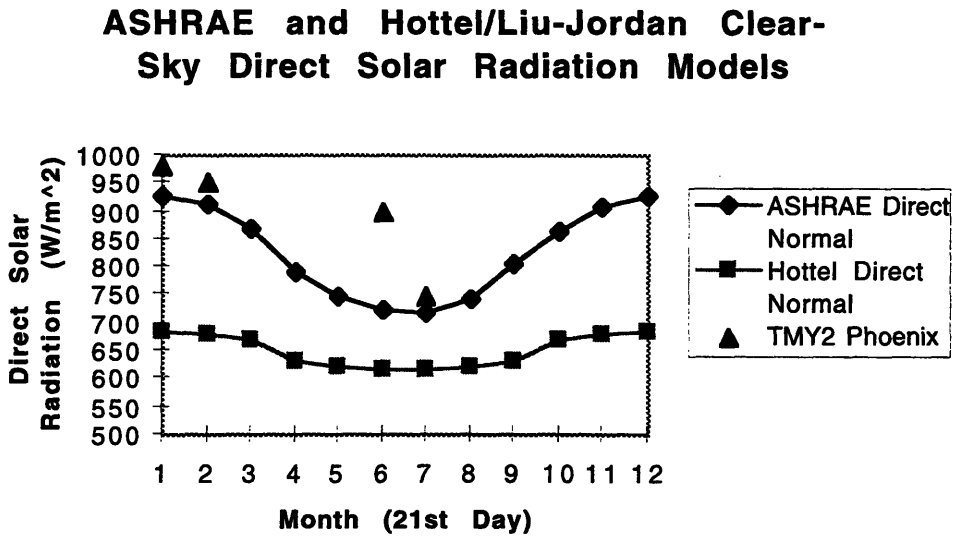

Figure 11. Comparison of ASHRAE and Hottel/Liu-Jordan clear-sky direct radiation models

Depending on the month, the Hottel/Liu-Jordan model yields 15-25% less direct normal radiation than the ASHRAE model. In order to determine which model best predicted actual direct normal radiation at this solar altitude, a rough comparison was made using actual measured solar radiation data in Phoenix, AZ. Phoenix was selected because of the clear skies often observed there. For several days surrounding January, February, June and July 21, the maximum direct normal radiation at a solar altitude of approximately 30° was recorded. These data are also plotted in **Figure 11**. The ASHRAE model shows the best agreement with the measured data, although its predictions fall below the measured values by 4–20%. The Hottel/Liu-Jordan model predictions fall 18-32% below the measured data. The origin of these shortfalls is not clear.

For solar altitudes of 10°, the range of prediction discrepancies between the two clear-sky models increases to 20-44%. For a 70° solar altitude (roughly the maximum observed in Boston), the discrepancy range is 6-15%.

At this stage, the major boundary conditions affecting the thermal behavior of the sub-zones have been discussed: solar radiation and outside dry-bulb temperature. The role of the solar radiation is to heat the outside surface of the exterior walls and to contribute to internal solar gains via transmission through glazing. The outside temperature is a key ingredient in determining both the rate of convection and infrared radiation[5] heat transfer to the outside surfaces of the exterior walls and also the rate of heat transfer resulting from infiltration of outside air into the conditioned space.

In the next sections (C through N), simple mathematical models will be developed for describing heat transfer through and among the many components of a sub-zone. Once the individual components of the model are described, they will be assembled in matrix form into a single model (section O).

C. Conduction and the Finite Difference Approximation

When a physical system, such as a concrete wall, is subjected to unsteady boundary conditions (*e.g.*, a varying temperature, convection coefficient or solar heat flux), its thermal mass moderates the propagation of the thermal stimulus through the system. The heat flux arriving at a wall surface when the sun emerges from behind clouds is not immediately felt on the inside of the wall. Depending on the thickness of the wall, the effect of the sun may not be observed at the inside wall surface until hours later. In other words, the material exhibits a time-dependent response.

This time dependence is captured in the diffusion equation, which describes the transient one-dimensional[6] conduction of heat through a uniform material:

---

[5] In this model, outside convection and radiation heat transfer coefficients are lumped into a single coefficient relating the rate of heat transfer to the exterior surface to the surface and outside air temperatures. This coefficient will be discussed in a later section.

[6] The consequences of making the assumption of 1-D conduction will be examined in the next section.

$$k\frac{\partial^2 T}{\partial x^2} = \rho c_p \frac{\partial T}{\partial t} \ ,$$

(29)

where k, ρ and c_p are the thermal conductivity, density and specific heat of the material. There are several techniques for solving differential equations such as (29). Given steady or periodic boundary conditions, it is relatively straightforward to solve the differential equation analytically in the time or Laplace domain. The analytic solution is complicated by the juxtaposition of layers of different materials [27] and rendered nearly unattainable by non-periodic boundary conditions.[7] Since building walls are almost always composite and since solar radiation and outside temperatures are not neatly periodic, a simpler, numerical solution was chosen to model conduction in this study. This method, the finite difference method, involves the discretization of the continuous differential equation.

Before equation (29) is transformed into discrete, finite difference form, a simpler equation will be examined to illustrate the discretization technique and to describe the Crank-Nicolson finite difference model used in the program.

Consider the following equation:

$$\frac{d\Theta}{dt} = -\frac{1}{\tau}\Theta(t)$$

(30)

Replacing the derivatives with Δ's,

$$\Theta(t+\Delta t) - \Theta(t) \approx -\frac{\Delta t}{\tau}\Theta(?)$$

(31)

---

[7] Solutions *may* be obtained, however. Duhamel's Theorem may be used to develop a time-domain solution (see [27], Chapter 5), and the z-transform method may be used as well. Frequency-domain approximate solutions could be obtained by representing the roughly periodic boundary conditions by their first few Fourier series harmonics. Solutions using this technique are described widely in the literature. For example, see [3].

The unusual notation on the right-hand side of (31) reflects the uncertainty involved in selecting the time at which Θ should be evaluated. Certainly, for very small Δt, $\Theta(t)$ may be used with little resulting error. This approach is taken in the forward difference Euler method. However, for larger time steps, considerable error may be introduced. Instability is also a possibility when employing explicit methods such as the forward difference Euler or the Runge-Kutta methods [17]. The backward difference Euler method replaces $\Theta(?)$ with $\Theta(t+\Delta t)$. The Crank-Nicolson method is a compromise between the two Euler methods. It sets:

$$\Theta(?) = \frac{\Theta(t) + \Theta(t + \Delta t)}{2} \qquad (32)$$

Both the backward difference Euler and the Crank-Nicolson methods are called *implicit* methods. While more challenging to implement, since they may require solution of a set of simultaneous equations, the implicit methods are unconditionally stable. Solving (31) for $\Theta(t+\Delta t)$ using (32) yields:

$$\Theta(t + \Delta t) = \Theta(t) \times \frac{\left(1 - \frac{\Delta t}{2\tau}\right)}{\left(1 + \frac{\Delta t}{2\tau}\right)}, \qquad (33)$$

which is recognizable as the first few terms of the expansion of the analytical solution to (30):

$$\Theta(t) = \Theta_0 \times \exp\left(\frac{-t}{\tau}\right) = \Theta_0 \times \frac{\exp\left(\frac{-t}{2\tau}\right)}{\exp\left(\frac{t}{2\tau}\right)} = \Theta_0 \times \frac{\left(1 - \frac{t}{2\tau} + \ldots\right)}{\left(1 + \frac{t}{2\tau} + \ldots\right)} \qquad (34)$$

Consider an infinite slab of homogeneous material, divided into equally spaced segments of width Δx:

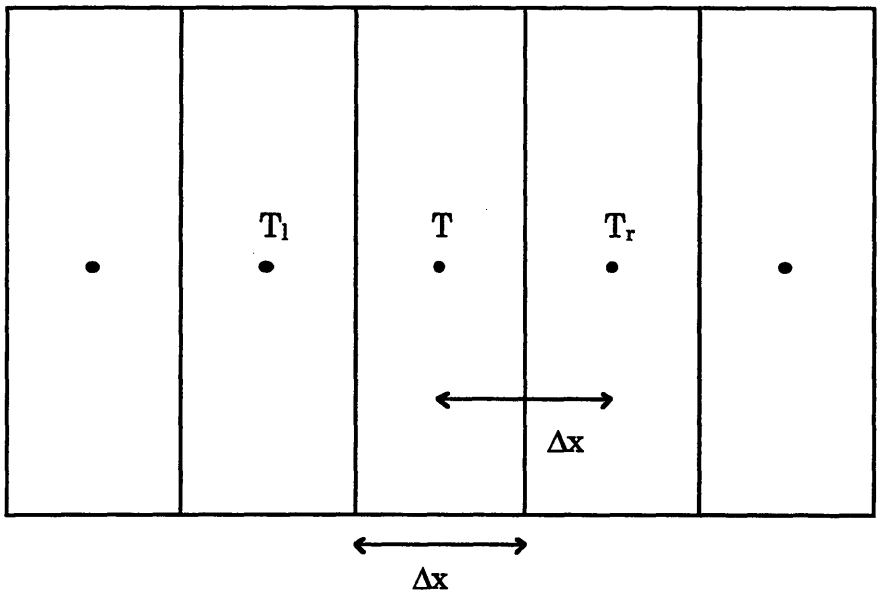

Figure 12. Infinite slab (in y and z directions)

The finite difference equation describing the behavior of the temperature T may be written in Crank-Nicolson form:

$$\rho c_p \frac{(T' - T)}{\Delta t} \approx \frac{k}{2}\left(\frac{\left(T_r' - T'\right)}{\Delta x^2} + \frac{\left(T_l' - T'\right)}{\Delta x^2}\right) + \frac{k}{2}\left(\frac{\left(T_r - T\right)}{\Delta x^2} + \frac{\left(T_l - T\right)}{\Delta x^2}\right), \quad (35)$$

where the prime (') represents T evaluated at t+Δt. In order to determine the temperature distribution within the slab, equation (35) must be solved for every temperature node in the slab. Since the thermal response of one slab segment is coupled to that of its neighbors, a system of simultaneous equations must be solved.

Equation (35) serves as the basis for modeling the exterior wall and the floor, both of which are thermally massive and exhibit transient conduction.[8]

[8] Both elements are treated mathematically as thermally massive elements. However, choice of building materials and thicknesses may render the elements practically devoid of thermal mass.

D. Exterior Wall

1. Thermal Model

The conduction through the exterior wall of the sub-zone is modeled using the Crank-Nicolson finite difference approximation of the one-dimensional diffusion equation, (35). This equation can be generalized to handle composite walls and a host of boundary conditions.

Consider a wall composed of two layers of material, a and b (**Figure 13**). Each layer is divided into segments containing a single temperature node. The segments adjoining the a-b interface share a common temperature node, T_{ab}. A key assumption of this model is that the temperature at each node is uniform throughout the segment (or segments, in the case of T_{ab}) containing it.

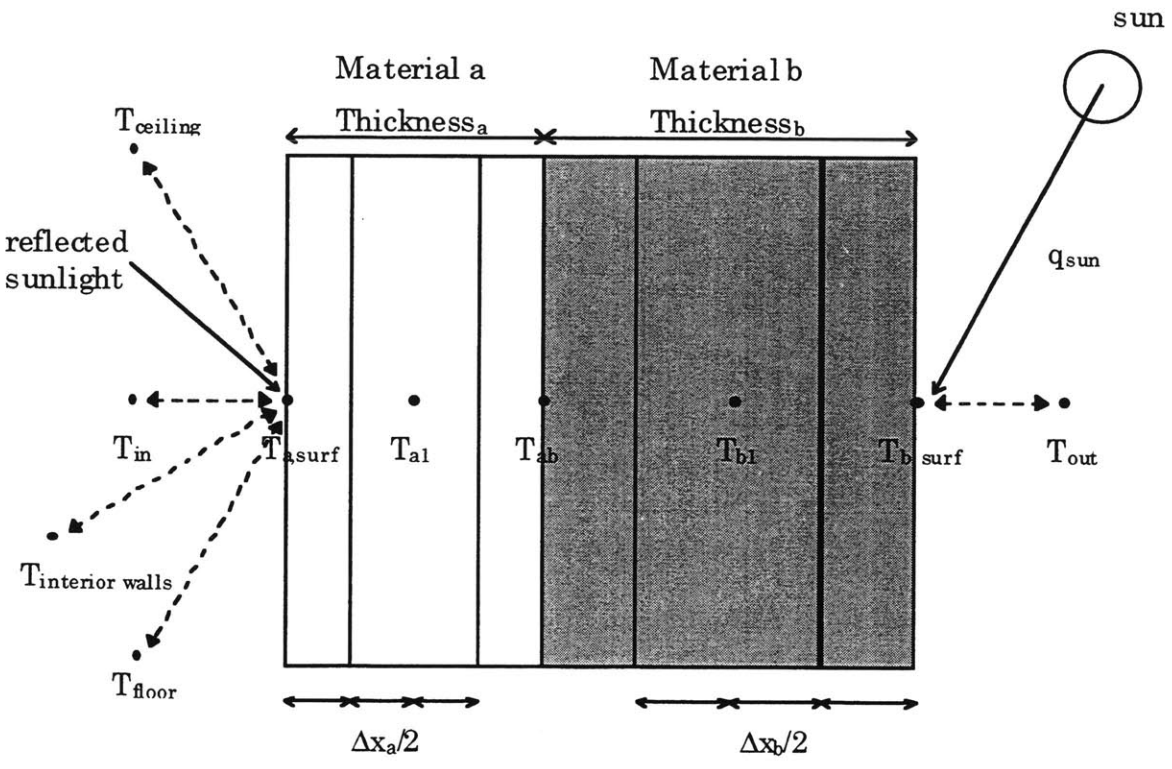

Figure 13. Composite exterior wall divided into sections (dotted lines represent convection, IR radiation, or both)

The equation derived above, (35), can be altered to fit the circumstances shown in **Figure 13.** In this case, not all the Δx's are identical. For a node inside the wall, (*i.e.*, T_{a1}, T_{ab}, T_{b1}), equation (35) becomes:

$$\left(\rho_l c_{p,l}\frac{\Delta x_l}{2}+\rho_r c_{p,r}\frac{\Delta x_r}{2}\right)\frac{(T'-T)}{\Delta t}\approx\frac{1}{2}\left(\frac{\left(T_r'-T'\right)}{\Delta x_r/k_r}+\frac{\left(T_l'-T'\right)}{\Delta x_l/k_l}\right)+\frac{1}{2}\left(\frac{\left(T_r-T\right)}{\Delta x_r/k_r}+\frac{\left(T_l-T\right)}{\Delta x_l/k_l}\right) \qquad (36)$$

Notice that for a node surrounded by a single material, equation (36) reduces to (35). $\Delta x_r/k_r$ may be rewritten as R_r, the thermal resistance between the node under consideration and the node to its right. R_l can be formed analogously.[9] Capacitances may also be formed:

$$\rho_r c_{p,r}\frac{\Delta x_r}{2}=\frac{C_r}{2}\ , \qquad (37)$$

where C_r is the capacitance (per unit area) of the material between the node under consideration and the node to its right. C_l is similarly defined. The capacitance defined in this way may also be called "thermal mass" (per unit wall area). The total capacitance located at a node is $(C_r+C_l)/2$. If the node lies at the material surface, as do $T_{a,surf}$ and $T_{b,surf}$, the total capacitances would be $C_r/2$ and $C_l/2$, respectively. With the change of notation just introduced, it becomes straightforward to perform an energy balance at each node, including those on the surfaces.

[9] It should be noted that this is the thermal resistance for a unit area of material in the y-z plane. To find the full resistance of a segment, the resistance must be divided by the area of the segment normal to the direction of heat flux.

Consider again the wall depicted in **Figure 13**. Material a has 3 nodes ($n_a = 3$) and material b also has 3 nodes ($n_b = 3$). The total number of nodes in the wall is $n_a + n_b - 1 = 5$ (the node at T_{ab} is counted only once). Using:

$$C_a = \rho_a c_{p,a} \Delta x_a = \rho_a c_{p,a} \frac{\text{Thickness}_a}{n_a - 1} \qquad (38)$$

and

$$C_b = \rho_b c_{p,b} \Delta x_b = \rho_b c_{p,b} \frac{\text{Thickness}_b}{n_b - 1} \ , \qquad (39)$$

energy balances can be performed for each node:

For <u>internal nodes</u>, such as T_{a1},[10]

$$(C_a)\frac{(T'_{a1} - T_{a1})}{\Delta t} \approx \frac{1}{2}\left(\frac{(T'_{ab} - T'_{a1})}{R_a} + \frac{(T'_{a,surf} - T'_{a1})}{R_a}\right) + \frac{1}{2}\left(\frac{(T_{ab} - T_{a1})}{R_a} + \frac{(T_{a,surf} - T_{a1})}{R_a}\right), \qquad (40)$$

This equation is also valid for the node T_{b1} if all a's are replaced with b's.

For <u>junction nodes</u>, such as T_{ab}:

$$\left(\frac{C_a}{2} + \frac{C_b}{2}\right)\frac{(T'_{ab} - T_{ab})}{\Delta t} \approx \frac{1}{2}\left(\frac{(T'_{b1} - T'_{ab})}{R_b} + \frac{(T'_{a1} - T'_{ab})}{R_a}\right) + \frac{1}{2}\left(\frac{(T_{b1} - T_{ab})}{R_b} + \frac{(T_{a1} - T_{ab})}{R_a}\right), \qquad (41)$$

For the <u>inside wall surface node</u>:

[10] Internal nodes are those nodes not at the junction between two dissimilar materials.

$$\frac{C_a}{2}\frac{(T'_{a,surf}-T_{a,surf})}{\Delta t} \approx \frac{1}{2}\left(\begin{array}{l} \dfrac{\left(T'_{a1}-T'_{a,surf}\right)}{R_a}+\dfrac{\left(T_{a1}-T_{a,surf}\right)}{R_a} \\ +h_{in}\left(T'_{in}-T'_{a,surf}\right)+h_{in}\left(T_{in}-T_{a,surf}\right) \\ +h_{r,wall->floor}\left(T'_{floor}-T'_{a,surf}\right)+h_{r,wall->floor}\left(T_{floor}-T_{a,surf}\right) \\ +h_{r,wall->walls}\left(T'_{walls}-T'_{a,surf}\right)+h_{r,wall->walls}\left(T_{walls}-T_{a,surf}\right) \\ +h_{r,wall->ceiling}\left(T'_{ceiling}-T'_{a,surf}\right)+h_{r,wall->ceiling}\left(T_{ceiling}-T_{a,surf}\right) \\ +q'_{sun,reflected}+q_{sun,reflected} \end{array}\right), \tag{42}$$

where the middle four lines on the right-hand side of (42) represent convection to the wall surface from the inside air, radiation from the floor, interior walls and ceiling. $q_{sun,reflected}$ is the amount of sun (per unit area of exterior wall) entering the room through any glazing that is absorbed on the inside surface of the exterior wall. The convection and radiation coefficients are all defined in terms of the exterior wall surface area. These coefficients will be discussed in greater detail in sections L and N.

For the <u>outside wall surface node</u>:

$$\frac{C_b}{2}\frac{(T'_{b,surf}-T_{b,surf})}{\Delta t} \approx \frac{1}{2}\left(\begin{array}{l} \dfrac{\left(T'_{b1}-T'_{b,surf}\right)}{R_b}+\dfrac{\left(T_{b1}-T_{b,surf}\right)}{R_b} \\ +h_{out}\left(T'_{out}-T'_{b,surf}\right)+h_{out}\left(T_{out}-T_{b,surf}\right) \\ +q'_{sun}+q_{sun} \end{array}\right), \tag{43}$$

where q_{sun} is given by:

$$q_{sun} = \alpha_{solar} \times I_{tot,\ surface} \tag{44}$$

and α_{solar} is the solar absorptivity of the exterior wall surface.

2. Wall Model Simplifications

While the finite difference method offers a simple and very flexible way of modeling conduction through a building wall subject to unsteady boundary conditions, it does not provide the exact solution except in the limiting case where Δx and Δt approach zero. However, an exact solution is not necessarily required in one part of a model when there are known uncertainties associated with other model inputs and components. The purpose of making wall model simplifications is to determine whether calculation time can be significantly reduced while introducing an acceptable level of uncertainty.

Two simplifications to the wall model are currently built into the model. Both methods accelerate the calculation process by reducing the number of temperature nodes within the wall (or, equivalently, increasing Δx). To predict heat transfer in a wall with N nodes, N simultaneous equations must be solved for every time step. Hence, the fewer the nodes, the shorter the calculation time.

The user may vary the number of nodes assigned to each material in the wall. The individual layers in a wall (*e.g.*, sheathing, insulation and gypsum wall board) may be broken up into an arbitrary number of sub-layers. For example, the gypsum wall board layer could be characterized by three temperature nodes (one at each surface and one in the center) or by two nodes (one at each surface). The impact these changes have on the building's annual energy usage will be assessed in a later section.

A more drastic measure may be taken to reduce calculation time: the layers of the different materials in the wall may be collapsed to form one "equivalent" layer of a single homogeneous material. This "equivalent" layer can have as few as two nodes in it. The properties of the "equivalent" layer are determined using:

$$C_{equiv} = \sum_{i=1}^{\text{Num Layers}} C_{layer\ i}\ , \qquad (45)$$

where $C_{layer\ i}$ is obtained from equation (38) with $n_a = 2$.

$$R_{equiv} = \sum_{i=1}^{Num\ Layers} R_{layer\ i}\ ,$$

(46)

where

$$R_{layer\ i} = \frac{Thickness_{layer\ i}}{k_{layer\ i}}$$

(47)

Unless specifically requested, this major simplification is not performed by the program.

3. Uncertainties and Sources of Error

Many factors contribute to the overall uncertainty associated with the heat transfer calculated through the wall modeled in the last two sections. It is the goal of this section to identify some of the origins and rough magnitudes of the uncertainties associated with the different factors.

a) Material Properties

The values for the thermophysical properties of the different components forming a wall can show considerable variation depending on the source of the information, the age and condition of the material and the material's moisture content. Precise identification of the building material is sometimes a critical factor as well. By way of illustration, consider two common building materials, softwood studs (fir or pine, for example) and fiberglass batt insulation. The ASHRAE Fundamentals Handbook[11] and Incropera and DeWitt[12] are the sources of the material properties listed below.

[11] [1] Chapter 24, Table 4.
[12] [17] Table A.3.

	Density	Thermal Conductivity	Specific Heat
	kg/m^3	W/mK	J/kgK
ASHRAE			
Southern Pine (cross grain)	570-659	0.144-0.161	1630
Spruce-Pine-Fir (cross grain)	392-502	0.107-0.130	1630
Incropera & DeWitt			
Softwoods (fir, pine)	510	0.12	1380
Yellow pine (cross grain)	640	0.15	2805
White pine (cross grain)	435	0.11	
Fir (cross grain)	415	0.11	2720
Fir (radial)	420	0.14	2720
ASHRAE			
Glass Fiber (approx 140mm)	10-16	0.0378	*
Incropera & DeWitt			
Glass Fiber, paper faced	16-40	0.035-0.046	*

Table 1. Comparison of material properties from two different sources.

*Values for the specific heat may be found in [25], page 151.

Examination of **Table 1** reveals that the precise wood used to make the stud affects its thermal conductivity and density dramatically. Depending on which source is used and the specific type and cut of wood used to represent "softwood," the thermal conductivity can vary as much as 50% and the density as much as 68%. The maximum variation in specific heats listed is 103%.

Fiberglass batt insulation shows a similar wide range in possible values from which to choose. The maximum value for thermal conductivity exceeds the minimum value by 31% and the maximum density exceeds the minimum by 300%.

It seems unlikely that the architect or designer will be able to specify accurately the building material properties to within even 20-30%. This condition is further aggravated by the fact that for some building materials, the thermophysical properties are strongly dependent on moisture content and aging [7].

b) Handbook Properties versus Installed Properties

Kuehn [22] and Kuehn and Maldonado [23] have shown that the handbook values for material properties can differ significantly from those measured in a real wall section. These researchers made "center of cavity" measurements in four different wall types in order to eliminate any possible two-dimensional effects associated with the studs.[13]

The results of the first study indicated that although the thermal resistances (R-values) of the individual wall components differed from the ASHRAE handbook values by as much as 181%, the "center of cavity" R-value for the entire wall thickness showed good agreement with the handbook wall R-value calculation. The range of deviation from the handbook calculations for the different wall sections was -3% to 8%. For the individual wall components, the most significant measured deviations from the handbook values occurred in the inner and outer layers, which included the inner and outer film resistances. The insulation layer of the walls (either fiberglass batt or cellulose) showed measured deviations from handbook values in the range of -16 to 9%.

The second study revealed similar discrepancies between measured and tabulated material property values. Material property values were obtained by choosing the values that produced the best agreement between a one-dimensional simulation and the measured transient heat flux and temperature distribution within the four walls.

The "best-fit" thermal conductivity values for the batt and cellulose insulation exceeded the handbook values by 25%. The thermal conductivity for polystyrene sheathing was 25% lower than the handbook value, while that for polystyrene insulation exceeded the handbook value by 50%. Finally, the measured wood stud thermal conductivity exceeded the handbook value by 74%.

The thermal mass per unit volume (ρc_p) of the wall components was also determined in the same fashion. A similar range of deviations from

---

[13] A "center of cavity" R-value measurement is one made in a region of the wall far from any studs, such as at the centerline of the insulation, equidistant from the neighboring studs.

handbook values was reported. The estimated uncertainty of all "best-fit" parameters was 10%.

Several possible causes were presented for the discrepancies between the measured and tabulated material properties. The higher observed thermal conductivity of the wooden stud was linked to the nails driven into it. Measured R values in excess of the handbook values may have indicated the presence of contact resistance or air films within the wall. Measured thermal conductivities exceeding the handbook values may have arisen from air gaps along the edges of the insulation, especially near the stud. Moisture was also a potential culprit.

c) Two-Dimensional Heat Transfer

Due to the presence of structural framing in the wall (*e.g.*, studs or window framing), heat transfer through the wall is not a strictly one-dimensional process. Nevertheless, it is possible to approximate the heat transfer through the wall as occurring via several parallel one-dimensional paths, one through the insulation and the other through the stud, for example. Such an approach is adopted in the current study. However, in a real wall, thermal gradients develop perpendicular to the wall normal and two- or three-dimensional heat transfer arises.

There are several methods for modeling parallel-path heat transfer through a wall. The simplest method makes use of the assumption that an isothermal condition exists on both inner and outer faces of the stud/ insulation layer. One-dimensional heat transfer through the stud, for example, is determined solely by the temperature difference across the stud, its cross-sectional area and its R-value. One-dimensional heat transfer through the insulation is governed by the same temperature difference and by its cross-sectional area and R-value. If A_{stud} and A_{ins} are the fractions of wall surface area comprised of stud and insulation, and k_{stud} and k_{ins} are the thermal conductivities of the stud and insulation, then an effective k value for the composite layer may be formed:

$$k_{eff} = A_{stud}k_{stud} + A_{ins}k_{ins} \qquad (48)$$

Similarly, effective densities and specific heats for the composite layer may also be formed:

$$\rho_{eff} = A_{stud}\rho_{stud} + A_{ins}\rho_{ins} \qquad (49)$$

and

$$c_{p,eff} = A_{stud}c_{p,stud} + A_{ins}c_{p,ins} \qquad (50)$$

It is this very simplified model that is used in the program despite the warning given by Kuehn and Maldonado.[14]

Another parallel-path method, recommended by ASHRAE, is to calculate the thermal resistance through the wall assuming isothermal conditions at the wall's inner and outer surfaces rather than at the boundaries of the stud/insulation layer. Such a calculation amounts to finding two separate wall R-values, one for conduction through the stud sections of the wall and one for conduction through the insulation sections of the wall. These two R-values can then be combined in parallel to determine an overall wall R_{eff}. There are several reasons why this approach was not employed in the current study:

1) If an R_{eff} is found that incorporates the heat transfer through studs and through insulation, this single R-value describes the thermal resistance of the entire wall. If the thermal mass in the wall is treated consistently, then it must be lumped together to form a single C_{eff} for the entire wall. The requirement of using such a gross simplification was not desired.

2) If the two R-values are not combined, then it is possible to retain a realistic profile of the capacitance in the wall (it need not be lumped together). However, if the two parallel paths for heat transfer through the wall are to be considered independently, then the number of wall equations to be solved doubles.

[14] [23] pg. 56.

The difference in overall wall R-values calculated using the two parallel-path techniques just described is 2% for a standard 2x6 wood stud wall construction.

The drawback of using these parallel-path techniques is that the effective framing percentage for the wall in question must be known in order to properly calculate the wall's R-value. Use of the actual framing percentage (or A_{stud}, defined above) is likely to lead to incorrect assessment of the wall's thermal resistance [22]. Unfortunately, the researcher must resort to experiment or two-dimensional conduction calculations to determine the wall's effective framing percentage. For the wall types examined by Kuehn [22], actual wall framing percentages of 6, 6, 9 and 9% had to be replaced by effective values of 11, 16, 10 and 30% to match the measured wall R-values. Kuehn and Maldonado [23] showed that use of "best-fit" material properties reduced the difference between actual framing percentages and the effective framing percentages required to match overall wall thermal resistance. Using the "best-fit" material properties, the reported effective framing percentages were 6.7, 6.7, 11.4 and 5.6% for the same four wall types. The impact of using an unadjusted framing percentage on the annual energy loads will be investigated in a later section.

d) Whole-Wall versus Clear-Wall R-Values

According to Christian and Kosny [9], additional measures must be taken to determine the actual thermal performance of walls in buildings. Walls are not isolated structures, but are connected to the roof and other walls. Typical measurements or two-dimensional heat conduction simulation will yield accurate predictions of heat transfer only through the "clear wall," the portion of the wall containing no windows and no connections to the roof or other walls. However, these authors argue that edge effects play a significant role in heat transfer through the wall and must be taken into account. Their measurements revealed that a "whole-wall" R-value accounting for conduction through all portions of a typical 2x6 wood stud wall was 16% lower than the "clear wall" R-value for the same wall.

e) Other Considerations and Summary of Wall-related Uncertainties

Several additional sources of uncertainty related to modeling the wall should be considered. The first source is the selection of the exterior surface solar absorptivity, α_{solar}. White paint, with a nominal $\alpha_{solar} = 0.26$, may peel or darken with age, increasing its solar absorptivity. Fading may be an issue for other materials. The impact of changing solar absorptivities will be investigated in a later section.

The second additional source considered in this section is the determination of appropriate wall areas to use in the calculations. A consequence of using a one-dimensional model to describe three-dimensional conduction is that it is not clear which face of the exterior wall should be used to determine the wall surface area. The surface area of the inner face of a wall of a typical 2x6 frame house may be 3-5% smaller than that of the outer face.

To summarize, the sources of uncertainty inherent in the model for exterior wall heat transfer include:

Material Properties:
- -Selection of proper material
- -Which value to select when a range of possible values is given for a particular material
- -Agreement of handbook and experimental material properties

Approximation to 2-D Heat Transfer:
- -Use of isothermal condition at surfaces of insulation/stud layer
- -Selection of appropriate framing percentage

Overall Model for Wall:
- -Use of "clear-wall" versus "whole-wall" R-value
- -Use of a single composite layer to describe entire wall (optional)
- -Selection of wall surface area

Finite Difference Approximation:
- -Finite Δt and Δx

Solar Absorptivity of Exterior Surface

Although not mentioned above, uncertainties in these factors are also important in determining the uncertainty associated with the rate of heat transfer through the wall:

Incident Solar Radiation (especially effects of shading by trees, buildings)

Outside convection/radiation coefficient

Infiltration of air

E. Floor

1. Thermal Model

The thermal model used to describe the floor is nearly identical to that used to describe the exterior wall. The only difference is the set of boundary conditions at the top and bottom surface of the floor. Heat transfer through the floor, as for the wall, is considered to be strictly one-dimensional. For the case of the slab-on-grade floor, perimeter losses are considered as a separate, independent heat transfer mechanism.

Figure 14 shows the two-layer floor model with the associated boundary conditions. $T_{\text{exterior wall}}$ in this figure is identical to $T_{a,\,\text{surf}}$ in **Figure 13**.

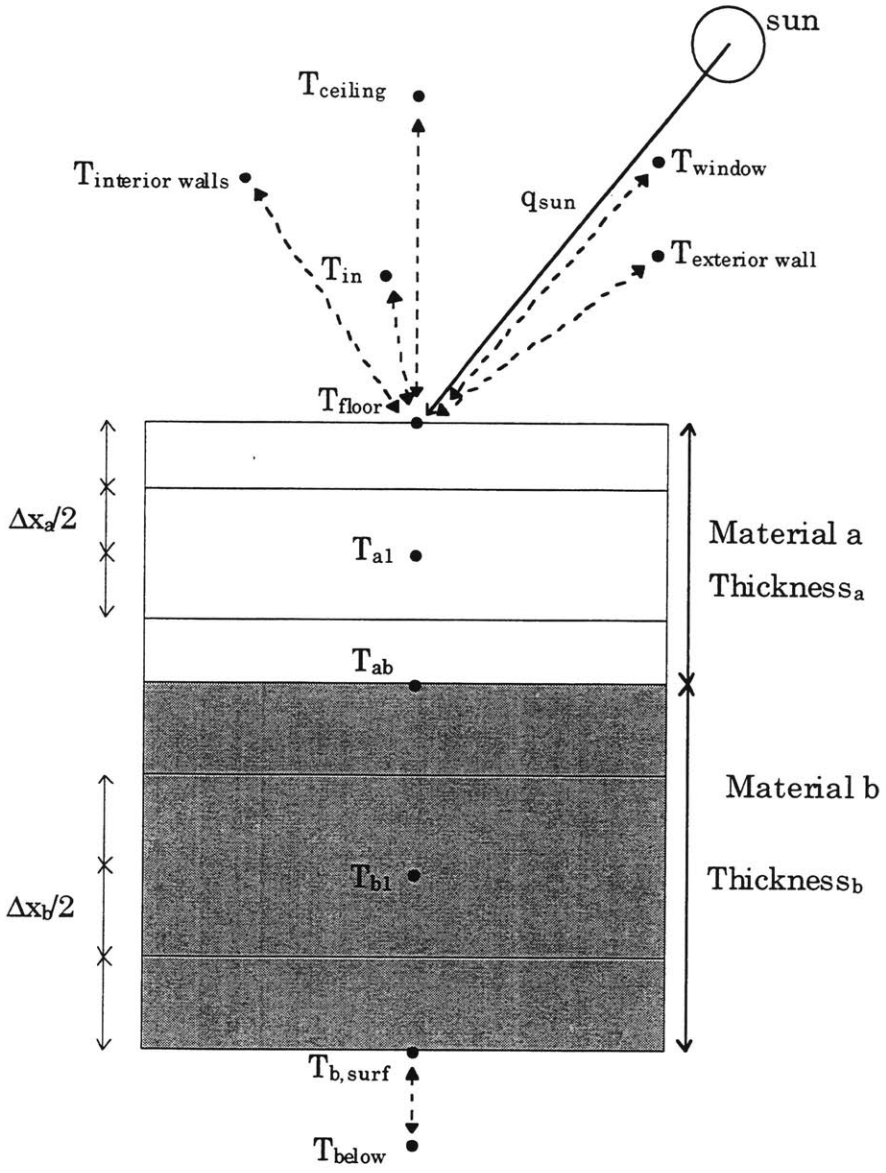

Figure 14. Two-layer floor shown with boundary conditions (dotted lines represent convection, IR radiation, or both)

The energy-balance equations for the different nodes expressed in Crank-Nicolson finite difference form are as follows:

For internal nodes, such as T_{a1},[15]

$$\left(C_a\right)\frac{\left(T'_{a1}-T_{a1}\right)}{\Delta t}\approx\frac{1}{2}\left(\frac{\left(T'_{ab}-T'_{a1}\right)}{R_a}+\frac{\left(T'_{floor}-T'_{a1}\right)}{R_a}\right)+\frac{1}{2}\left(\frac{\left(T_{ab}-T_{a1}\right)}{R_a}+\frac{\left(T_{floor}-T_{a1}\right)}{R_a}\right) \tag{51}$$

This equation is also valid for the node T_{b1} if all a's are replaced with b's and T_{floor} is replaced with $T_{b,\,surf.}$ (C_a and R_a are defined in section D.1.)

For junction nodes, such as T_{ab}:

$$\left(\frac{C_a}{2}+\frac{C_b}{2}\right)\frac{\left(T'_{ab}-T_{ab}\right)}{\Delta t}\approx\frac{1}{2}\left(\frac{\left(T'_{b1}-T'_{ab}\right)}{R_b}+\frac{\left(T'_{a1}-T'_{ab}\right)}{R_a}\right)+\frac{1}{2}\left(\frac{\left(T_{b1}-T_{ab}\right)}{R_b}+\frac{\left(T_{a1}-T_{ab}\right)}{R_a}\right) \tag{52}$$

For the floor's upper surface node:

$$\frac{C_a}{2}\frac{\left(T'_{floor}-T_{floor}\right)}{\Delta t}\approx\frac{1}{2}\left(\begin{array}{l}\dfrac{\left(T'_{a1}-T'_{floor}\right)}{R_a}+\dfrac{\left(T_{a1}-T_{floor}\right)}{R_a}\\ +h_{floor}\left(T'_{in}-T'_{floor}\right)+h_{floor}\left(T_{in}-T_{floor}\right)\\ +h_{r,floor->wall}\left(T'_{wall}-T'_{floor}\right)+h_{r,floor->wall}\left(T_{wall}-T_{floor}\right)\\ +h_{r,floor->window,\,eff}\left(T'_{window}-T'_{floor}\right)\\ +h_{r,floor->window,\,eff}\left(T_{window}-T_{floor}\right)\\ +h_{r,floor->walls}\left(T'_{walls}-T'_{floor}\right)+h_{r,floor->walls}\left(T_{walls}-T_{floor}\right)\\ +h_{r,floor->ceiling}\left(T'_{ceiling}-T'_{floor}\right)\\ +h_{r,floor->ceiling}\left(T_{ceiling}-T_{floor}\right)\\ +q'_{sun}+q_{sun}\end{array}\right), \tag{53}$$

[15] Internal nodes are those nodes not at the junction between two dissimilar materials.

where the middle seven lines of (53) represent convection to the floor surface from the inside air, radiation from the exterior wall, window, interior walls and ceiling. q_{sun} is the total amount of sunlight entering the room that is absorbed by the floor (per unit floor area). Determination of q_{sun} will be discussed in a later section. The convection and radiation coefficients are all defined in terms of the floor surface area. These coefficients will be discussed in greater detail in sections L and N.

For the floor's lower surface node:

$$\frac{C_b}{2}\frac{(T'_{b,surf}-T_{b,surf})}{\Delta t} \approx \frac{1}{2}\left(\begin{array}{l}\dfrac{\left(T'_{b1}-T'_{b,surf}\right)}{R_b}+\dfrac{\left(T_{b1}-T_{b,surf}\right)}{R_b} \\ +h_{below}\left(T'_{below}-T'_{b,surf}\right)+h_{below}\left(T_{below}-T_{b,surf}\right)\end{array}\right) \qquad (54)$$

Note that the lower surface of the floor becomes adiabatic if h_{below} is set to zero. h_{below} is a combined convection/radiation heat transfer coefficient.

There are three different types of floors encountered in typical dwellings: floors between living spaces, floors over an unheated basement or crawl space and slab-on-grade floors.

It is straightforward for the program to treat floors above a living space because the air temperature in the sub-zone below is determined by the thermal simulation for that space. No further modeling need be introduced.

In the case of the unheated basement and slab-on-grade floors, however, additional approximations must be made. According to McQuiston and Parker,[16] the only significant heat losses from slab-on-grade floors occur at the perimeter of the slab during the heating season. Perimeter losses are calculated according to the following formula:

$$q_{slab,perim} = F \times P(T_{in} - T_{out}) \,, \qquad (55)$$

[16] [25] pg. 177.

where F is the perimeter heat transfer coefficient (W/m°C), P the perimeter length (m) and T_{in} and T_{out} are the inside and outside air temperatures, respectively.

For the purposes of this model, the air temperature in unheated basements is assumed to fall between a nominal ground temperature of 10°C and the setpoint temperature of the nearest occupied zone.[17] For such a space,

$$T = 10°C + \text{Weight Factor} \times (T_{setpoint} - 10°C), \quad (56)$$

where Weight Factor is a parameter between 0 and 1. The air temperature of this space may also be arbitrarily fixed. This last model is extremely approximate and should be improved in the future.

2. Floor Model Simplifications

The same two simplifications described for the exterior wall model may be applied to the model for the floor. The first involves reducing the number of nodes in each floor layer (to a minimum of two nodes per layer for multi-layer floors and one node for single-layer floors) and the second, more drastic, simplification involves collapsing the floor into a single homogeneous layer described by a minimum of one node. (The minimum for the wall was two nodes).

3. Uncertainties and Other Sources of Error

The same points discussed in the section on wall uncertainties apply to the floor as well. Several additional points should be considered, however.

As will become evident in a later section when the relative importance of heat losses through different portions of the building envelope are compared, losses through the basement or floor slab can be substantial. However, accurate predictions of heat losses from floor slabs and basements

[17] [25] pg. 255.

are very difficult to achieve. Calculations are complicated by non-negligible two-and three-dimensional effects and a dependence on soil properties as well as its moisture content. Much work has been devoted to the study of ground-coupled systems [10,20,21,26,32,34].

The slab-on-grade perimeter heat loss calculation method described above is very simple to implement into a model, yet there are many uncertainties associated with its use. The ASHRAE Fundamentals Handbook gives some limited guidance in selecting the perimeter heat loss coefficient, F.[18] Typical values for F are about 0.86 W/m°C and 1.5 W/m°C for insulated and uninsulated perimeters, respectively. These values depend on exterior wall construction and also on the severity of climate (as described by the number of degree-days). If it is assumed that all slabs are insulated, use of the typical F = 0.86 W/m°C will have at most a ±7% error for sites with more than 2900 heating degree days (base 18 °C). This error estimate reflects merely the range of possible values given in the handbook table. It does not reflect variation in F due to soil type, soil moisture content, construction quality, proximity to other buildings or other factors. A rough estimate of the overall uncertainty in F is at least ±25%.

The method used to estimate the unheated basement temperature is extremely approximate. Its use is not recommended without further improvements.

F. Glazing

1. Thermal Model

A simplified model using solar heat gain factors (SHGF) was adapted from procedures described by the ASHRAE Fundamentals Handbook and by McQuiston and Parker.[19] This model assumes that the glazing is not spectrally selective. A more detailed model for spectrally-selective glazing involves the use of solar heat gain coefficients (SHGC). Guidance for use of this model is provided in the ASHRAE source cited.

---

[18] [1] pg. 27.12.

[19] See [1] Chapter 29 and [25] Chapter 6.

Two components of heat transfer through glazing must be addressed: transmission of solar radiation and conduction. These components are not mutually independent, however, since solar energy absorbed by the window is eventually conducted toward the two surfaces of the glass. The following nodal model was constructed to approximate the processes occurring in the glazing (**Figure 15**).

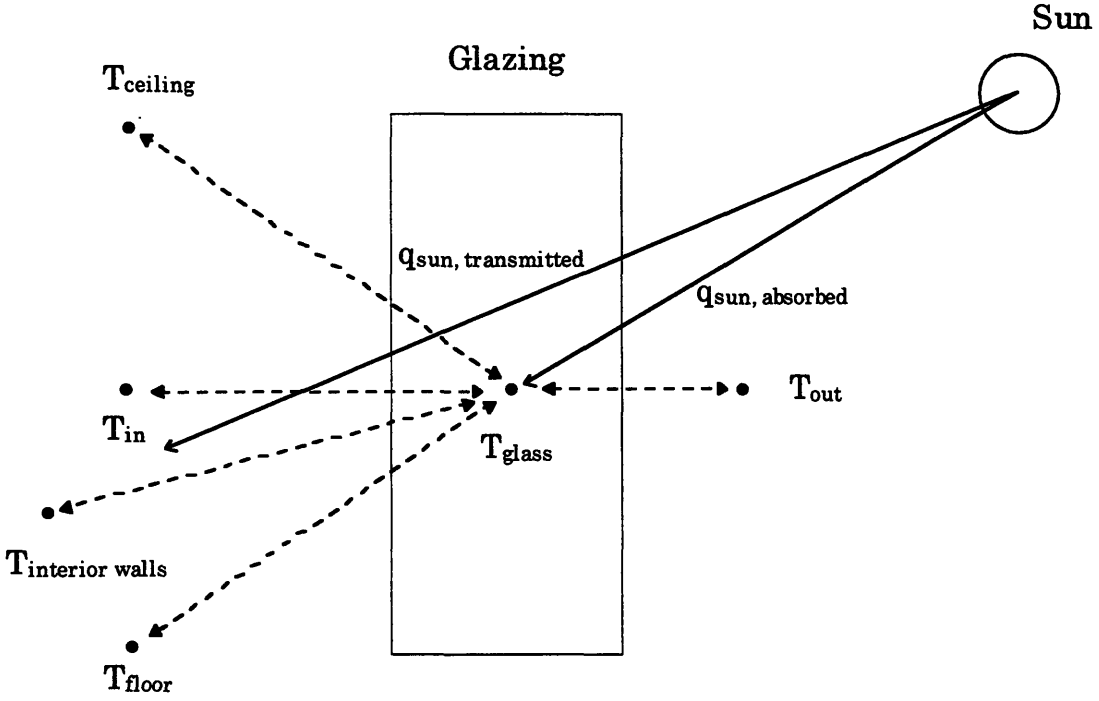

Figure 15. Nodal model of glazing showing boundary conditions (dotted lines represent convection, IR radiation, or both)

The amount of incident radiation absorbed and transmitted by the glazing is determined in the following manner:

• The diffuse ($I_{d,total}$) and direct (I_D) radiation incident on the exterior window surface are calculated using measured or modeled radiation data as described above. The angle of incidence, θ, is also determined.

• The shading coefficient, SC, of the window must be supplied. This coefficient is tabulated for a variety of window types by the sources cited above. It represents the fraction of radiation transmitted or absorbed by a

particular glazing type (at a particular angle of incidence) relative to that transmitted or absorbed by double-strength, single-pane clear glass.

- The absorbed radiation per unit window area is given by:

$$q_{sun,absorbed} = SC \times \left(I_D \sum_{j=0}^{5} a_j \cos^j(\theta) + 2 \times I_d \sum_{j=0}^{5} \frac{a_j}{(j+2)} \right) \quad (57)$$

The expression within the parentheses is also referred to as the absorbed solar heat gain factor, or ASHGF.

- The transmitted radiation per unit window area is given by:

$$q_{sun,transmitted} = SC \times \left(I_D \sum_{j=0}^{5} t_j \cos^j(\theta) + 2 \times I_d \sum_{j=0}^{5} \frac{t_j}{(j+2)} \right), \quad (58)$$

where both t_j and a_j are given in tabular form by the two references cited above. It should be noted that the values given by the two sources differ. The values used in the program are:

j	a_j	t_j
0	0.01154	-0.00885
1	0.77674	2.71235
2	-3.94657	-0.62062
3	*8.57881	*-7.07329
4	-8.38135	9.75995
5	3.01188	-3.89922

Table 2. Coefficients for use in equations (57) and (58)

*Instances where the two sources disagreed on the coefficients.

The expression within the parentheses in equation (58) is known as the transmitted solar heat gain factor, or TSHGF.

The amount of heat transfer through the window via conduction is a linear function of the overall U-value for the window, which is provided by the

user. This value should represent the entire window, including the center of glass, edge and frame. For a window of unit area:

$$\frac{1}{U} = \frac{1}{h_{in(conv+rad)}} + R_{glazing} + \frac{1}{h_{out}} ,$$

(59)

where $R_{glazing}$ is the thermal resistance of the window in the absence of interior and exterior film resistances and

$$h_{in(conv+rad)} = h_{in} + h_{r,window->floor} + h_{r,window->walls} + h_{r,window->ceiling}$$

(60)

Implicit in the use of equations (59) and (60) is the assumption that all surfaces in radiative contact with the window are at a common temperature, T_{in}. This is not necessarily the case.

Given a window U-value and the outdoor and indoor film coefficients, it is possible to calculate $R_{glazing}$.

The model shown in **Figure 15** contains a single node in the middle of the window, regardless of the number of window panes. This node may lie in the air space between the panes or it may lie within a glass pane. The reason behind this unintuitive approach is that a one-node window description minimizes calculation time and also provides a model that does not need to be adjusted to account for multiple glazings. In a real double-glazed window, some radiation is absorbed by the inner lite and some by the outer lite. With just one node to absorb radiation in the model, it was decided to place the node in the center of the window's thermal resistance. Placing the node on the inner or outer surface of the window (for a double-glazed window) would have led to an unrealistic weighting of the amount of absorbed radiation exiting the interior and exterior window surfaces.

Given this major approximation, the conduction heat transfer through the window is calculated as follows:

• The thermal resistance between the window node and the inner surface is taken to be $R_{glazing}/2$, as is the thermal resistance between the window node and the outer surface.

• This thermal resistance may be added in series to the outside film resistance in order to find an effective outside heat transfer coefficient:

$$\frac{1}{h_{out,eff}} = \frac{1}{h_{out}} + \frac{R_{glazing}}{2} \qquad (61)$$

However, formation of effective heat transfer coefficients for the inward-facing side of the glazing is more complicated. With the proper choice of R_E, the following thermal circuits may be shown to be equivalent:

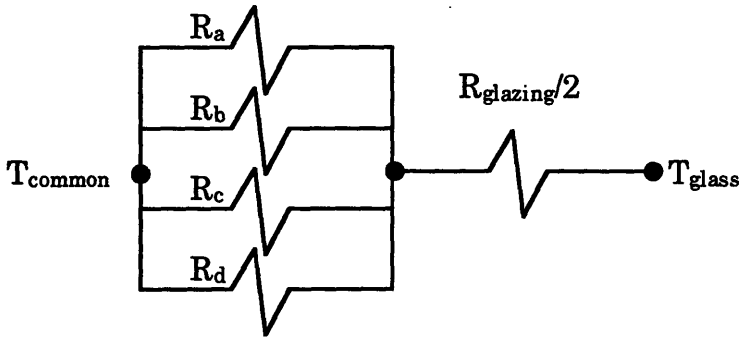

is equivalent to

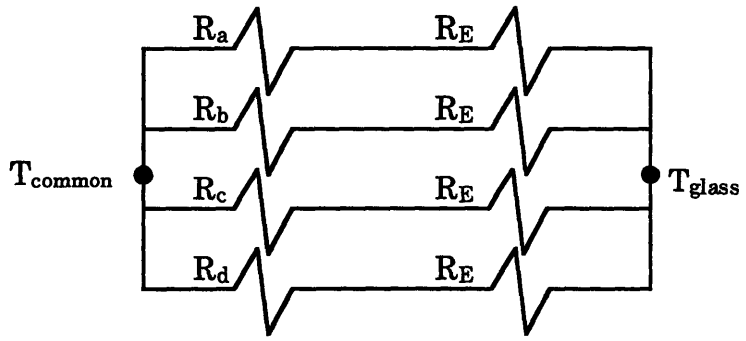

Figure 16. Equivalent thermal circuits for the inner portion of the glazing

T_{common} represents the inside air temperature, which is assumed to be identical to the surface temperatures of the floor, interior walls and ceiling.

R_a, R_b, R_c, R_d represent the inverses of the window-floor, window-interior walls, window-ceiling and window-air heat transfer coefficients.

For the heat transfer from T_{common} to T_{glass} to be identical in the two thermal circuits, R_E must be selected to satisfy:

$$\left[\frac{1}{\sum_{i=a}^{d}\frac{1}{R_i}}+\frac{R_{glazing}}{2}\right]^{-1}=\sum_{i=a}^{d}\frac{1}{R_i+R_E}$$

(62)

• The non-linear equation (62) is solved numerically to determine R_E. Given R_E, effective heat transfer coefficients for the inner surface of the window may be found. For example:

$$\frac{1}{h_{r,window->floor,eff}}=\frac{1}{h_{r,window->floor}}+R_E$$

(63)

• In this model, the thermal mass of the window is ignored. Consequently, the window node temperature is assumed to reach a steady state immediately. Therefore, the window node temperature at time t+Δt, or T_{window}', is a function of the surrounding conditions and inputs at the time t+Δt alone. In concert with the finite difference equations describing the other components of the sub-zone, the following equation allows solution of the window node temperature:

$$h_{out,eff}\left(T'_{window}-T'_{out}\right)+h_{in,eff}(T'_{window}-T'_{in})+h_{r,window->floor,eff}(T'_{window}-T'_{floor})+$$
$$h_{r,window->ceiling,eff}(T'_{window}-T'_{ceiling})+h_{r,window->walls,eff}(T'_{window}-T'_{walls})=q'_{sun,absorbed}$$

(64)

2. Uncertainties

The uncertainties associated with this rough window model are numerous. Treatment of solar radiation will be addressed first, followed by the treatment of conduction.

a) Solar Radiation Absorption and Transmission

The primary modeling uncertainty with respect to the treatment of solar radiation lies in the use of solar heat gain factors (SHGF) and the shading coefficient (SC) to determine the amount of sunlight absorbed by and transmitted through the glazing. As mentioned in the ASHRAE Handbook, the model works well for single- and double-pane clear glass and for tinted single-pane glass. However, the model cannot necessarily be accurately generalized to situations where spectrally-selective coatings, such as low-emissivity coatings, are used. In certain cases, according to Reilly *et al.* [31], the shading coefficient method can lead to a 35% over-prediction of transmitted solar heat gain. For more detailed calculations, the SHGC method should be adopted.

Another factor influencing the quality of the estimate of transmitted and absorbed solar radiation is the presence of shading, not only from intentional shading devices, but also from neighboring trees and buildings. No treatment of window shading by any means is incorporated into the program. Neglect of this factor could lead to an over-prediction of transmitted and absorbed radiation by 100% or more. The importance of this uncertainty will be determined in Chapter IV.

b) Conduction

The U-value entered by the user plays a critical role in determining the rate of heat transfer through the window. Whole-window U-values are readily available from tables. In one source,[20] the U-values are specified for winter conditions (windspeed = 24 km/hr, $T_{out} = -18°C$), while for still conditions, the same source shows that the U-values are 15% lower. This variability is due to the dependence of the outside convection coefficient on windspeed. A single outside convection coefficient (to be discussed in more detail in section N) and

[20] [1] Chapter 29, Table 5.

a single window U-value are used for all conditions throughout the entire year. The impact of uncertainty in h_{out} (and consequently U) will be assessed in a later section.

The introduction of effective heat transfer coefficients at the inner surface of the glazing requires the single assumption that the air and all interior surfaces of the sub-zone are isothermal. Given this assumption, the model used above to describe heat transfer through the window gives identical results to what would have been determined using the U-value of the window and the inside and outside air temperatures. The good agreement between the load predictions of this model and those of Energy-10 in the absence of solar radiation gives further credence to this model. (See Chapter VI.)

Another issue to consider is the fact that the program uses a single area to describe the window. The whole-window U-value is associated with conduction through both the glazing and the window frame, while solar radiation transmission occurs through the glazed area alone. This inconsistency may be especially important for windows with dividers, but even for fixed windows with no dividers, the ratio of the transparent area to the total area can be as low as 0.8.

The impact of the modeling assumption that the absorption of sunlight occurs in the center of the glazing's thermal resistance will be investigated.

G. Ceiling

1. Thermal Model

To minimize calculation time, the ceiling is modeled as a pure thermal resistance with no thermal mass. Like the window, it attains steady-state conditions immediately in this model. **Figure 17** shows the ceiling and the inputs affecting its temperature.

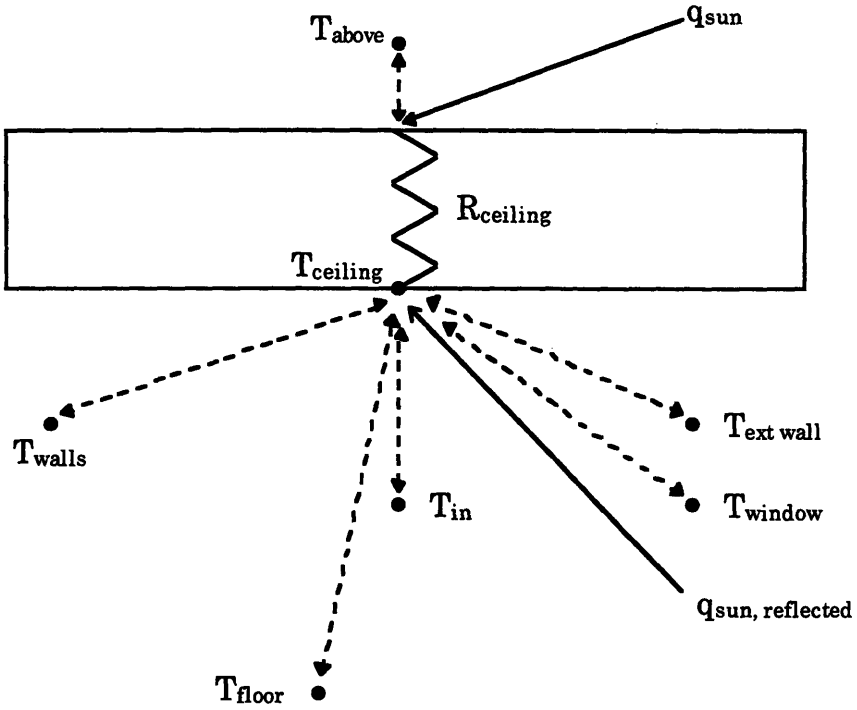

Figure 17. Ceiling thermal model (dotted lines represent convection, IR radiation, or both)

The heat balance equation for the node at $T_{ceiling}$ is:

$$\frac{\left(T'_{ceiling} - T'_{above}\right)}{\left(R_{ceiling} + 1/h_{above}\right)} + h_{ceiling}(T'_{ceiling} - T'_{in}) + h_{r,ceiling->floor}(T'_{ceiling} - T'_{floor}) +$$
$$h_{r,ceiling->walls}(T'_{ceiling} - T'_{walls}) + h_{r,ceiling->wall}(T'_{ceiling} - T'_{wall}) +$$
$$h_{r,ceiling->window,eff}(T'_{ceiling} - T'_{window}) = q'_{sun,reflected} \qquad (65)$$

The subscript "wall" refers to the inside surface of the exterior wall, while the subscript "walls" refers to the interior walls. Convection and radiation coefficients are defined in terms of the ceiling area. $q_{sun,\ reflected}$ represents reflected solar radiation absorbed by the ceiling per unit ceiling area. The calculation of $q_{sun,\ reflected}$ will be presented in a later section. T_{above} refers to

the air temperature above the ceiling. It may represent the temperature of the upstairs sub-zone or the well-ventilated attic temperature (outside temperature). In the first case, $R_{ceiling}$ is equal to the total resistance of the floor layers of the upstairs sub-zone and h_{above} is equal to h_{floor} of the upstairs sub-zone.[21] This option is not fully implemented into the model. Another available option (which is pictured in **Figure 17**) is to assume that the upper surface of the ceiling is actually the roof surface. In this case, $h_{above} = h_{out}$ and T_{above} is equal to the sol-air temperature of the roof surface:

$$T_{above} = T_{out} + \frac{\alpha_{solar,roof} q_{sun}}{h_{out}} \qquad (66)$$

Note that for this last case, the attic is not ventilated. The attic is strictly a resistive element connecting the inside ceiling surface temperature and the sol-air temperature.

2. Uncertainties

Some of the uncertainties associated with the exterior wall model should be considered for the ceiling model as well, namely: uncertainties associated with material properties and with the determination of overall R-values. A few additional points merit attention:

- Radiation between the attic floor and the underside of the roof is not accounted for in the well-ventilated attic setup, despite the fact that a major fraction of the heat transfer within the attic space occurs via radiation.[22] Neglect of attic radiation may lead to a considerable underestimation of summer cooling loads as well as errors in the heat load estimate. If the upper surface of the ceiling corresponds to the roof, however, then $R_{ceiling}$ may be chosen to so that radiation within the attic space is accounted for.

- The ceiling does not truly lack thermal mass.

---

[21] A combined convection/radiation coefficient would be more accurate.
[22] [7] pg. 147.

H. Interior Walls

1. Thermal Model

The model for the interior walls also neglects the presence of any thermal mass.[23] Consequently, steady-state conditions are assumed to be present at the node describing the surface temperature of the interior walls. When calculating the walls' surface temperature, the assumption is made that the walls are adiabatic, *i.e.*, there is no heat transfer through the wall to neighboring sub-zones or zones. (The role of conduction in inter-sub-zone heat transfer is not neglected, however. See section K.) **Figure 18** shows the sub-zone component temperatures affecting the temperature of the interior walls node.

[23] The rationale for this modeling assumption is two-fold. First, the walls do not represent actual partitions in the zone–they merely provide resistance to heat transfer among sub-zones. Second, calculation times may be reduced if the walls' surface temperature alone is considered in the calculations.

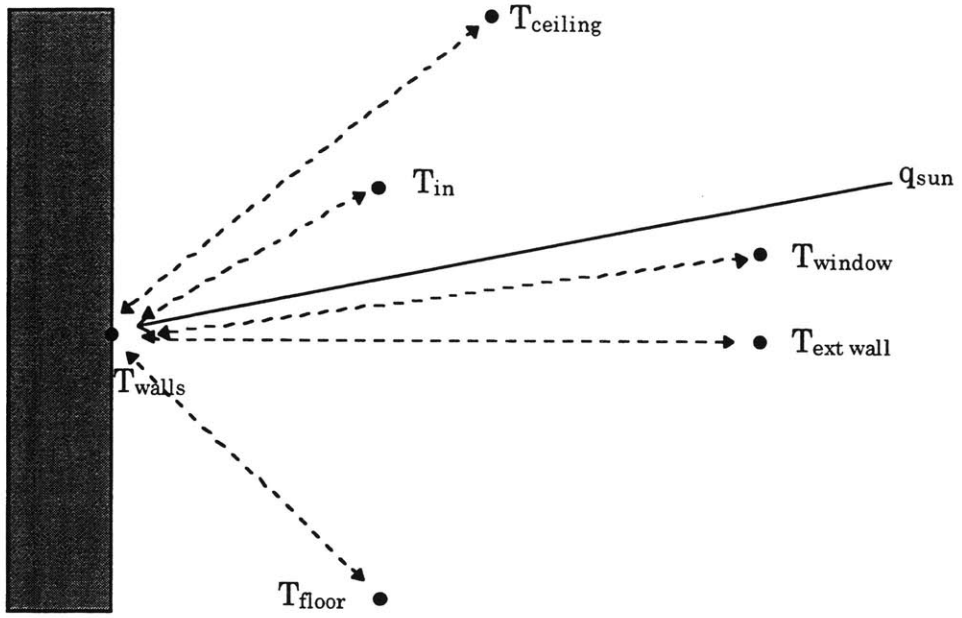

Adiabatic Wall

Figure 18. Model components influencing the temperature of the interior walls (dotted lines represent convection or IR radiation)

The energy-balance equation for the interior walls surface node, T_{walls}, is:

$$h_{in}(T'_{walls} - T'_{in}) + h_{r,walls->floor}(T'_{walls} - T'_{floor}) + h_{r,walls->ceiling}(T'_{walls} - T'_{ceiling}) + h_{r,walls->wall}(T'_{walls} - T'_{wall}) + h_{r,walls->window,eff}(T'_{walls} - T'_{window}) = q'_{sun} \quad (67)$$

q_{sun} is equal to the amount of incoming solar radiation (per unit area of interior walls) that is absorbed by the interior walls. Again, the subscript "wall" refers to the exterior wall and the heat transfer coefficients are defined in terms of interior wall area.

2. Uncertainties

There are two principal sources of uncertainty associated with this description of the heat transfer occurring at the surface of the interior walls: the solar absorptivity of the surface and the assumption that the surface is adiabatic. The impact of the first uncertainty on estimated heat and cooling loads will be examined in a later section. The second assumption may in fact be quite a good one if the neighboring sub-zone air temperatures are very close to that of the sub-zone in question. This issue will be explored below.

I. Air

1. Thermal Model

In this program, the air in the sub-zone is considered to have negligible thermal mass.[24] It interacts with the sub-zone surfaces solely via convection. Sub-zone air temperature is additionally affected by infiltration of outside air, by floor slab perimeter losses, by heat transfer to other sub-zones and by internal heat gains. These additional factors will be addressed in separate sections. Room air temperature is kept within setpoints by adding heat or cooling directly to the air. Air temperature control is also addressed in a separate section. The following energy-balance equation for sub-zone air assumes that the air temperature is free to float unimpeded by the heating or cooling system:

$$h_{in}A_{walls}(T'_{in} - T'_{walls}) + h_{in}A_{wall}(T'_{in} - T'_{wall}) + h_{in,eff}A_{window}(T'_{in} - T'_{window}) +$$
$$h_{floor}A_{floor}(T'_{in} - T'_{floor}) + h_{ceiling}A_{ceiling}(T'_{in} - T'_{ceiling}) + h_{infiltration} \times ACH(T'_{in} - T'_{out}) +$$
$$F \times P(T'_{in} - T'_{out}) + (UA)_{wall\ to\ left\ sub\text{-}zone}(T'_{in} - T'_{in,\ left\ sub\text{-}zone}) +$$
$$(UA)_{wall\ to\ right\ sub\text{-}zone}(T'_{in} - T'_{in,\ right\ sub\text{-}zone}) = q'_{internal}\ , \qquad (68)$$

where $h_{infiltration}$ is defined by equation (73) and ACH is the number of air changes per hour in the sub-zone. The U-values in this equation account for

---

[24] The decision to ignore the thermal mass of the air was motivated by simplicity. It may be desirable to incorporate it into a future version of the program.

both conduction and convection heat transfer between neighboring sub-zones. The units of U are W/°C per unit area of shared wall. The other convection coefficients have the usual definition. F and P were defined in section E.1 of this chapter.

$q_{internal}$ is equal to the total internal heat gain to the sub-zone air arising from occupants and electricity usage. Based on an estimate of the building's monthly electricity usage in kWh, the average electrical power flowing into each sub-zone is determined.[25] This constant power is added to the 24-hour average heat gain from occupants (70 W/person) to form $q_{internal}$. This very approximate method of accounting for internal gains was added to the model after all calculations were performed in the remainder of the thesis. Therefore, internal heat gains from occupants and electricity usage were neglected in all calculations presented.

The program uses two additional approximations to solve equation (68). It assumes that:

$$T'_{\text{left sub-zone}} \cong T_{\text{left sub-zone}} \quad \text{and}$$
$$T'_{\text{right sub-zone}} \cong T_{\text{right sub-zone}} \qquad \textbf{(69)}$$

The reason for the additional approximation is that it allows the program to avoid solving for the thermal response of all sub-zones simultaneously. The computational cost of such a simultaneous solution is prohibitive, as will be discussed in section O of this chapter.

The question may arise as to whether it is possible for this model to consider a uniform air temperature throughout all sub-zones. As a consequence of the approximations made in equation (69), this is not possible. If the U-value governing heat transfer between sub-zones is increased by many factors of 10 (in an attempt to equalize sub-zone temperatures) the resulting load predictions are meaningless.

Consider the following scenario in the heating season. Let the initial temperatures of the south- and east-facing sub-zones be 20°C. If inter-sub-

[25] The power is divided equally among all sub-zones. In a setup where the sub-zone floor areas are different, the power could be allocated by floor area.

zone heat transfer is governed by the U-values presented in section K, then the temperatures calculated at the next time step could be 21°C in the south-facing sub-zone and 20°C in the east sub-zone, for example.[26] However, if the U-value between sub-zones is very high (such as 500,000 W/m²°C), then when the new south sub-zone temperature is calculated (based on the same initial conditions), its change will be severely constrained by the initial temperature of the east sub-zone. The consequence of this constraint is that it is very difficult for sub-zone temperatures to rise above initial values. In one trial, the sub-zone temperatures had risen to only 20.5°C by mid-summer, which is clearly not a reasonably scenario. Adjusting the size of the time steps used in the finite difference method did not ameliorate the situation.

The moisture content of the air in the sub-zones is modeled very simply. Using the TMY2 data for relative humidity (RH), dew point temperature and atmospheric pressure (P), the humidity ratio of the outside air is determined:[27]

$$W = 0.62198 \frac{RH \times p_{v,s}}{P - p_{v,s}} ,$$

(70)

where $p_{v,s}$ is the saturated vapor pressure in Pascals. It is given by:

$$\ln(p_{v,s}) = C_1/T_{\text{dew point}} + C_2 + C_3 T_{\text{dew point}} + C_4 T_{\text{dew point}}^2 + C_5 T_{\text{dew point}}^3 + C_6 \ln(T_{\text{dew point}})$$
$$C_1 = -5.8002206 \times 10^3$$
$$C_2 = 1.3914993$$
$$C_3 = -4.8640239 \times 10^{-2}$$
$$C_4 = 4.1764768 \times 10^{-5}$$
$$C_5 = -1.4452093 \times 10^{-8}$$
$$C_6 = 6.5459673$$

(71)

The dew point temperature used in equation (71) is in degrees Kelvin.

---

[26] Due, perhaps, to the different amount of insolation received by the two sub-zones.
[27] [1] Chapter 6.

The humidity ratio of the inside air is identical to that of the outside air except when it exceeds the user-defined setpoint. In that case, latent heat is removed from the air to maintain the air at the setpoint humidity ratio. Since no internal latent gains are included in the model, infiltration is the only source of moisture to the sub-zone air. Calculation of the latent cooling loads will be discussed in section O.

2. Uncertainties

Aside from the uncertainty associated with heat transfer coefficients, which will be discussed below, four sources of modeling error are introduced with the incorporation of equation this air model into the program.

The first is the assumption that the air does not have any significant thermal mass. By a quick analysis, the thermal mass of the air should play a small role even in the lightweight building described in the next chapter. The thermal mass of the air in the south-facing sub-zone, for example, is equal to approximately 4% of the thermal mass of the entire lightweight exterior wall. The percentage is even lower for a three-inch concrete floor, or a massive concrete wall.

In many simulation programs, such as HVACSIM+ and Energy-10, the thermal capacitance of the air is lumped together with that of room furnishings and other non-massive objects. In order to follow this approach, an assumption is made about the quantity of "light-weight" thermal mass in the room. Yet as soon as objects are introduced into the room, detailed ray-tracing programs must be used to keep track of the radiative processes occurring within the space. Since no particulars are known about the room at the early design stage for which this program is intended, it was decided to ignore any thermal mass contributions from lightweight furnishings and the air. The impact of such an assumption will be investigated in Chapter VI.

The impact of the second modeling approximation ($T'_{neighbor} \cong T_{neighbor}$) may be investigated by examining the rate of change of the sub-zone air temperatures. If the rate of change is large, then the assumption that $T'_{neighbor} \cong T_{neighbor}$ is not a good one. However, the impact of such an error may be minimal if the heat transfer coefficient determining the rate of convective

exchange between the two spaces is small. Also, reducing the size of the time steps used in the finite difference solutions would tend to minimize the impact of the assumption. These issues will be investigated in a later section.

The argument for the third assumption–that the moisture content of the sub-zone air tracks that of the outside air–does not hold water if there are significant latent loads in the sub-zone. These may arise from occupants, plants and cooking, for example. Incorporation of these factors and the complex issue of moisture storage in sub-zone materials is beyond the scope of this study.

A fourth modeling assumption that has not yet been discussed is that the air in the sub-zone is well-mixed at a single temperature. Depending on the system used for space conditioning, this assumption may be a poor one. An understanding of the impact of this assumption may be achieved via detailed studies using computational fluid dynamics.

J. Infiltration and Natural Ventilation

1. Thermal Model

The model described in this section is designed to take into account heat and cooling loads caused by the exchange of indoor and outdoor air. Infiltration is the uncontrolled, unintentional exchange of air, while ventilation is the controlled exchange of air, such as that induced by opening the windows to cool the house on a summer night. Both infiltration and ventilation play a very important role in determining overall heat and cooling loads. However, since its action is uncontrolled, the infiltration rate in a particular house is extremely difficult to predict with reliable accuracy.

a) Infiltration

The driving force behind infiltration is a difference in the air pressures inside and outside the building. These pressure differences arise from both temperature differences between the indoor and outdoor air (stack effect) and the effects of wind. Local wind pressure is strongly dependent on details of

the building's form in addition to influences from nearby vegetation, buildings and terrain.

Given a pressure difference across apertures in the building envelope, air will pass into or out of the building. These apertures may consist of cracks around windows and doors, undampered bathroom or clothes drier vents, chimneys, and unsealed openings cut to bring electric or telephone lines into the home. In all but the tightest houses, these flaws in the building envelope are innumerable and are immeasurable without special equipment.

Reeves *et al.* summed up the situation as follows [30]: "Infiltration rates are extremely difficult to predict accurately for a residence because of the numerous variables that are involved, the complexities of the interactions among the variables and the inability to exactly determine the magnitude of the variables."

Faced with this seemingly intractable situation, there are several methods the researcher may use to estimate infiltration rates.

By far the simplest method is to assume a constant infiltration rate based on the "tightness" of the building construction. Peterson [28] shows a range of 0.37 to 0.86 air changes per hour for tightly constructed to loosely constructed houses. (One air change represents an exchange of indoor and outdoor air equal in volume to the interior volume of the house.) This simple method was chosen for use in this program. The rate of heat transfer from the inside air due to infiltration is given by:

$$q_{infiltration} = h_{infiltration} \times ACH(T_{in} - T_{out}) , \qquad (72)$$

where

$$h_{infiltration} = \frac{\rho_{air} \times c_{p,air} \times Volume}{3600} \qquad (73)$$

More complicated models have been developed that relate infiltration rates to wind speed and temperature differences. The basic form of a common empirical relation is:

$$\text{Infiltration rate} = A + B(\Delta T) + DV_{wind} \,, \qquad (74)$$

where A, B and D are fitting parameters, ΔT is the indoor-outdoor temperature difference and V_{wind} is the local wind speed. Both Peterson [28] and Coblentz and Achenbach [11] make use of equation (74), but with different values for A, B and D.

Further details, such as building height, terrain class, and effective leakage area or equivalent crack length, are accounted for in models proposed by Sherman and Grimsrud [33] and Reeves *et al.* [30].

b) Natural Ventilation

The program gives the user the option of specifying a higher air change rate to be used when warranted by outside conditions. For example, if the outside temperature rises above the minimum setpoint temperature during the heating season, the higher air change rate is used. This corresponds to the occupants opening the windows and doors to bring in fresh air. Similarly, in the cooling season, occupants may open windows to bring in cool night air. The alternate air change rate is used in the cooling season when the outside temperature falls below the maximum temperature setpoint.

2. Uncertainties

Even using the more detailed model described by Sherman and Grimsrud, some predictions of air infiltration rates were as much as 150% above and 70% below actual measurements.[28] Factors such as quality of construction and building material choice play a large role in infiltration, as does the presence of chimneys and ventilation fans. Elkins and Wensman [12] reported that the presence of a fossil-fuel heating system could increase the rate of infiltration 74% relative to that observed in an electrically-heated home. Peterson [28] mentioned a test in which shower and kitchen fans increased the air change rate of a home from 0.5 to 1.5 ACH.

---

[28] [33] pg. 806.

Given the magnitude of the uncertainties just described, the simple assumption of a constant air change rate seems justified for the purposes of this program. The effect of an uncertainty in the air change rate will be assessed in a later section.

K. Neighboring Sub-Zones

1. Thermal Model

The implementation of this model describing the flow of heat between neighboring sub-zones was introduced briefly in section I. As one looks into a sub-zone from its window there are two rear walls, one on the left and one on the right. These walls are common to this sub-zone and the left and right sub-zones. In the event of a temperature imbalance between the current sub-zone and the left sub-zone, for example, heat transfer will occur via two pathways: conduction through the common wall and convection through any openings in the wall. The program allows the user to supply a single U-value to be used in the following equation describing heat loss from air in this sub-zone to the air in the left sub-zone:

$$q_{\text{-> left sub-zone}} = (UA)_{\text{wall to left sub-zone}}(T_{in} - T_{\text{in, left sub-zone}}) \qquad (75)$$

Estimation of the above UA follows:

For an insulated 2x4 wood stud interior wall with 1/2" gypsum wall board on both sides, with the stud comprising 15% of the surface area, the U-value for the wall is 0.40 W/m^2°C. (A convection coefficient of 3.08 W/m^2°C was used on both sides of the common wall.[29]) For a rectangular building with ceiling height = 2.743 m (9 ft) and width and length = 11.8 and 7.87 m (for a total area = 1000 ft^2), A for the common wall is 19.4 m^2. Therefore UA = 7.8 W/°C if conduction through the wall is considered exclusively.

---

[29] A better choice would be to include the effects of radiation by using a combined radiation/convection heat transfer coefficient. Using 8.35 W/m^2°C (the ASHRAE value for interior vertical surfaces), the wall U-value is 0.48. Since the U-value shown above was used for all calculations in the next chapters, the radiation contribution was not discussed in the main text.

As summarized by Bauman *et al.* [5], Weber and Kearney [40] found that for two spaces connected by a door-like opening, the rate of heat transfer between the two spaces is governed by:

$$q = A_{\text{opening size}} h_{iz} \Delta T_{iz} \,, \tag{76}$$

where h_{iz} ("iz" representing inter-zonal) is given by:

$$h_{iz} = C(0.73)(H_A \Delta T_{iz})^{0.5} \,, \tag{77}$$

where C is a constant between 0.65 and 1 (determined by aperture geometry) and H_A is the height of the opening. Setting C = 1, H_A = 2.44 m, and ΔT_{iz} = 2°C yields h_{iz} = 1.6 W/m²°C. If the door opening is 1m wide, then UA = 3.9 W/°C if the only heat transfer between sub-zones occurs through the opening.

The average U for the entire common wall, accounting for both convection through the single door opening and conduction through the wall, is 0.55 W/m²°C.[30] This U value is defined in terms of the full area of the common wall. If desired, the U for the wall alone or for the opening alone could be used.

2. Uncertainties

The model described in the preceding section entails several assumptions:

- It is assumed that a constant U-value for the common wall is appropriate for use at all times.
- To calculate this U-value, certain material properties were assumed.
- When calculating conduction heat transfer through the common wall, (which is assumed to be massless) the surface temperatures

[30] Note that this whole-wall U-value would be 0.62 W/m²°C had radiation been considered. As shown in Chapter IV, the impact on annual loads of ignoring the radiation contribution is negligible.

calculated in section H are not used. The air temperatures alone for the two sub-zones are used. Also, the conduction through the wall does not directly influence interior wall surface temperatures.

- It is assumed that equation (77) is applicable to the triangular geometry of the sub-zones used by the program. (It was developed using a rectangular geometry.)

At this early stage in the design, it is not clear what kinds of openings exist between the sub-zones. In fact, the entire construct of the sub-zones is somewhat artificial. Therefore, it is likely that considerable uncertainty is associated with the use of the U-values presented above. However, if the temperature differences between zones are generally small, the influence of the neighboring zones and the uncertainties in the way they are modeled may not significantly impact the quality of the overall load calculations. It is shown in Chapter III that the contribution of inter-sub-zone heat transfer has a negligible impact on overall annual loads.

L. Long-Wave Radiation Heat Transfer

1. Sub-Zone View Factors

In order to predict the rate of radiation heat transfer between two surfaces, the view factor between those surfaces must first be found. View factors among different surfaces in the program's triangular sub-zone geometry will be determined in this section.

The next figure shows a plan view the South-facing sub-zone and the angles and dimensions needed to determine the surface-to-surface view factors.

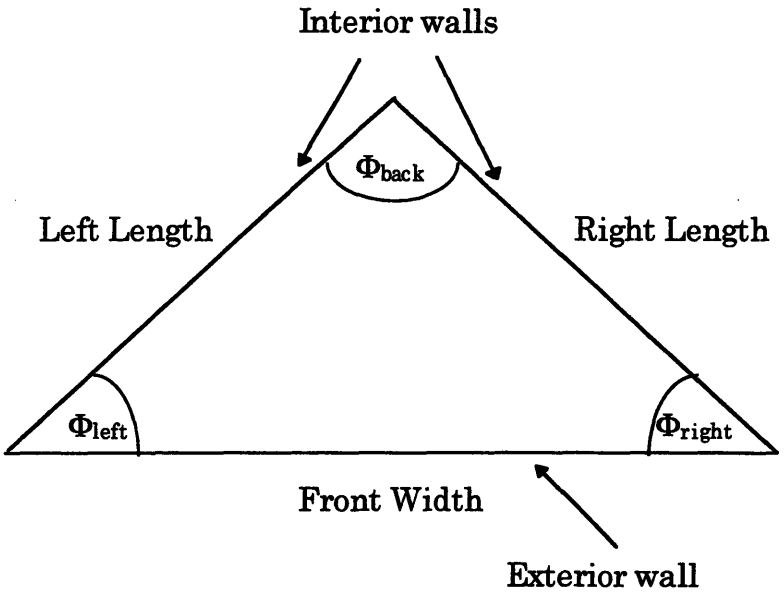

Figure 19. Plan of South-facing sub-zone

To give concrete examples of the view factors derived in the remainder of this section, the following dimensions are given to a 1000 ft² building:

Front Width (width of South and North faces) = 11.8 m
Side Width (width of East and West faces) = 7.87 m
Height = 2.743 m
Left Length = Right Length = 7.09 m
$\Phi_{left} = \Phi_{right} = 0.5882$ radians = 33.7°

$F_{front->left}$, or the view factor from the front wall (the exterior wall) to the left wall, and similarly $F_{left->right}$ and $F_{right->front}$ are given by:

$$F_{front->left} = F(\Phi_{left}, \text{Left Length, Height, Front Width}) = 0.287,$$
$$F_{left->right} = F(\Phi_{back}, \text{Right Length, Height, Left Length}) = 0.070,$$
$$F_{right->front} = F(\Phi_{right}, \text{Front Width, Height, Right Length}) = 0.477, \quad (78)$$

where $F(\Phi,a,b,c)$ is given by [36]:

$$
\begin{aligned}
F\times(\pi Y) = &-\frac{\sin(2\Phi)}{4}\left[\begin{array}{l} XY\sin(\Phi)+\left(\frac{\pi}{2}-\Phi\right)\left(X^2+Y^2\right) \\ +Y^2\tan^{-1}\left(\frac{X-Y\cos(\Phi)}{Y\sin(\Phi)}\right) \\ +X^2\tan^{-1}\left(\frac{Y-X\cos(\Phi)}{X\sin(\Phi)}\right)\end{array}\right] \\
&+\frac{\sin^2(\Phi)}{4}\left\{\begin{array}{l}\left(\frac{2}{\sin^2(\Phi)}-1\right)\ln\left[\frac{\left(1+X^2\right)\left(1+Y^2\right)}{1+Z}\right] \\ +Y^2\ln\left[\frac{Y^2(1+Z)}{(1+Y^2)Z}\right]+X^2\ln\left[\frac{X^2(1+X^2)^{\cos(2\Phi)}}{Z(1+Z)^{\cos(2\Phi)}}\right]\end{array}\right\} \\
&+Y\tan^{-1}\left(\frac{1}{Y}\right)+X\tan^{-1}\left(\frac{1}{X}\right)-\sqrt{Z}\tan^{-1}\left(\frac{1}{\sqrt{Z}}\right) \\
&+\frac{\sin(\Phi)\sin(2\Phi)}{2}X\sqrt{1+X^2\sin^2(\Phi)}\left[\begin{array}{l}\tan^{-1}\left(\frac{X\cos(\Phi)}{\sqrt{1+X^2\sin^2(\Phi)}}\right) \\ +\tan^{-1}\left(\frac{Y-X\cos(\Phi)}{\sqrt{1+X^2\sin^2(\Phi)}}\right)\end{array}\right] \\
&+\cos(\Phi)\int_0^Y\sqrt{1+\xi^2\sin^2(\Phi)}\left[\begin{array}{l}\tan^{-1}\left(\frac{X-\xi\cos(\Phi)}{\sqrt{1+\xi^2\sin^2(\Phi)}}\right) \\ +\tan^{-1}\left(\frac{\xi\cos(\Phi)}{\sqrt{1+\xi^2\sin^2(\Phi)}}\right)\end{array}\right]d\xi\,,
\end{aligned}
\tag{79}
$$

where

$$
\begin{aligned}
X &= a/b\,, \\
Y &= c/b\,, \\
Z &= X^2+Y^2-2XY\cos(\Phi)
\end{aligned}
\tag{80}
$$

Using the relation:

$$A_1 F_{1->2} = A_2 F_{2->1} ,$$

(81)

it is straightforward to find $F_{right->left}$, $F_{front->right}$ and $F_{left->front}$ (0.070, 0.287, 0.477 respectively). Since the interior walls are given a single temperature node, it is helpful to determine a view factor from the exterior wall to the interior walls and vice versa:

$$F_{front->interior\ walls} = F_{front->left} + F_{front->right} = 0.573$$

(82)

and

$$F_{interior\ walls->front} = \frac{\text{Front Width}}{(\text{Left Length} + \text{Right Length})} \times F_{front->interior\ walls} = 0.477$$

(83)

It then follows that:

$$F_{front->ceiling} = F_{front->floor} = \frac{(1 - F_{front->interior\ walls})}{2} = 0.213$$

(84)

$$F_{ceiling->front} = F_{floor->front} = \frac{(\text{Height} \times \text{Front Width})}{\text{Ceiling Area}} \times F_{front->floor} = 0.297$$

(85)

Using similar manipulations, the following view factors are derived:

$$F_{left->floor} = F_{right->floor} = 0.226$$
$$F_{floor->left} = F_{floor->right} = 0.189$$

(86)

$$F_{\text{floor->interior walls}} = F_{\text{ceiling->interior walls}} = 0.379$$
$$F_{\text{interior walls->floor}} = F_{\text{interior walls->ceiling}} = 0.226$$

(87)

$$F_{\text{floor->ceiling}} = F_{\text{ceiling->floor}} = 0.324$$

(88)

$$F_{\text{interior walls->interior walls}} = 0.070$$

(89)

A single approximation is made by the program with regard to the view factors. (No other approximations are necessary since the view factors are determined exactly from the geometry of the space.) This approximation is that the view factor from the window to the sub-zone surfaces is identical to that from the exterior wall (front) to the sub-zone surfaces. The motivation for this assumption is that little is known about the window. Only the window's percentage of overall exterior wall area is specified, not its location and particular dimensions. Especially given the complexity of view factor determination (*e.g.*, equation (79)) it was deemed unreasonable to assume a particular window location and size in order to find exact view factors from this window to the sub-zone surfaces.

2. Long-Wave Radiation Heat Transfer Coefficients

a) Thermal Model

In order to calculate the long-wave radiation heat transfer coefficients between sub-zone surfaces, infrared emissivities for all surfaces must be specified. To provide further numerical examples of the coefficients calculated, the following emissivities (ε_{IR}) were chosen:

$$\varepsilon_{IR,\,\text{floor}} = 0.94$$
$$\varepsilon_{IR,\,\text{walls and ceiling}} = 0.90$$
$$\varepsilon_{IR,\,\text{window}} = 0.93$$

(90)

The net rate of radiative heat transfer between two surfaces is given by:

$$q_{1->2} = \frac{\sigma(T_1^4 - T_2^4)}{\frac{1-\varepsilon_1}{\varepsilon_1 A_1} + \frac{1}{A_1 F_{1->2}} + \frac{1-\varepsilon_2}{\varepsilon_2 A_2}} ,$$

(91)

where σ, the Stefan-Boltzmann constant, equals 5.67×10^{-8} W/m^{2}K^{-4}. Equation (91) is not strictly correct, since radiation heat transfer from surface 1 to surface 2 via surface 3, for example, is neglected. This approximation will be justified in Chapter IV, where it is shown that its impact on annual heat and cooling loads is negligible.

The program linearizes equation (91) using the common approximation:

$$T_1^4 - T_2^4 \approx 4T_m^3(T_1 - T_2) ,$$

(92)

where T_m is equal to the mean of T_1 and T_2 expressed in degrees Kelvin. This approximation is most accurate when the temperature difference between surfaces in radiative contact is small. This linear approximation is essential to the simultaneous solution of the temperature node heat-balance equations. The program assumes a single T_m for the entire simulation. Based on a review of the annual average sub-zone surface temperatures, the heating season minimum setpoint is the temperature that best approximates T_m. Certainly this assumption introduces additional uncertainty into the calculations. The importance of the value of T_m will be assessed in a later section. Using equation (92), equation (91) may be approximated:

$$q_{1->2} \approx \frac{4\sigma T_m^3(T_1 - T_2)}{\frac{1-\varepsilon_1}{\varepsilon_1 A_1} + \frac{1}{A_1 F_{1->2}} + \frac{1-\varepsilon_2}{\varepsilon_2 A_2}}$$

$$\equiv h_{1->2} A_1 (T_1 - T_2) \equiv h_{2->1} A_2 (T_1 - T_2)$$

(93)

Finally:

$$h_{r,1->2} = \frac{1}{A_1} \times \frac{4\sigma T_m^3}{\frac{1-\varepsilon_1}{\varepsilon_1 A_1} + \frac{1}{A_1 F_{1->2}} + \frac{1-\varepsilon_2}{\varepsilon_2 A_2}} = \frac{1}{A_1} \times \frac{4\sigma T_m^3}{\frac{1-\varepsilon_1}{\varepsilon_1 A_1} + \frac{1}{A_2 F_{2->1}} + \frac{1-\varepsilon_2}{\varepsilon_2 A_2}} \quad (94)$$

The two different versions of equation (94) differ only due to the use of equation (81). Note that $h_{r,1->2}$ is defined in terms of A_1. $h_{r,2->1}$, which is defined in terms of A_2, is given by:

$$h_{r,2->1} = \frac{A_1}{A_2} h_{r,1->2} \quad (95)$$

Repeated use of equations (94) and (95), along with the assumption that $T_m = 293K$, yields the following set of radiative heat transfer coefficients valid for the north- and south-facing sub-zones. Each coefficient is defined in terms of the area of the first subscript. Whenever the exterior wall (front) or the window areas were needed, actual areas were used, *i.e.*, $A_{\text{Exterior Wall}}$ = 0.9x(Front Width x Height) and A_{window} = 0.1x(Front Width x Height), since the percentage glazing used was 10%. All coefficients are given in SI units.

$$\begin{aligned}
h_{r,\text{floor->exterior wall}} &= 1.46; \; h_{r,\text{exterior wall->floor}} = 1.17 \\
h_{r,\text{floor->window}} &= 0.17; \; h_{r,\text{window->floor}} = 1.20 \\
h_{r,\text{floor->interior walls}} &= 2.06; \; h_{r,\text{interior walls->floor}} = 1.23 \\
h_{r,\text{exterior wall->interior walls}} &= 2.94; \; h_{r,\text{interior walls->exterior wall}} = 2.20 \\
h_{r,\text{exterior wall->ceiling}} &= 1.16; \; h_{r,\text{ceiling->exterior wall}} = 1.45 \\
h_{r,\text{window->ceiling}} &= 1.19; \; h_{r,\text{ceiling->window}} = 0.17 \\
h_{r,\text{ceiling->interior walls}} &= 2.02; \; h_{r,\text{interior walls->ceiling}} = 1.21 \\
h_{r,\text{window->interior walls}} &= 3.12; \; h_{r,\text{interior walls->window}} = 0.26 \\
h_{r,\text{floor->ceiling}} &= h_{r,\text{ceiling->floor}} = 1.75
\end{aligned} \quad (96)$$

Recall that in section F effective convection and radiation heat transfer coefficients were introduced for the window to account for the placement of the window temperature node in the middle of $R_{glazing}$. For completeness, the results of this adjustment are summarized here. Assumptions: $U_{glazing}$ (manufacturer's whole-window value) = 2.6 W/m²°C; h_{in} = 3.08 W/m²°C; h_{out} = 34 W/m²°C.

$$h_{in(conv+rad)} = 8.59$$
$$R_{glazing} = 0.24 \qquad (97)$$

(SI units. See equations (59) and (60) for definitions.)

$$h_{in,eff} = 1.33;\ h_{out,eff} = 6.72 \qquad (98)$$

$$h_{r,window->floor,\ eff} = 0.79;\ h_{r,floor->window,\ eff} = 0.11$$
$$h_{r,window->ceiling,\ eff} = 0.79;\ h_{r,ceiling->window,\ eff} = 0.11$$
$$h_{r,window->interior\ walls,\ eff} = 1.33;\ h_{r,interior\ walls->window,\ eff} = 0.11 \qquad (99)$$

b) Summary of Radiation-Related Uncertainties

The program's treatment of IR radiation occurring within the sub-zone contains several uncertainties. The important modeling uncertainties involve:

- The assumption that the view factors from the window to sub-zone surfaces are identical to those from the exterior wall to the same surfaces.
- The assumption that the non-linear radiative exchange may be represented by a linear approximation and that a single mean temperature (T_m) may be used for the entire year.
- The assumption that no furnishings exist in the sub-zone that complicate view factor determination.
- The assumption that the surfaces in the sub-zone behave as gray bodies, emitting and absorbing long-wave radiation isotropically.

The primary parameter uncertainty in this portion of the model is that of the emissivity values used for the sub-zone surfaces.

Where possible, the importance of these uncertainties will be explored in a later section.

3. Exterior Surface Long-Wave Radiation

Ideally, radiation and convection occurring at the exterior of the building envelope would be treated individually, as done within the sub-zone. However, several obstacles prevented implementation of this approach. These obstacles included the lack of a simple method for determining the surface temperatures and view factors for the neighboring environment, including the sky. Rather than introducing another set of approximations, it was decided to use the combined convection/radiation heat transfer coefficient suggested by ASHRAE.[31] This coefficient describes heat transfer between the exterior envelope surface and ambient air.

M. Distribution of Sunlight within Sub-zone

The accurate determination of the distribution of incoming solar radiation within a sub-zone requires detailed information about window dimensions and position as well as detailed information about the interior space. Solar position can be coupled with room geometry to yield the exact portion of the room illuminated by beam radiation at any given time. However, as most energy simulation programs are not robust enough to treat the illuminated patch of floor differently from the rest of the floor, for example, solar radiation is typically modeled as being evenly spread over the different room surfaces. One such model was constructed by Athienitis and Stylianou [2], who developed algorithms for determining the ratio of total daily solar radiation absorbed by the floor to that absorbed by the other surfaces in a rectangular room.

---

[31] [1] pg. 24.2.

1. Model

In this program, a simple assumption is made about where incoming solar radiation (both beam and diffuse) impinges upon the sub-zone surfaces. It is assumed that 50% of all incoming radiation is evenly distributed on the floor, while the rest is evenly distributed on the interior walls. The amount of sunlight initially absorbed by each surface is determined by the solar absorptivities of the surfaces. Solar radiation not initially absorbed is assumed to be reflected isotropically within the space. View factors are used to determine the distribution of reflected light in the sub-zone. All reflected light is absorbed by the next surface it encounters.[32]

Defining $\%_{\text{sun->floor}}$ to be the portion of incoming light striking the floor first, and $\%_{\text{sun->walls}}$ (or $100\% - \%_{\text{sun->floor}}$) to be the portion striking the interior walls first, it is possible to establish the amount of sunlight absorbed by all sub-zone surfaces. $\%_{\text{glazed}}$ is defined to be the percentage of the exterior wall covered by glazing. The solar absorptivities of the interior walls (white paint) and floor (dark tile) are 0.26 and 0.7, respectively.

Percentage of incoming sunlight absorbed by the floor =

$$\%_{\text{sun->floor}} \times \alpha_{\text{solar,floor}} + \%_{\text{sun->walls}} \times (1 - \alpha_{\text{solar,walls}}) \times F_{\text{interior walls->floor}} \qquad (100)$$

Percentage of incoming sunlight absorbed by the interior walls =

$$\%_{\text{sun->walls}} \times \alpha_{\text{solar,walls}} + \%_{\text{sun->floor}} \times (1 - \alpha_{\text{solar,floor}}) \times F_{\text{floor->interior walls}} + \%_{\text{sun->walls}} \times (1 - \alpha_{\text{solar,walls}}) \times F_{\text{interior walls->interior walls}} \qquad (101)$$

Percentage of incoming sunlight absorbed by the ceiling =

$$\%_{\text{sun->floor}} \times (1 - \alpha_{\text{solar,floor}}) \times F_{\text{floor->ceiling}} + \%_{\text{sun->walls}} \times (1 - \alpha_{\text{solar,walls}}) \times F_{\text{interior walls->ceiling}} \qquad (102)$$

---

[32] With the exception of the window. It is assumed that all reflected light striking the window is transmitted.

Percentage of incoming sunlight absorbed by the exterior wall =

$$\%_{sun->floor} \times (1 - \alpha_{solar,floor}) \times F_{floor->wall} \times (100\% - \%_{glazed})$$
$$+\%_{sun->walls} \times (1 - \alpha_{solar,walls}) \times F_{interior\ walls->wall} \times (100\% - \%_{glazed})$$

(103)

For the South-facing sub-zone described earlier, all incoming solar radiation is accounted for and is absorbed as follows:

Floor: 43.4%
Interior Walls: 21.3%
Ceiling: 13.2%
Interior Surface of Exterior Wall: 19.9%
Lost through window: 2.2%

2. Summary of Uncertainties

Built into the model just described is the significant assumption that furnishings within the sub-zone do not affect the distribution of solar energy. The presence of carpeting, for example, would certainly have a major impact on the amount of solar energy absorbed by the floor. The initial estimate that 50% of incoming sunlight strikes the floor is simply an estimate. The impact of the percentage chosen will be investigated in a later section.

Another important modeling assumption is that light not initially absorbed by the surface it strikes is scattered isotropically. This is not always the case for tile floors, for example. However, if the sunlight is reflected off the floor, it will most likely strike the interior walls. Adjustment of $\%_{sun->floor}$ could account for the additional reflection, but such a fine point is unlikely to have a significant impact on the program's output.

The certainty with which surface solar absorptivities can be specified is unclear. These values may change with time as surfaces age. The impact of varying the surface absorptivities will be assessed in a later section.

N. Convection Heat Transfer

1. Thermal Model

The treatment of convection heat transfer in the program is extremely simplified. Justification for this approach will be explored in the next subsection on uncertainties.

The rate of heat transfer via convection from a surface of uniform temperature T_s to well-mixed air of temperature T_{air} is given by:

$$q_{convection} = h_c A_{surface}(T_s - T_{air}) \qquad (104)$$

Constant convection coefficients were selected for year-round use based on heat transfer coefficients given by ASHRAE.[33] The radiative component of the overall heat transfer coefficients given by this source was removed by Bauman *et al.*,[34] yielding the following set of convection heat transfer coefficients for use inside the sub-zone:

For vertical surfaces: $h = 3.08\ W/m^2°C$
For floors: $h = 4.04\ W/m^2°C$
For ceilings: $h = 0.95\ W/m^2°C$

(105)

Since the program makes use of a combined convection-radiation heat transfer coefficient at the outside surface of the sub-zone, the overall heat transfer coefficient provided by ASHRAE was selected for year-round use:[35]

$$h_{out} = 34.0\ W/m^2°C \qquad (106)$$

---

[33] [1] pg. 24.2, Table 1.
[34] [5] pg. 218.
[35] Assuming winter conditions, with windspeed = 6.7 m/s.

2. Discussion of Uncertainties

The rate of convection heat transfer at the different surfaces within a room is sensitive to many factors, including the geometry of the space, the orientation of the surface of interest, the temperature difference between the surface and the air, and the local air speed. An additional obstacle for the model developer is that the last two variables mentioned may be time- and location-dependent. A non-uniform temperature distribution may arise on a surface in the vicinity of thermal breaks and windows, for example. Air speed is also a local phenomenon, dependent on local temperature distributions. It may also be strongly time-dependent, such as in a space conditioned by a forced-air heating or cooling system.

Even if one assumes a constant air-surface temperature difference and surface orientation, a wide range of convection coefficients may be found in the literature describing natural convection. Bauman *et al.*[36] found that the presence of horizontal barriers (floor and ceiling) within a room delayed the onset of turbulence for flow along a vertical surface, leading to laminar conditions in their test cell.[37] For a room 2.7m in height and with a temperature difference of 2.8°C between the wall and air, the convection coefficient for a vertical surface derived from their correlation is 2.05 W/m²°C. The ASHRAE correlation[38] for similar conditions (laminar flow) yields 1.43 W/m²°C, while that for turbulent conditions yields 1.85 W/m²°C. Khalifa and Marshall [19] show that for the same surface-air temperature difference, convection coefficients for vertical surfaces in the literature range from 1.4 to 3.2 W/m²°C.[39] These researchers report an even higher value (3.7 W/m²°C) for a vertical wall opposite a fan heater.

The constant convection coefficient for vertical surfaces used by the program (3.08 W/m²°C) falls within the range of reported values. However, the value of the constant coefficient was based on a surface-air temperature difference of 5.6°C, somewhat larger than typical differences observed between opaque surfaces and the inside air. This temperature difference may be more typical of that found between glazing and the indoor air.

---

[36] [5] pg. 217.

[37] The investigators used a scaled water test cell, to eliminate radiation effects. They contend that the results found within the test cell are valid for an air-filled room.

[38] [1] pg. 3.12.

[39] The lower bound is about 1.8 W/m²°C if laminar flow is excluded.

Bauman *et al.* also explored the spatial dependence of the convection coefficients. Simulation results showed that for vertical indoor surfaces, the convection coefficient ranged from a low of –2.2 to a high of 2.8 W/m²°C.[40] The floor convection coefficient varied between 0.8 and 3.4 W/m²°C, while ceiling coefficients varied between 0.5 and 1.8 W/m²°C. (Compare with coefficients selected in equation (105).)

From the evidence just presented, there is great uncertainty as to what convection coefficients should be selected for use in simulations. For this reason, it was decided to use constant convection coefficients that depended only on surface orientation. The impact on overall predicted energy use of the choice of indoor convection coefficients will be examined in a later section.

As mentioned above, the coefficient used to determine the rate of heat transfer at the exterior surface of the building accounts for both convection and radiation. According to ASHRAE,[41] for a vertical surface this value ranges from 8.29 W/m²°C for still air to 34.0 W/m²°C for a windspeed of 6.7 m/s. For some conditions, use of coefficients as large as 500 W/m²°C may be warranted.[42] Due to the surface heat transfer coefficient's strong dependence on windspeed and the large variation of windspeeds expected at the surface, a great deal of uncertainty exists as to which value to choose. The importance of the value chosen will be assessed in a later section.

O. Synthesis of Building Model Components

Energy-balance equations for the various building model components have been developed in sections B through N of this chapter. These equations incorporate material properties and thicknesses, sub-zone geometry, and boundary conditions such as outside temperature and solar radiation. Simultaneous solution of the full set of component equations for each hourly time step throughout the year provides the program with the information

---

[40] The negative value arose from their definition that heat flow from the air to the surface is positive. Below a window, the falling, cold air is warmed by the surface, leading to a negative convection coefficient.

[41] [1] pg. 24.2, Table 1.

[42] Such as when wet siding dries after rainfall. See [23].

needed to calculate annual heat and cooling loads. The solution of the component energy-balance equations will be discussed in this section. The next section will demonstrate how the resulting information is used to calculate building energy loads.

In order to solve the set of simultaneous component equations, they are first assembled into matrix form. The procedure will be demonstrated using the equations for the temperature node at the outside surface of the exterior wall and the temperature node on the surface of the interior walls. Note that the first temperature node contains thermal mass, while the second does not. The heat-balance equations are repeated for convenience:

$$\frac{C_b}{2}\frac{(T'_{b,surf}-T_{b,surf})}{\Delta t} \approx \frac{1}{2}\left(\begin{array}{l} \dfrac{\left(T'_{b1}-T'_{b,surf}\right)}{R_b}+\dfrac{\left(T_{b1}-T_{b,surf}\right)}{R_b} \\ +h_{out}\left(T'_{out}-T'_{b,surf}\right)+h_{out}\left(T_{out}-T_{b,surf}\right) \\ +q'_{sun}+q_{sun} \end{array}\right), \tag{43}$$

$$h_{in}(T'_{walls}-T'_{in})+h_{r,walls->floor}(T'_{walls}-T'_{floor})+h_{r,walls->ceiling}(T'_{walls}-T'_{ceiling})+ h_{r,walls->wall}(T'_{walls}-T'_{wall})+h_{r,walls->window,eff}(T'_{walls}-T'_{window})=q'_{sun} \tag{67}$$

Equation (43) may be rewritten using the following collection of terms:

$$W \equiv \frac{0.5\Delta t}{C_b/2} \tag{107}$$

$$\left\{1+\frac{W}{R_b}+W\times h_{out}\right\}T'_{b,surf}-\frac{W}{R_b}T'_{b1}=$$
$$\left\{1+\frac{W}{R_b}-W\times h_{out}\right\}T_{b,surf}+\frac{W}{R_b}T_{b1}$$
$$+W\left\{h_{out}(T'_{out}+T_{out})+q'_{sun}+q_{sun}\right\}$$

(108)[43]

Equation (67) may be rewritten:

$$\left\{h_{in}+h_{r,walls->floor}+h_{r,walls->ceiling}+h_{r,walls->wall}+h_{r,walls->window,eff}\right\}T'_{walls}$$
$$+\left\{-h_{in}\right\}T'_{in}+\left\{-h_{r,walls->floor}\right\}T'_{floor}+\left\{-h_{r,walls->ceiling}\right\}T'_{ceiling}$$
$$+\left\{-h_{r,walls->wall}\right\}T'_{wall}+\left\{-h_{r,walls->window,eff}\right\}T'_{window}$$
$$=q'_{sun}$$

(109)[44]

A generalized form of both of these equations is:

[Coefficients] × [Temperatures at next time step] =
[Coefficients] × [Temperatures at current time step]
+ [Boundary conditions]

(110)

All component equations may be written in this form and combined into a single matrix equation:

$$\hat{\mathbf{A}}\mathbf{T}' = \hat{\mathbf{B}}\mathbf{T}+\mathbf{C}\,,$$

(111)

---

[43] This equation accounts for the solar radiation properly if instantaneous solar radiation is given at time t and t+Δt. However, the solar radiation data at t+Δt given in the TMY2 format actually reflects radiation between t and t+Δt. Therefore, the Crank-Nicolson averaging of solar heat gain at time t and t+Δt is not needed. To correct this equation for TMY2 data usage, q_{sun} should be set equal to q_{sun}'.

[44] The TMY2 format effectively gives instantaneous solar radiation halfway between the current time step and the next. In this case, the assumption is made that the instantaneous radiation at the next time step is equal to that at the midpoint between time steps.

where $\hat{\mathbf{A}}$ and $\hat{\mathbf{B}}$ represent coefficient matrices derived from the individual component equations and $\mathbf{T}'$ and $\mathbf{T}$ represent the temperatures at all temperature nodes at the next and current time steps, respectively. $\mathbf{C}$ is the vector containing all boundary conditions.

Given initial temperatures at all the temperature nodes, the vector of temperatures at the next time step is calculated as follows:

- Using matrix multiplication and addition, the right-hand side of equation (111) is condensed to a single vector, $\mathbf{D}$.
- The equation $\hat{\mathbf{A}}\mathbf{T}' = \mathbf{D}$ is solved for $\mathbf{T}'$ using LU decomposition [29].
- This $\mathbf{T}'$ becomes the next $\mathbf{T}$ to be used in equation (111).

The entire procedure is repeated to calculate node temperatures at hourly time intervals throughout the year.

The accuracy of this algorithm was validated using the exact solution for conduction through a slab. Details are available in Appendix 1.

It was further validated by comparison with results obtained using the Runge-Kutta and Euler methods to solve the differential equations associated with the different temperature nodes. Those explicit methods were abandoned due to the instability encountered when the behavior of typical light-weight wall elements was modeled using hourly time steps. As mentioned above, the implicit method the program uses is unconditionally stable.

To give the reader a better feel for the matrix equation (111), the elements of a typical sub-zone are shown in shorthand form. The sub-zone has three layers in the exterior wall, each containing two nodes (for a total of four wall nodes, since interface nodes are counted once). The floor is comprised of two layers. An "X" in the matrix represents one or more constant (non-zero) coefficient terms. For example, these are the same coefficient terms that are used to multiply the temperature terms in equations (108) and (109). The X's representing these coefficient terms appear in rows 6 and 8 of the matrices, respectively.

$$\begin{bmatrix} X & X & & & & & & & & \\ X & X & X & & & X & X & X & X & \\ & X & X & X & & & X & X & X & \\ & & X & X & X & & & & & \\ & & & X & X & X & & & & \\ & & & & X & X & & & & \\ & X & & & & & X & X & X & X \\ & X & X & & & & X & X & X & X \\ & X & X & & & & X & X & X & X \\ & X & X & & & & X & X & X & X \end{bmatrix} \times \begin{bmatrix} T'_{floor,bot} \\ T'_{floor,top} \\ T'_{wall,\ inside\ face} \\ T'_{wall,2} \\ T'_{wall,3} \\ T'_{wall,\ outside\ face} \\ T'_{window} \\ T'_{walls} \\ T'_{ceiling} \\ T'_{in} \end{bmatrix} =$$

$$\begin{bmatrix} X & X & & & & & & & & \\ X & X & X & & & X & X & X & X & \\ & X & X & X & & & X & X & X & \\ & & X & X & X & & & & & \\ & & & X & X & X & & & & \\ & & & & X & X & & & & \\ & & & & & & & & & \\ & & & & & & & & & \\ & & & & & & & & & \\ & & & & & & & & & \end{bmatrix} \times \begin{bmatrix} T_{floor,bot} \\ T_{floor,top} \\ T_{wall,\ inside\ face} \\ T_{wall,2} \\ T_{wall,3} \\ T_{wall,\ outside\ face} \\ T_{window} \\ T_{walls} \\ T_{ceiling} \\ T_{in} \end{bmatrix}$$

$$+ \begin{bmatrix} T_{below} \\ \text{Sun hitting floor} \\ \text{Sun hitting inside of wall} \\ - \\ - \\ T_{out},\ \text{Sun hitting outside of wall} \\ T_{out},\ \text{Sun absorbed by window} \\ \text{Sun hitting walls} \\ \text{Sun hitting ceiling, } T_{above}, \text{ Sun hitting roof} \\ \text{Infiltration, Slab perimeter losses, Neighbors, Internal gains} \end{bmatrix}$$

(112)

For even this simple sub-zone, with a small number of nodes used to describe the floor and walls, ten simultaneous equations must be solved. Since the time required to obtain the solution scales as the number of equations to the third power [29], it is of vital importance to minimize the number of temperature nodes in the model. It is for this reason that the "major" simplifications of the exterior wall and floor layers were introduced in sections D.2 and E.2.

Time constraints were also the principal motivation behind the division of the zone into sub-zones. If a single rectangular zone were to be considered as one space, the total number of equations to solve simultaneously (assuming the same number of nodes in the exterior walls and floor) would be 24: 4 for the windows, 2 for the floor, 16 for the walls, 1 for the air, and 1 for the ceiling. Because of the cubic dependence of calculation time on the number of equations, it is much faster to complete four simultaneous solutions of 10 equations than one single simultaneous solution of 24 equations.[45]

P. Control of Sub-Zone Temperatures and the Determination of Heat and Cooling Loads

The control mechanism used to maintain the sub-zone temperature within a specified range is very closely linked to the determination of building energy usage. Details of the program's approach will be described in this section.

Since the program explicitly allows for the use of thermal mass in the building, it was decided that the room temperature should be allowed to float within a specified range. Were the temperature maintained at a constant value, the usefulness of thermal storage would be compromised. This range is specified by the user. Heating and cooling seasons are also specified by the user. During the heating season, the home can accrue no cooling load and

[45] All other things being equal, the single simultaneous solution of 24 equations would take about 3.5 times longer than the four simultaneous solutions of 10 equations. The complexity of determining window->window view factors in a single space also contributed to the decision to break the room into sub-zones, as did the fact that the interior of a real building is almost always divided into rooms.

during the cooling season, no heat load can be accrued. The rationale for this decision was that homeowners are unlikely to use their heating or cooling system out of season. They are more likely to open up the house to warm it up in the summer or to enjoy the free cooling than to turn on the furnace.

1. Standard Procedure

For the sake of brevity, only the procedure for calculating the heat load will be discussed in detail. The method for calculating the sensible cooling load is completely analogous. The procedure will be described in example form. For this example, assume that the user-specified allowable inside air temperature range is 20-25°C. The example is illustrated in **Figure 20.**

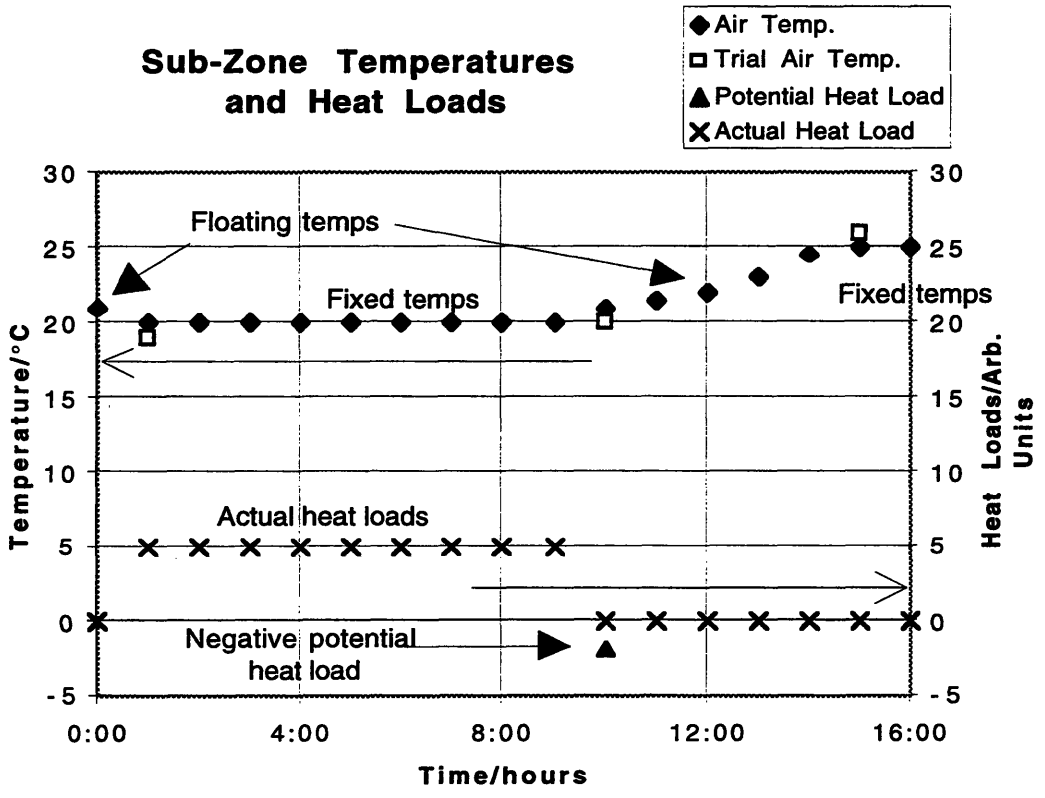

Figure 20. Example temperature and heat load histories

The year begins at 12:00 a.m. January 1. Initial temperature values are estimated for this time assuming steady-state heat transfer conditions between the room air and the outside. For illustration purposes, assume that the initial inside air temperature is 21°C. Given this vector of node temperatures, **T**, node temperatures are calculated for 1:00 a.m., **T'**.

The 1:00 a.m. air temperature value is queried. Since there are no external heat gains to the sub-zone on a winter night and the heating system is not on, the air temperature has dropped to 19°C. Since the temperature is below the minimum temperature setpoint, this change is not allowed by the program. The program backs up to original 12 a.m. temperatures and calculates new 1 a.m. sub-zone temperatures assuming that the air is maintained at 20°C by the heating system.

Given the revised 1:00 a.m. temperatures, the rate at which heat is being transferred from the sub-zone air is calculated. Convection heat transfer to all internal surfaces as well as infiltration and perimeter slab losses and internal gains are included. This rate is multiplied by the 3600 seconds in an hour to yield a *potential* heat load in Joules for the period between 12 and 1 a.m. Provided that there is a net heat loss from the 20°C air, this *potential* heat load is considered to be the *actual* heat load, or the amount of heat that must be supplied in order to maintain the air temperature at 20°C.[46]

Assume that there are no significant heat gains into the sub-zone until 9 a.m., when the sunlight begins to warm up the space. 9 a.m. temperatures are used to calculate 10 a.m. temperatures, still assuming a fixed, 20°C air temperature. However, when the potential heat load is calculated for the 9-10 a.m. period, it is negative, due to the incoming solar radiation and the warmer outside air temperature. When this negative potential load is obtained, the program returns to the 9 a.m. sub-zone temperatures and recalculates 10 a.m. temperatures, this time allowing the air temperature to float unconstrained. The new 10 a.m. air temperature calculated is 21°C and there is no heat load for the 9-10 a.m. period.

The air temperature is allowed to float until it exceeds either endpoint of the specified range. Suppose that the amount of incoming solar radiation exceeds the ability of the thermal mass in the floor and exterior wall to store

---

[46] In other words, if there are net heat gains to the 20°C air, the *actual* heat load = 0.

the heat. Using 2 p.m. temperatures, a 3 p.m. air temperature of 26°C is calculated. A similar mechanism to the one described above is put into effect to keep the air temperature within the specified range. The program backs up to the 2 p.m. temperatures and calculates new 3 p.m. temperatures assuming that the air temperature is held fixed at 25°C.

As before, a potential heat load is calculated. If the potential load is negative (*i.e.*, the sub-zone air experiences a net heat gain), then it is assumed that the occupants will increase ventilation (by opening windows or doors) to maintain the 25°C temperature. No cooling load or heat load is assessed.

Suppose that the temperature is thus held fixed until 4 p.m. Using 4 p.m. sub-zone temperatures and a fixed 25°C air temperature, the 5 p.m. potential load is found to be positive. This load is not considered actual heat load, but rather serves to signal the program to revert to the original 4 p.m. temperatures and recalculate 5 p.m. sub-zone temperatures allowing the air temperature to float. The temperature then floats down through the evening hours until the next predicted air temperature falls below 20°C and the whole process begins again.

To summarize, the actual heat load is defined to be the amount of heat that must be supplied to the sub-zone air to maintain the air temperature at the minimum allowable value. No heat load accrues when the air temperature floats above the minimum setpoint. The analogous definition and procedure hold for the calculation of cooling loads. In that case, cooling loads accrue only when the air temperature is at the maximum allowable value and there is a net heat gain to the sub-zone air that must be removed by cooling. Heat loads and cooling loads are calculated independently for the various sub-zones. The loads are combined at year-end to obtain overall zone, or building, loads.

The method used for calculating the latent cooling load is analogous to the degree-day method used for calculating sensible loads. For every hour that the outside humidity ratio, W_{out}, exceeds the inside humidity ratio setpoint (currently $W_{in,\,setpoint} = 0.008$ kg vapor/kg dry air), the sensible load is given by:

$$\text{Latent Load (Joules)} = 3600 \frac{h_{infiltration} ACH}{c_{p,air}} \left(W_{out} - W_{in,setpoint} \right) \Delta h_{evaporation} \qquad (113)$$

where the quotient before the parentheses is equivalent to the mass flow rate of air into the sub-zone in kg/s. $\Delta h_{evaporation}$ is the enthalpy of evaporation evaluated at the midpoint of the allowed temperature range, expressed in J/kg vapor. The annual latent load is equal to the sum of all hourly loads. Note that the latent cooling load is calculated entirely independently of the sensible cooling load.

2. Accelerated Procedure

An accelerated method for calculating annual sensible heat and cooling loads has been built into the program. The manner in which heat and cooling loads are calculated at any given time is identical to that described above. However, in the accelerated version, the sub-zone's boundary conditions are average conditions that do not reflect the day-to-day variation present in the actual weather data. The actual weather data from each month are reduced to form an average day for that month. For example, the 1 a.m. temperature on the average January day is equal to the average of all 1 a.m. temperatures recorded in January. The solar radiation data is also averaged in the same manner.

The accelerated load calculations are performed as follows:

The program calculates the full zone's expected heat load for the average January day by combining the daily loads from all sub-zones. Using the sub-zone temperatures calculated for the end of this average day as new initial temperatures, the program recalculates the heat load for the same average day. This process continues until the difference between the most

recent daily heat load calculation and the penultimate daily heat load calculation falls below a specified tolerance level, such as 0.5% of the zone's total daily heat load. Once the tolerance level has been satisfied, heat load calculations for the month of January are complete: the monthly heat load is simply the most recent daily heat load multiplied by the number of days in the month.

The program advances to February and the procedure is repeated. In this way, the heat load or the cooling load is calculated for each month of the year. As will be seen in a later section, the acceleration resulting from the use of this technique is dramatic, especially for light-construction buildings.

At this point, provisions have not been made for calculating the latent cooling load using the accelerated procedure.

III. Demonstration of Simulation Results

The remaining chapters of this document are devoted to the study of the performance of the building energy simulation program described in the last chapter as well as its sensitivity to a wide variety of input parameters. This chapter will set the stage for the following three chapters. The particular buildings and building sites to be studied will be introduced in section A. Simulation results from these base-case buildings will be presented in section B.

A. Site and Building Descriptions

Two sites were selected to investigate the performance of the program: Boston, Massachusetts and Phoenix, Arizona. Heat loads dominate annual energy requirements for residential buildings in Boston, while cooling loads dominate the annual energy requirements in Phoenix. **Table 3** summarizes site statistics for the two building locations.

Site	Latitude	Longitude	Mean Annual Max. Temperature	Mean Annual Min. Temperature	Heating Degree Days (base 20°C)	Cooling Degree Days (base 27°C)
Boston, MA	42° 22' N	71° 2' W	35.4 °C	-17.6 °C	3784.7 °C-days	22.4 °C-days
Phoenix, AZ	33° 26' N	112° 1' W	46.0 °C	-1.4 °C	1093.1 °C-days	803.9 °C-days

Table 3. Selected site statistics[47]

Since the degree-days measure does not incorporate the effect of solar radiation, the importance of cooling in both locations is significantly understated by this measure. The importance of heating in Phoenix is likewise overstated by this measure. The temperature extremes given above and simulation results shown in section B better illustrate the relative importance of heating and cooling in the two locations.

[47] Degree-day calculations were performed with TMY2 weather data, while ASHRAE Fundamentals (Chapter 26) provided the annual mean temperatures. The heating degree days were calculated using 20°C as the base temperature, while the cooling degree days were calculated using 27°C.

A lightweight and a thermally massive home were selected for use in this study. The two simple, rectangular buildings have identical footprints, volumes and orientations, and differ only in composition. A summary of building attributes follows in **Table 4** and **Table 5**.

Features Common to Both Buildings		
Footprint size	92.9	m^2
Volume	254.85	m^3
Widths of South and North faces	11.8	m
Widths of East and West faces	7.87	m
Height of Exterior Walls	2.74	m
Temperature Setpoints		
Minimum	20	°C
Maximum	27	°C
Infiltration/Natural Ventilation		
Air change rate	0.5	ACH
Nat'l ventilation air change rate	0.5	ACH
Air density	1.2	kg/m^3
Air specific heat	1000	J/kg°C
Δh evaporation	2554200	J/kg vapor
Convection Coefficients		
h_in	3.08	W/m^2°C
h_floor	4.04	W/m^2°C
h_ceiling	0.95	W/m^2°C
h_out	34	W/m^2°C
Solar Absorptivities		
Outside surface of exterior wall	0.26	
Roof surface	0.5	
Interior surfaces of all walls	0.26	
Floor surface	0.7	
%Sun->floor	50%	
IR Emissivities		
Floor surface	0.94	
Glazing	0.93	
Interior surfaces of all walls	0.9	
Ground Reflectance	0.2	
Glazing		
Double-pane, wood frame	U = 2.6	W/m^2°C
Area (percentage of each exterior wall area)	20%	
Shading Coefficient	0.90	
Window node location	0.50	
Ceiling		
R-value, excluding films	R = 3.81	m^2°C/W
Floor Slab (insulated)		
Perimeter loss coefficient	F = 0.86	W/m°C

Table 4. Summary of building dimensions and parameters

Features of the Lightweight Building					
Exterior Wall Composition	2x6 wood frame				
	Layer thickness	Density	Specific Heat	Thermal Conductivity	Layer R-value
(interior layer first)	m	kg/m^3	J/kg°C	W/m°C	m^2°C/W
Gypsum Wall Board (0.5")	0.0127	1249	1089	0.160	0.079
Fiberglass (80% of layer)	0.1397	32	837	0.043	
Wood Stud (20% of layer)	0.1397	433	2387	0.109	2.475
Sheathing	0.033	160	837	0.055	0.596
				Total R Value	3.150
Floor					
Concrete slab on grade (3")	0.0762	2243	837	1.731	
Features of the Massive Building					
Exterior Wall Composition	Concrete masonry wall				
	Layer thickness	Density	Specific Heat	Thermal Conductivity	Layer R-value
(interior layer first)	m	kg/m^3	J/kg°C	W/m°C	m^2°C/W
Gypsum Wall Board (0.5")	0.0127	1249	1089	0.160	0.079
Block (8")	0.2032	1842	837	0.796	0.255
Extruded Foam (3")	0.0762	40	1214	0.029	2.590
Sheathing (0.5")	0.0127	160	837	0.055	0.229
				Total R Value	3.154
Floor					
Concrete slab on grade (6")	0.1524	2243	837	1.731	

Table 5. Lightweight and massive building properties

As can be seen in the tables above, the two buildings are very similar. They differ almost exclusively in the amount of thermal mass used in construction. In order to isolate the effect of the thermal mass on building energy usage, the wall R-values for the two building types were made identical. The sheathing thickness in the lightweight construction was altered to make this possible.

Two nodes were used in each wall layer, while a single node was used in the floor. Justification for this choice follows in Chapter V.

The heating season used to generate the sample results is October 1 to May 31 for Boston and December 1 to February 28 for Phoenix.

B. Sample Simulation Results

Using the parameters outlined in the last section, hourly simulations were run for the entire year (all 365 days) for the lightweight and massive buildings at both sites. Shown in the following figures are the buildings' annual sensible loads as well as the loads for the individual sub-zones: South,

North, East and West. Calculations for the lightweight buildings required about 67 seconds of computation time on a 180 MHz Power Macintosh 8500, while the massive buildings required about 76 seconds (due to the additional wall node).

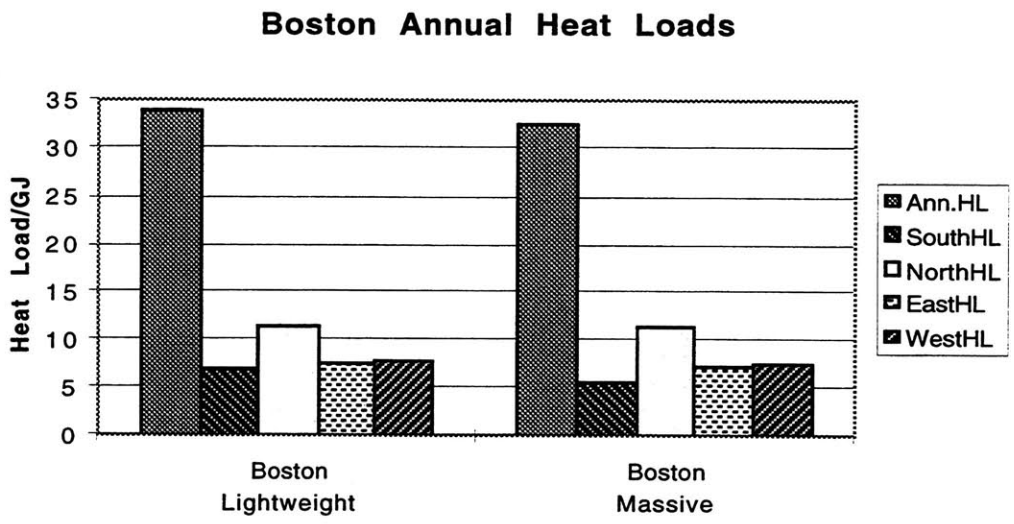

Figure 21. Boston annual heat loads

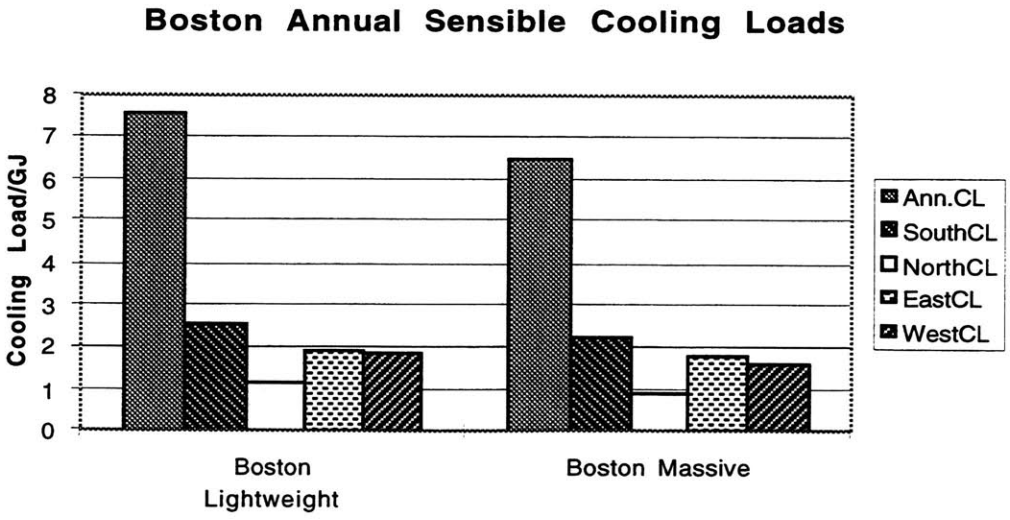

Figure 22. Boston annual sensible cooling loads

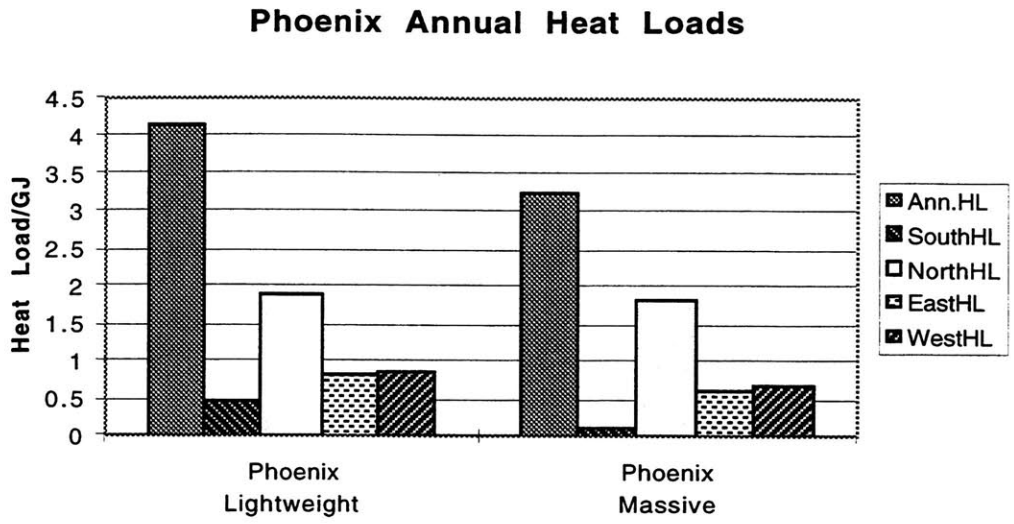

Figure 23. Phoenix annual heat loads

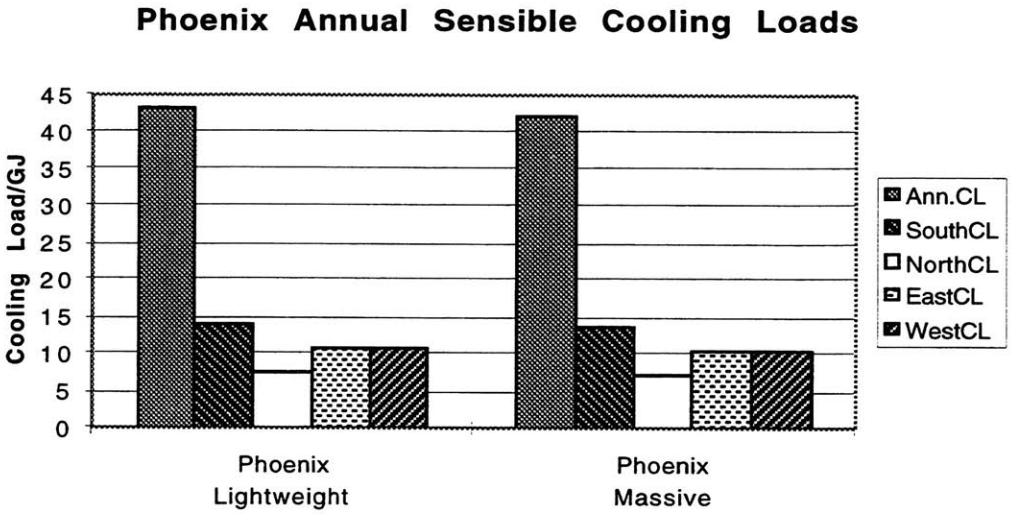

Figure 24. Phoenix annual sensible cooling loads

As shown in these figures, the Phoenix cooling load and the Boston heat load do indeed dominate the overall energy requirements for both building types. As expected, the heat load in the South-facing sub-zone is the smallest of all sub-zones, while that in the North is greatest. The loads in the East and West fall between the North and South extremes. The opposite case is

true for sensible cooling loads: the South-facing sub-zone has the largest cooling load, while the North-facing sub-zone has the smallest.

With this particular set of parameters, the additional thermal mass in the massive building provides less than 5% reduction of the dominant loads in each climate experienced by the lightweight buildings. As window area is increased, or natural ventilation introduced, the impact of the thermal mass on heat and cooling loads will be evident. These changes will explored later in this section.

Before investigating further the role of the thermal mass, the impact of the different building components on annual loads will be examined. Shown below in **Table 6** are annual heat gain contributions from each component in the building model in direct thermal contact with the interior air. The only component not formally introduced in the preceding chapter is the Exhaust. When the interior space overheats in the heating season, it is assumed that the occupants will open windows to satisfy the space's cooling load. When such a cooling load is incurred in the heating season, this load is called the Exhaust Load for the heating season. Conversely, if a heat load is incurred in the cooling season, this load is called the Exhaust Load for the cooling season.

The sign convention used for the load contributions is positive for heat gain to the room air and negative for heat loss from the room air. Since the behavior of the massive and lightweight buildings does not differ greatly, the results for massive buildings alone are shown. The sum of all heat load (cooling load) components yields the actual annual heat load (cooling load).

Some explanation is required to interpret the following two tables. **Table 6** shows the contributions to air heat gain during the heating season, while **Table 7** shows the contributions to air heat gain during the cooling season. The sum of the absolute value of each gain was found to obtain a measure of overall gain contributions. The "Source Contribution" columns represent the ratio of the individual source heat gains to the overall sum for each location. In **Table 6**, the most important heat loss contributor in Phoenix, infiltration, shows the largest negative percentage in the "Source Contribution" column. Likewise, the floor shows the largest positive percentage, representing the largest heat gain contribution.

Internal surfaces, such as the floor, ceiling and interior walls may be described as sources of heat gain since their surface temperatures sometimes exceed the air temperature. This may occur due to the absorption of solar radiation. When the temperatures of the internal surfaces fall below that of the air, then the heat gains associated with those surfaces become negative.

	Phoenix		Boston	
Gain Source	Heat Gain	Source Contribution	Heat Gain	Source Contribution
	GJ		GJ	
Window	-1.217	-9%	-5.460	-15%
Exterior Wall	0.526	4%	-2.137	-6%
Floor	2.518	19%	2.232	6%
Infiltration	-3.264	-25%	-13.814	-38%
Floor Slab Perimeter	-2.624	-20%	-10.999	-30%
Interior Walls	1.645	13%	-0.853	-2%
Ceiling	0.218	2%	-0.993	-3%
Adjacent Sub-zone	-0.001	0%	-0.001	0%
Exhaust	-1.073	-8%	-0.337	-1%

Table 6. Heating season heat gain contributions

It is clear from **Table 6** that infiltration and slab perimeter losses dominate the heat load in both Boston and Phoenix. Window losses follow in importance. The only significant heat gains to the air are from the floor in Boston and from the floor and interior walls in Phoenix. The relative importance of the floor contribution in Phoenix exceeds that in Boston as a consequence of the larger amount of solar radiation available in Phoenix. The large amount of exhaust shown for the Phoenix building indicates that a significant amount of overheating occurred in the defined heating season. Shortening the heating season would reduce this overheating. It is interesting to note that the two largest contributors to the annual heat losses in both locations also have considerable uncertainty associated with them.

	Phoenix		Boston	
Gain Source	Heat Gain	Source Contribution	Heat Gain	Source Contribution
	GJ		GJ	
Window	0.481	1%	-0.843	-5%
Exterior Wall	7.879	18%	1.937	11%
Floor	15.816	36%	5.044	29%
Infiltration	-0.447	-1%	-2.627	-15%
Floor Slab Perimeter	-0.346	-1%	-2.083	-12%
Interior Walls	14.764	34%	4.175	24%
Ceiling	3.668	8%	0.895	5%
Adjacent Sub-zone	0.001	0%	0.001	0%
Exhaust	0.121	0%	0.000	0%

Table 7. Cooling season heat gain contributions

Table 7 reveals that the most important cooling season heat gain contributors in Boston are the floor, interior walls, exterior wall and ceiling, in that order. Heat loss contributors are, in order of importance: infiltration, perimeter losses and window losses. In Phoenix, there are no significant heat loss contributors. In order of importance, cooling season heat gain contributions for the Phoenix building arise from the floor, interior walls, exterior wall and ceiling.

The importance of thermal mass becomes apparent when the amount of glazing in the exterior walls is increased. **Figure 25** shows how the heat load in Boston is affected by changes in the percentage of gross exterior wall area devoted to glazing (on all four exterior walls). The massive building is better able to store the increased amounts of incoming solar radiation for later use than the lightweight building. Consequently, its heat load is lower than that of the lightweight building. Its minimum load is reached when about 30% of the gross exterior wall area is glazed. At this point, heat losses through the increasing window area begin to outweigh the benefit of the increased solar radiation entering the space. Use of additional thermal mass for storage of solar energy shifts the location of the minimum load to a higher glazing percentage.

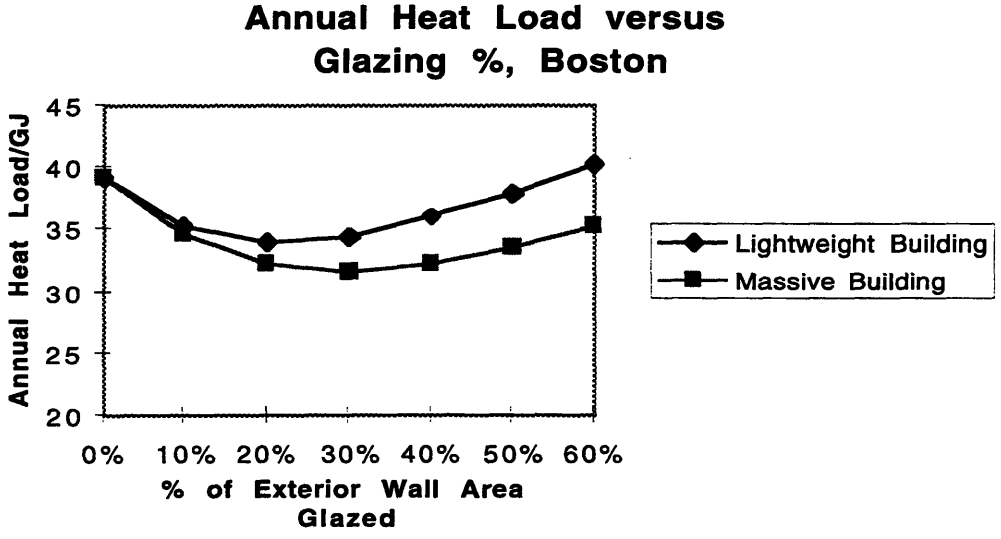

Figure 25. Annual heat load in Boston as a function of glazing % on all four exterior walls

The impact of thermal mass is also apparent in the cooling season when natural ventilation is implemented as a cooling strategy. As described in Chapter II, natural ventilation is introduced in the cooling season when the exterior air temperature falls below the maximum temperature setpoint of the interior air. Most often, this free cooling is available during the night. The more mass in the building, the better the coolness from the night air can be stored for use on the following day and the lower the sensible cooling load becomes. The cooling season in Phoenix is used to illustrate this point in the following figure. Note that if fans are used to increase the rate of ventilation, increased electricity usage should be considered.

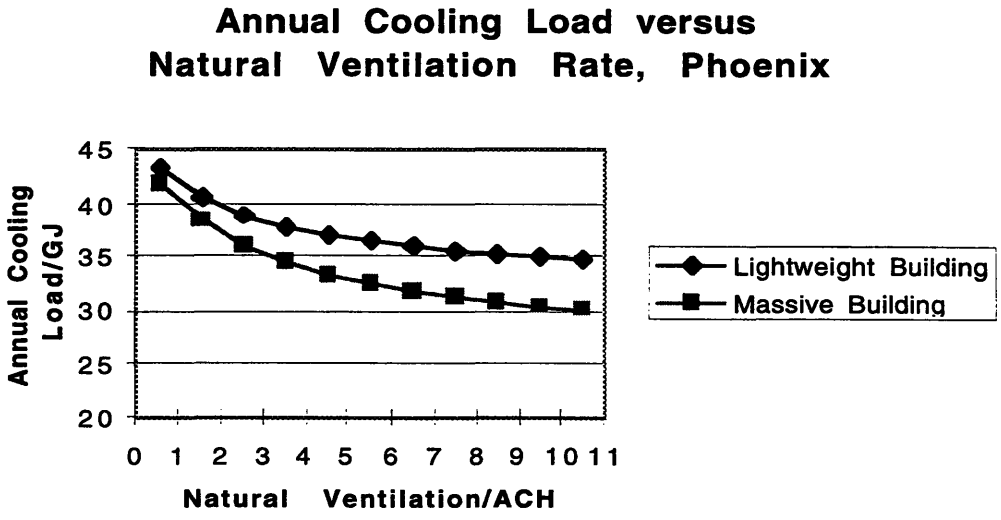

Figure 26. Annual cooling load dependence on rate of natural ventilation in Phoenix

IV. Impact Study of Input Uncertainties

As discussed in Chapter II, there exists a substantial number of uncertainties associated with parameter inputs to the building simulation program. These inputs include weather data, convection and radiation heat transfer coefficients and material properties.

For each program input, a rough estimate was made of a reasonable uncertainty band. The program then performed a set of annual energy calculations, stepping the parameter of interest through the prescribed uncertainty band to determine the resulting impact on annual sensible heat and cooling loads. Unless specifically noted otherwise, all cooling loads are sensible cooling loads.

This study was performed using both lightweight and massive buildings at the Boston site. The sections of this chapter will loosely follow the order in which building model components were introduced and described in Chapter II. The format of the chapter sub-sections will consist of presentations of the parametric studies in graphical form followed by a discussion of the results. At the end of the chapter, results will be summarized and discussed.

Shown in each figure is the percent deviation from the base loads as a function of a single input parameter. (Base loads are the loads calculated using the building data shown in **Table 4** and **Table 5**.) The base loads for the Boston buildings are given here for reference:

Lightweight Heat Load = 33.87 GJ
Lightweight Sensible Cooling Load = 7.57 GJ
Massive Heat Load = 32.36 GJ
Massive Sensible Cooling Load = 6.50 GJ
Latent Cooling Load = 1.033 GJ (lightweight and massive)

(114)

The abscissa in the charts below is either the model parameter of interest, a fixed adjustment to the parameter of interest, or a multiplier of the base-case parameter. For example, if the effect of an uncertainty band of ±50% for a particular parameter is to be studied, the multiplier in the

abscissa will range from 0.5 to 1.5. The value of the parameter used by the program is equal to the product of the base-case parameter and the multiplier.

A. Temperature and Solar Radiation Data

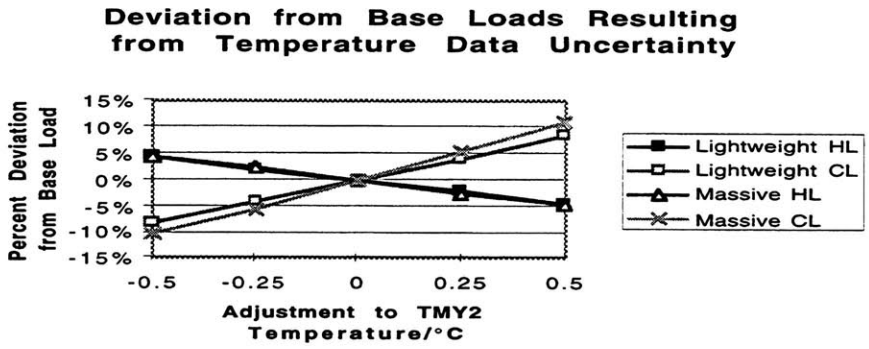

Figure 27. Effect of outside temperature data uncertainty

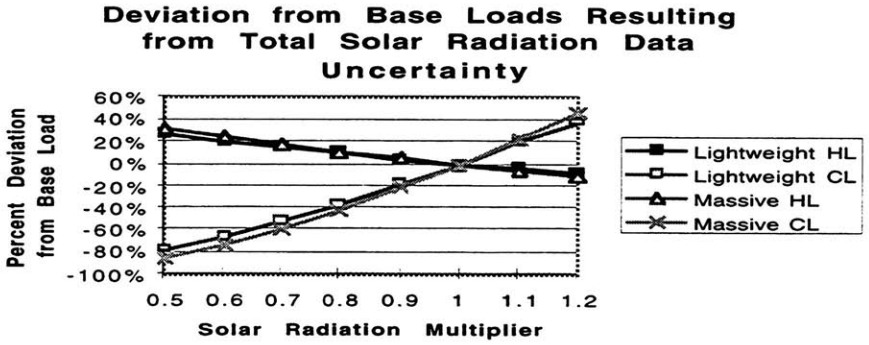

Figure 28. Effect of uncertainty in total solar radiation

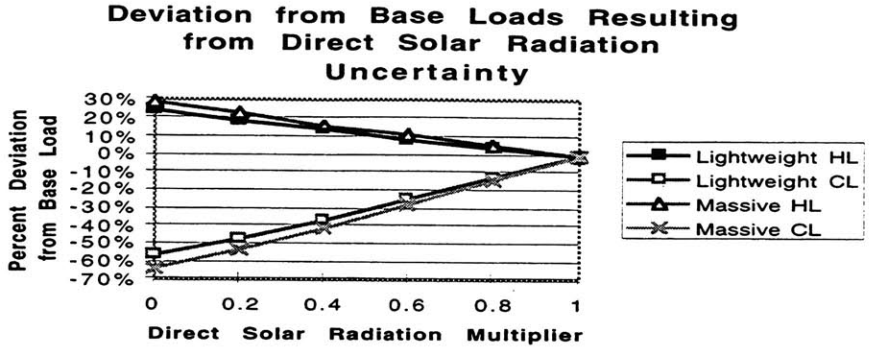

Figure 29. Effect of direct solar radiation uncertainty

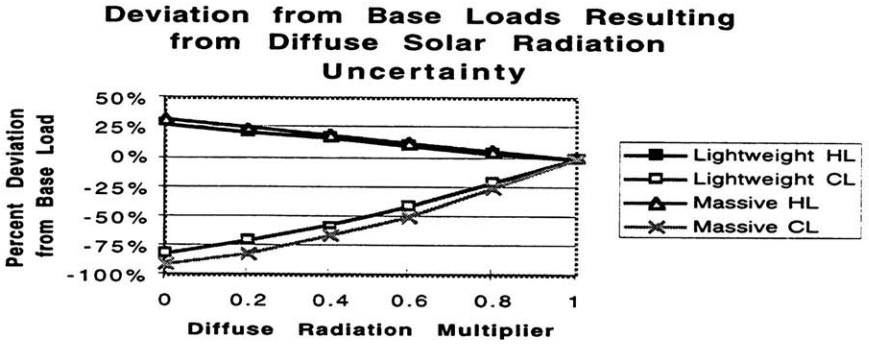

Figure 30. Effect of diffuse radiation uncertainty

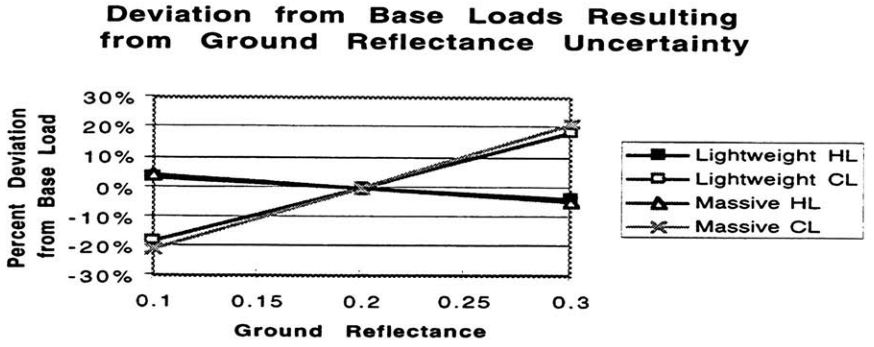

Figure 31. Effect of ground reflectance uncertainty

As can be seen in the preceding figures, uncertainty in the weather data can have a major impact on the calculated annual heat and cooling loads. A

conservative ±0.25°C estimate of temperature error leads to uncertainties in heat and cooling loads of ±2.5 and ±5% respectively.

The impact of uncertainty in the solar radiation data is even more dramatic. As described in Chapter II, the uncertainty in the TMY2 solar radiation data is ±13%. Even using a ±10% uncertainty band for total solar radiation, Boston heat loads vary by ±5% and the cooling loads by ±20%. If shading by vegetation and other buildings is considered to decrease overall radiation by 50%, then heat loads rise 30% and cooling loads drop 80%. Detailed information about site shading may not be available at the early design stages. Neglect of this information can lead to sizable errors in predicted energy use.

Figure 29 shows the effect of reducing the direct radiation incident on the building. Again, the effect is dramatic. It is interesting to compare the importance of direct and diffuse radiation. **Figure 30** is included for this purpose. For these buildings, diffuse radiation has a much greater impact on building energy usage than direct radiation. This arises due to the fact that all faces of the building receive diffuse radiation throughout the day, while direct radiation, although more intense, strikes each surface for a limited number of hours. The total annual diffuse radiation striking the four walls of the building comprises 58% of the total radiation striking the building walls. Only the South-facing wall receives more direct than diffuse radiation on an annual basis.

Note that if the direct and diffuse radiation are eliminated individually, the annual cooling loads decrease by about 60 and 85%, respectively, from the base-case values. The fact that the sum of these percentage reductions exceeds 100% indicates that cooling loads are not linear functions of incident solar energy. Consider an example where the direct and diffuse solar radiation are initially eliminated. A certain amount of diffuse (or direct) radiation may be re-introduced before any cooling load is incurred. Up to that point, sub-zone heat losses to the environment via infiltration, conduction through the window and exterior walls, *etc.*, exceed the gains from the small amount of diffuse (direct) radiation.

Also shown in this section is **Figure 31**, which shows the impact of the value used for the ground reflectance. It is included since this parameter plays a role in determining the amount of reflected radiation striking building

walls. The ground reflectance impacts the annual loads significantly: changes of ±50% relative to the base-case reflectance value correspond to ±5% deviations from the base annual heat load and ±20% deviations from the base annual cooling load.

B. Exterior Wall

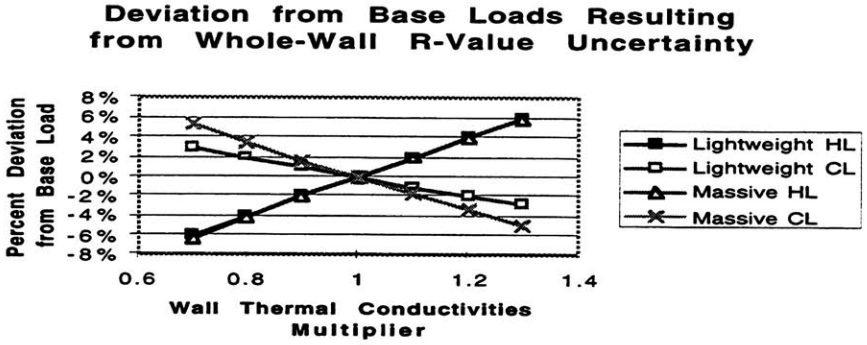

Figure 32. Effect of thermal conductivity of all wall layers

The preceding figure was generated by multiplying the thermal conductivity of every wall layer by the factor indicated in the abscissa.

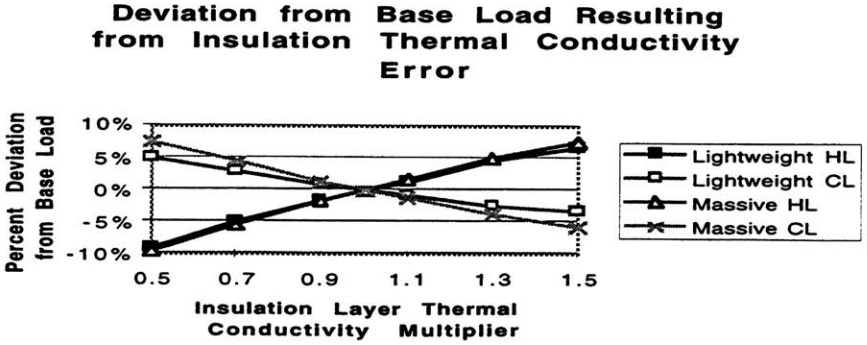

Figure 33. Effect of thermal conductivity of the insulation layer

In **Figure 33**, for the massive wall, the independent variable is the multiplier of the thermal conductivity of the extruded foam. For the

lightweight wall, it is the multiplier of the effective thermal conductivity of the entire insulation/stud layer that is varied.

The thermal mass of the gypsum wall board in both lightweight and massive buildings was varied by ±50%. In neither case did this change impact the annual loads by more than 1%.

Changing the thermal mass of the concrete blocks in the massive building by ±50% affected the annual loads by less than 1.5%.

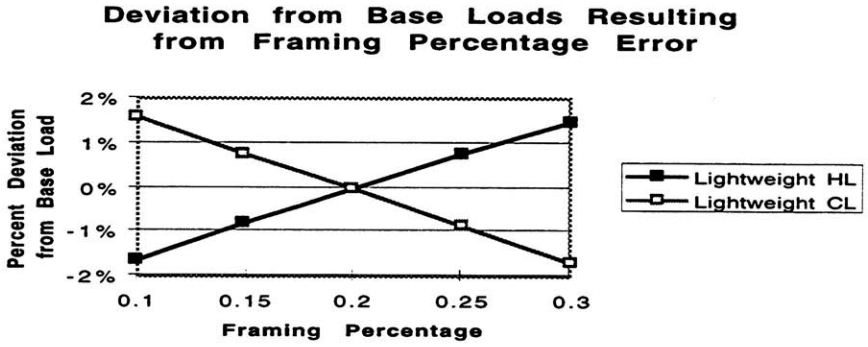

Figure 34. Effect of framing percentage in wood-frame wall

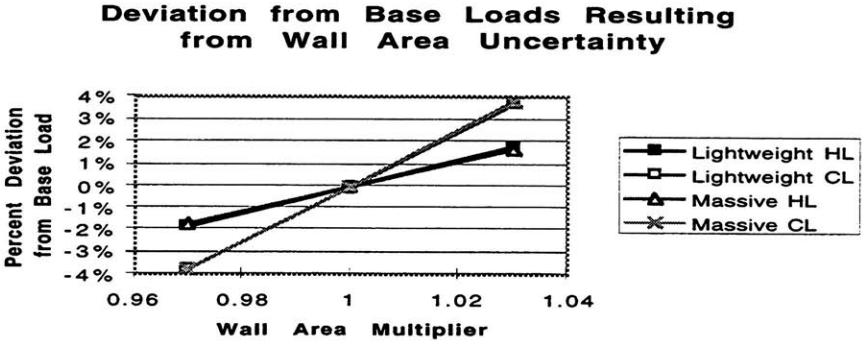

Figure 35. Effect of gross exterior wall area

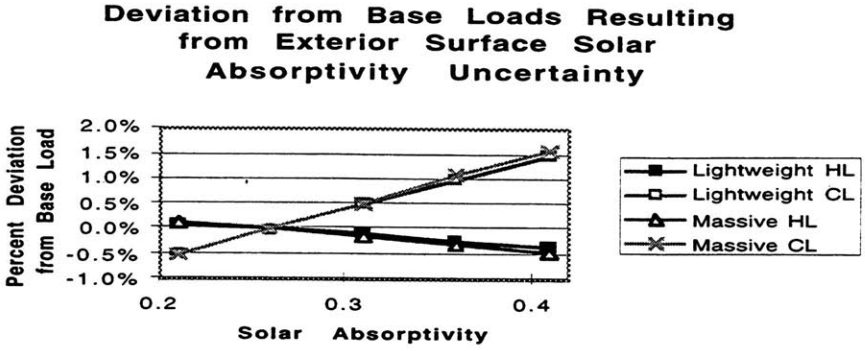

Figure 36. Effect of exterior wall surface solar absorptivity

Figure 32 explores the phenomenon reported by Christian and Kosny [9] regarding whole-wall versus clear-wall R-values. They reported that the whole-wall R-value was nearly 20% below the clear-wall value for a 2x6 wood-frame wall. An uncertainty band of ±20% corresponds to an overall uncertainty band on the order of ±4% for both heat and cooling loads.

Figure 33 shows that a ±50% uncertainty in the thermal conductivity of the insulation layer leads to roughly ±5-10% uncertainty in the annual loads. As discussed in Chapter II, such large uncertainties could be the consequence of improper accounting for moisture within the insulation, incorrect selection of the framing percentage, or selection of inappropriate material properties.

Use of 20% as the framing percentage for the wood-frame wall leads to less than 2% uncertainty in the annual loads. (The framing percentages required by Kuehn to match experimental R-values covered the range shown in **Figure 34**. See Chapter II.)

As shown by **Figure 35** and **Figure 36**, additional minor uncertainty in the overall loads results from uncertainties in the wall area used for calculations and the solar absorptivity of the exterior surface of the exterior wall.

C. Floor

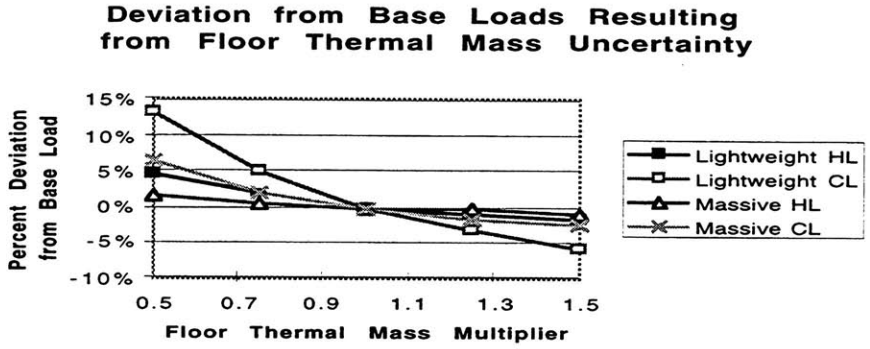

Figure 37. Effect of uncertainty in floor thermal mass

Altering the thermal conductivity of the floor slab by ±50% led to negligible changes in the annual loads (<±1%).

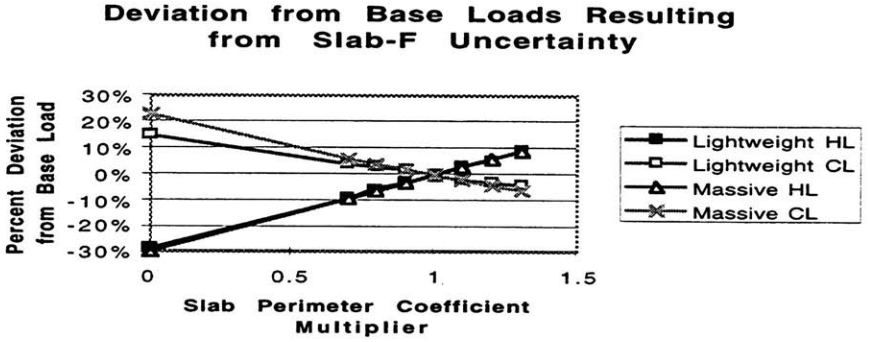

Figure 38. Effect of uncertainty in slab perimeter heat transfer coefficient, F

Figure 37 shows that, especially for the lightweight building, the thermal mass of the floor has a significant effect on the overall cooling load. Reduction of the base-case thermal mass by 50% leads to an increase of roughly 10% in the annual cooling load. Effects are more modest for the heat loads–on the order of ±2-5% deviation from the base loads for ±50% changes in the floor's thermal mass.

As **Figure 38** shows, a modest uncertainty band of ±30% in the floor perimeter heat transfer coefficient leads to an uncertainty band of ±10% for the heat and ±5% for the cooling loads. Ignoring the perimeter losses altogether (multiplier = 0) reduces heat loads by 30% and increases cooling loads by 20%.

D. Glazing

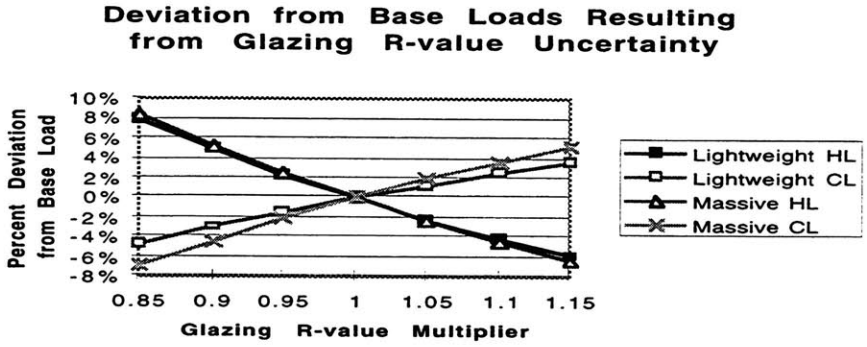

Figure 39. Effect of glazing R-value uncertainty

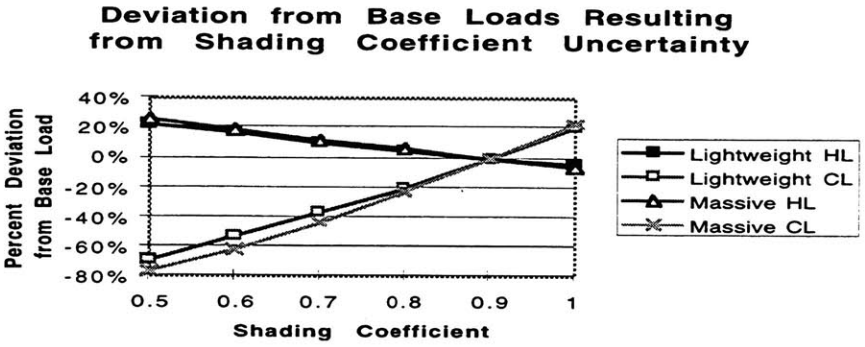

Figure 40. Effect of shading coefficient uncertainty

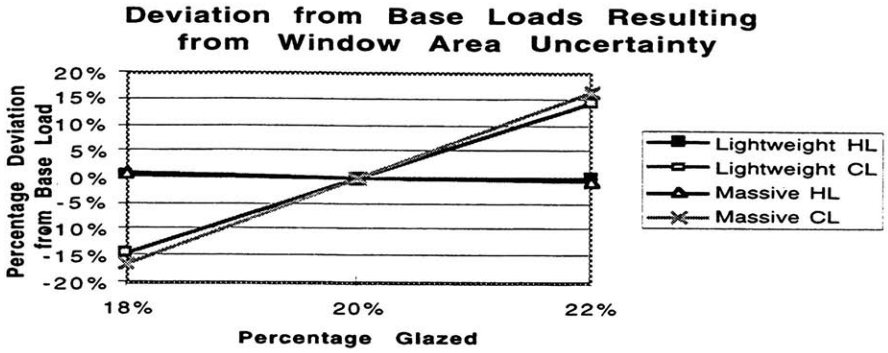

Figure 41. Effect of window area uncertainty

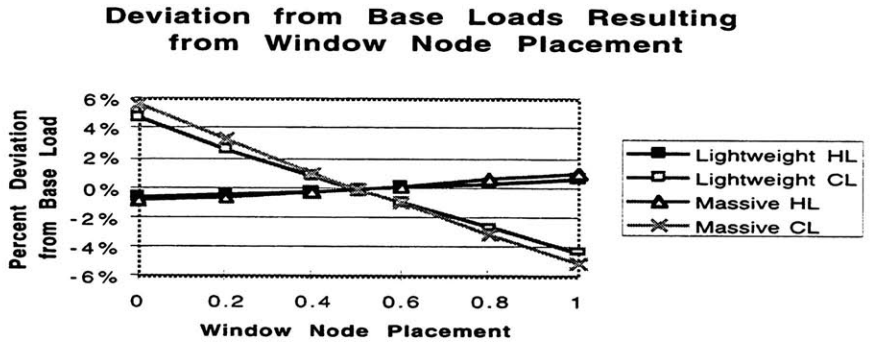

Figure 42. Effect of window node placement

Using a conservative estimate of ±10% uncertainty in the window R-value, **Figure 39** shows that the impact on annual load uncertainties is about ±4-5%.

The shading coefficient displays a more marked effect on annual loads. As shown in **Figure 40**, reducing the shading coefficient to 0.5 increases heat loads by about 20% and decreases cooling loads by about 70%. Such a decrease in the shading coefficient could be warranted by the presence of external shading due to trees or neighboring buildings, or by Venetian blinds on the inside of the window. If these effects are not considered during the early design phase (which may be a likely scenario) the predicted annual energy loads may be differ significantly from the actual loads.

Figure 41 shows the impact of a ±10% uncertainty in the base-case window area.[48] The percentage deviation is insignificant (<±1%) for the heat loads, although for the cooling loads, an uncertainty band of about ±15% is introduced. This large percentage corresponds to about ±1 GJ of annual cooling load.

As shown in **Figure 42**, the decision to locate the window node in the center of the glazing thermal resistance[49] introduces less than ±1% uncertainty into the heat load calculations and roughly ±5% uncertainty in the annual cooling load calculations. As expected, when the node is on the interior surface of the glass (position = 0), the absorbed solar radiation immediately adjacent to the conditioned space increases the cooling load and decreases the heat load. When the node is on the exterior surface of the glazing, the cooling load is reduced and the heat load increased.

E. Ceiling and Interior Walls

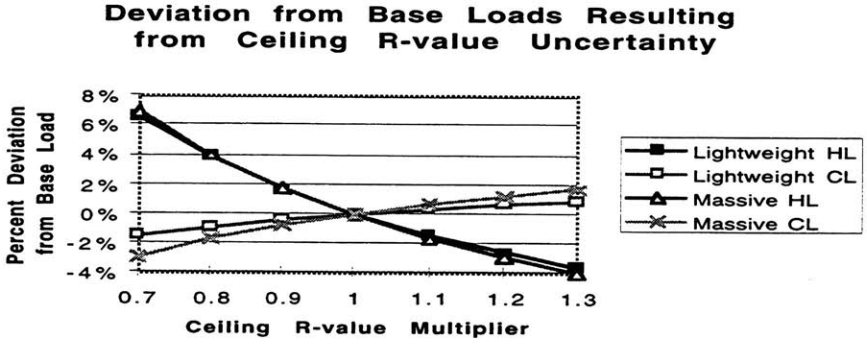

Figure 43. Effect of ceiling R-value uncertainty

[48] The base-case glazing area is 20% of the exterior wall area. Therefore, ±10% uncertainty corresponds to a range of 18 to 22% glazing of overall wall area.

[49] As described in Chapter II, this thermal resistance is the thermal resistance of the window when film effects are removed.

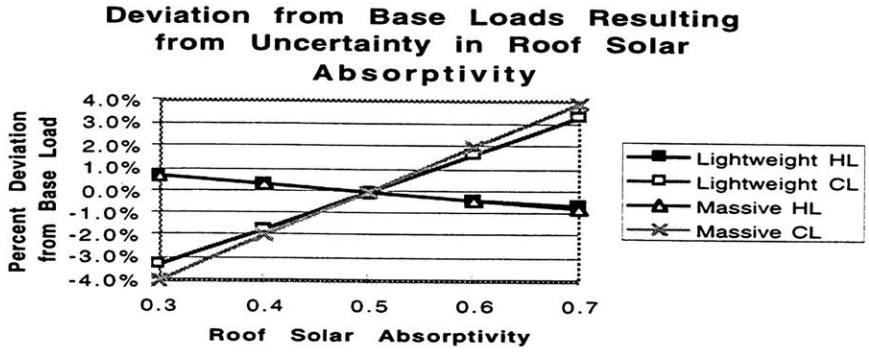

Figure 44. Effect of roof solar absorptivity uncertainty

Uncertainty in the thermal resistance of the ceiling significantly impacts the uncertainty in annual loads. Shown in **Figure 43** is a conservative estimate of the uncertainty of the ceiling R-value. Considering the problems involved in accurately specifying wall R-values, the uncertainty in the ceiling R-value may far exceed the range shown here. As shown in the figure, ±30% uncertainty in the R-value creates ±3-7% uncertainty in the predicted annual loads.

The impact of the solar absorptivity of the roof is shown in **Figure 44**, where it can be seen that the heat load is nearly unaffected by the choice of the coefficient. Estimated cooling load uncertainty as result of solar absorptivity uncertainty is ±3%.

The impact of an estimated ±50% uncertainty of inter-sub-zone U-values on the overall load calculations is negligible.

F. Infiltration

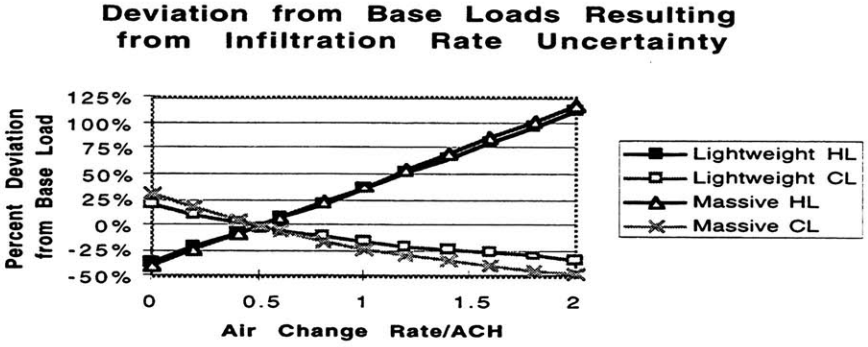

Figure 45. Effect of infiltration rate uncertainty

As discussed in Chapter II, there is a very substantial amount of uncertainty associated with infiltration. Since infiltration plays a major role in determining annual loads,[50] it contributes heavily to the overall uncertainty associated with the load calculations. **Figure 45** demonstrates the strong dependence of annual loads on the infiltration rate. The heat loads calculated for a medium-loose house, with an infiltration rate in the range of 0.5 to 1.0 ACH, may differ by as much as 40%, depending on what infiltration rates are specified. Even specifying the infiltration rate at 0.5 ± 0.3 ACH leads to an uncertainty in the calculated heat load of ±25%. The corresponding cooling load uncertainty is ±15%. Consideration of even larger uncertainties in the specified air change rate may be warranted. (See Chapter II.)

G. Long-Wave Radiation

The long-wave radiation emissivities of the different building surfaces were varied over the following ranges:

Glazing: 0.90 – 0.95
Floor: 0.88 – 0.96

[50] See Chapter III.B.

Walls and Ceiling: 0.88 – 0.92

These changes impacted annual loads negligibly.

The mean temperature used to form the radiation heat transfer coefficients was varied from 283 to 303 K. The resulting loads differed from the base-case loads (using T_{mean} = 293 K) by less than ±0.5%.

In order to assess the impact of any error associated with assuming that surface-to-surface radiation within the sub-zone occurs without reflection, all radiation heat transfer coefficients were simultaneously increased by 50%.[51] This change affected annual loads by less than 2% for both buildings.

H. Distribution of Sunlight within Sub-zone

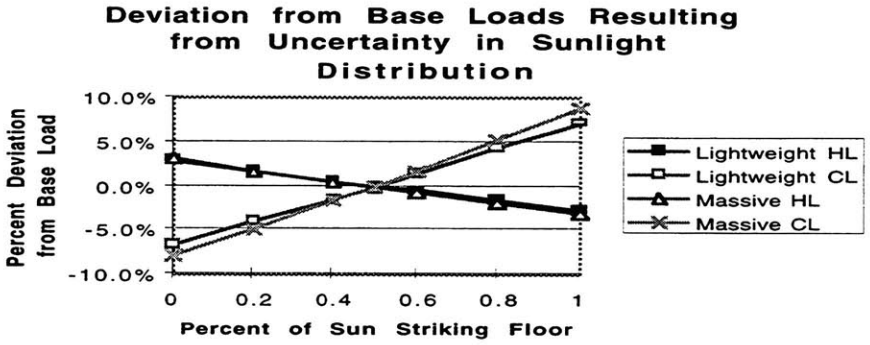

Figure 46. Effect of sunlight distribution uncertainty

As can be seen in **Figure 46**, the assumption that 50% of incoming sunlight strikes the floor first leads to errors of at most ±3% for the heat load and ±9% for the cooling load.

[51] Since reflection is ignored in the calculation of the radiation heat transfer coefficients described in Chapter II, the coefficients used in the model represent a lower-bound estimate. Hence the decision to probe the effect of increases in the coefficients.

Varying the solar absorptivity of the floor over the range [0.5 – 0.8] and of the inside wall surfaces over the range [0.2 – 0.4] affected predicted annual heat loads by less than 2% and annual cooling loads by less than 3%.

I. Convection Coefficients

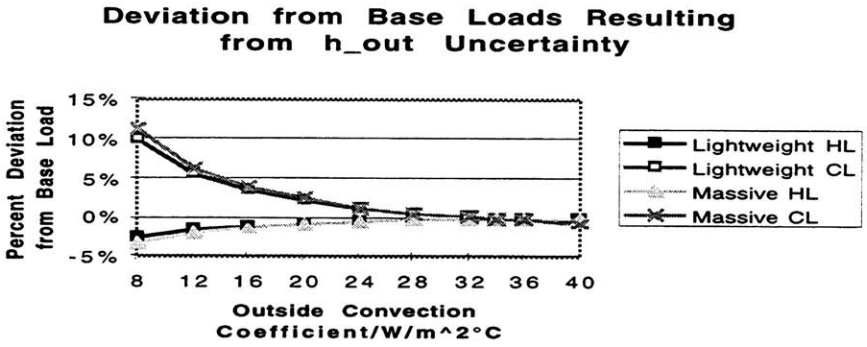

Figure 47. Effect of outside convection coefficient uncertainty

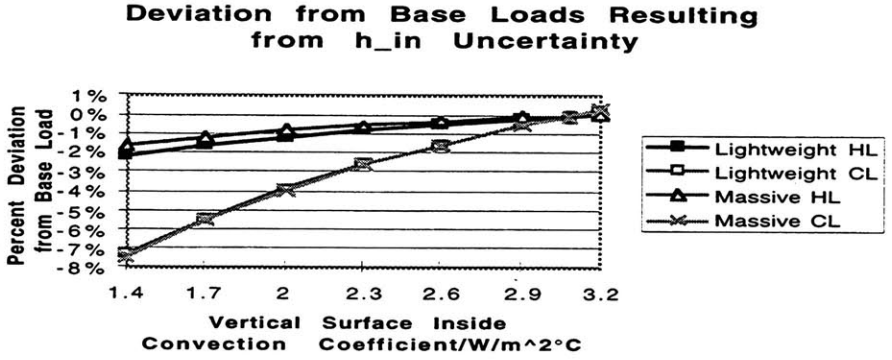

Figure 48. Effect of inside convection coefficient uncertainty

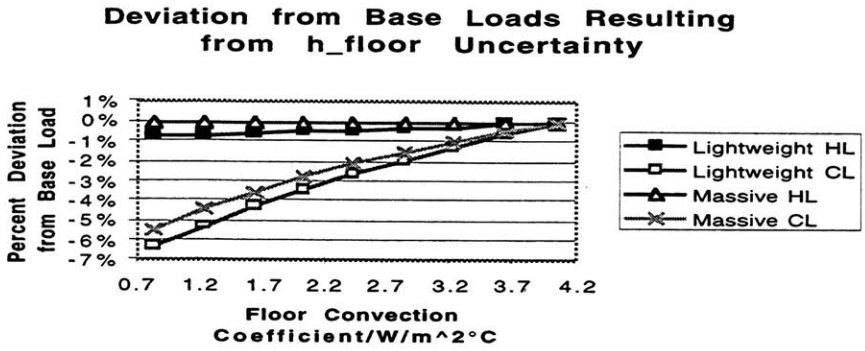

Figure 49. Effect of floor convection coefficient uncertainty

The exterior convection coefficient used in the program is that recommended by ASHRAE for winter conditions, 34 W/m²°C. If the coefficient for summer conditions, 22.7 W/m²°C, were used instead, the annual heat loads would be only 1% lower, while the annual cooling loads would be about 2% greater (see **Figure 47**). If the still-air value is used, 8.3 W/m²°C, then annual heat loads drop by about 3%, while cooling loads rise by about 10%. Since portions of a building may be well sheltered from the wind, and since windspeeds can be highly variable, it may be prudent to adopt the larger uncertainty bands associated with the outside convection coefficient (±3 and ±10%).

As shown in **Figure 48**, the maximum deviations from the base loads occur when the convection coefficient for laminar flow over a vertical surface is used. In this case, the annual heat loads are about 2% below the base heat loads and the annual cooling loads 7% below the base cooling loads. Since flow may be laminar at the inside wall surfaces [5], load uncertainties this large should be considered.

As can be seen in **Figure 49**, uncertainties in the floor convection heat transfer coefficient have little effect on the overall heat loads. The 5-6% decrease in the cooling load obtained when the lowest of convection coefficients is used amounts to an actual cooling load decrease of just 0.4 GJ.

Not pictured in this section are the predicted loads using ceiling convection heat transfer coefficients in the range 0.5 to 2.0 W/m²°C. Variation of $h_{ceiling}$ over this entire range led to overall deviations from the base loads of less than 2%.

J. Summary and Discussion of Uncertainties

Table 8 summarizes the uncertainties presented in the preceding nine sections.

Before attempting to draw conclusions about the overall uncertainty of the building simulation program, some clarifications regarding the information gathered in **Table 8** should be considered.

There are two principal types of inputs examined in this study: steady-state and time-dependent inputs. The descriptor steady-state implies that the value of the input is not affected by any time-varying environmental factors, such as windspeed or changing solar radiation. Material properties,[52] solar absorptivities and shading coefficients[53] are examples of steady-state inputs. The value chosen to represent the density of the concrete in the floor slab is of equal quality throughout the entire simulation. In other words, if the true density is 1800 kg/m^3, and 2000 kg/m^3 is input, then there exists a 10% error in this variable throughout the entire simulation.

The other kind of input varies with time. Examples include convection coefficients, which depend on instantaneous windspeeds, and solar radiation data. As mentioned above, the radiation data carries a ±13% uncertainty. This does not mean that 100% of the time the actual radiation might be 13% lower, for example. The error is generally time-dependent (barring systematic experimental error), sometimes positive, sometimes negative. Similarly, since the convection coefficients depend on instantaneous conditions, the actual convection coefficient may be at times higher and at times lower than the particular value chosen for use in the simulation.

Despite their different natures, these two types of inputs have been treated identically in the preceding sections. When attempting to determine how the uncertainty band associated with a particular input induces uncertainty in the overall loads, that particular input variable was given a series of constant values, each valid for the entire year simulated. Such an

---

[52] If changing moisture content and temperature dependence may be ignored.

[53] Of course, the solar absorptivity (and R-value) of the roof change with snow coverage, and the shading coefficient may change as leaves appear, grow, then fall from nearby deciduous trees.

approach is entirely reasonable for the steady-state inputs. However, for the time-dependent inputs, rigorous defense of the method is not possible.

The lack of promise of alternative approaches was the principal justification used for extending the treatment of the steady-state variables to the time-dependent ones. For example, the development and incorporation of a model linking the value of the external convection coefficient to instantaneous windspeed, wall surface temperature and air temperature necessarily introduces further uncertainties into the model, in addition to considerable complexity. Furthermore, it was not deemed appropriate to randomly vary the outside convection coefficient throughout the range of possible values on an hourly basis, especially since it was not clear what sort of distribution the randomly-selected values should form.[54]

Consequently, it should be kept in mind that uncertainty bands calculated for annual loads reflect an exaggerated impact of the uncertainty of the time-dependent inputs.

An additional point should be made about the uncertainties discussed here. Some variables, such as shading coefficients or solar absorptivities, are bounded on one side. Shading coefficients and solar absorptivities fall, by definition, between zero and one. The range of possible values for the shading coefficient cannot necessarily be centered about the value selected for use in the program. Specifically, the shading coefficient was set equal to 0.9. Its upper bound is 0.95 and lower bound is 0.5 (both estimated, the latter bound reflecting shading by neighboring buildings or vegetation). Use of the upper bound leads to an annual heat load prediction 2.7% lower than the base load, while use of the lower bound leads to an annual heat load 24.3% higher than the base load. For simplicity, the load uncertainty band associated with the shading coefficient is given in **Table 8** in terms of the magnitude of the larger deviation, *i.e.*, ±24.3%, rather than the more precise +24.3%/–2.7%.

Finally, these uncertainties were determined for two particular buildings at the Boston site. It turned out that the performance of these two buildings was very similar–only in certain circumstances did the additional thermal mass in the massive building significantly impact the predicted percentage deviations from the base annual loads. What has been attempted in this study has been to develop a sense of the possible uncertainties

[54] *e.g.*, top-hat, or Gaussian.

associated with building energy simulation programs, not a firm uncertainty band that may be applied to all buildings in all locations. Therefore, caution is advised when applying particular details of this information to other buildings.

Model Input	Heating Uncertainty	Cooling Uncertainty	Heating "Extreme" Case	Cooling "Extreme" Case
Temperature	3%	5%		
Total Radiation	5%	20%	30%	80%
Direct Radiation	10%	35%	25%	60%
Diffuse Radiation	15%	55%	30%	86%
Ground Reflectance	5%	20%		
Whole-Wall R-value	4%	4%		
Insulation Layer k	10%	6%		
Thermal Mass GWB	<1%	<1%		
Thermal Mass Concrete	<1.5%	<1.5%		
Framing Percentage	<2%	<2%		
Wall Area	2%	4%		
Solar Absorptivity	<0.5%	<1.5%		
Thermal Mass of Floor	4%	10%		
Floor k	<0.5%	<0.5%		
Floor Perimeter Coeff.	10%	5%		
Glazing U value	7%	5%		
Shading Coefficient	10%	40%	20%	70%
Window Area	<1%	15%		
Node Location	<1%	5%		
Ceiling R-value	7%	3%		
Inter-Sub-zone U-value	<.5%	<.5%		
Infiltration	25%	15%	40%	40%
IR Emissivities	<.1%	<.1%		
Tmean	<.5%	<.5%		
Neglect of IR Reflections	<2%	<2%		
Percent Sun on Floor	2%	5%		
Solar Absorptivities	<2%	<3%		
h_out	<1%	<2%	3%	10%
h_in	2%	7%		
h_floor	<1%	6%		
h_ceiling	<1%	<2%		
Estimated Overall Load Uncertainties	**±32%**	**±41%**	**±53%**	**±95%**

Table 8. Summary of load uncertainties resulting from individual model input uncertainties

Shown in **Table 8** are two sets of heat load and cooling load uncertainties. The first set reflects a more conservative estimate of the load uncertainties due to particular inputs. Where appropriate, this set uses only portions of the uncertainty ranges shown in the preceding sections. The

second set reflects a more complete, though perhaps extreme, estimate of the load uncertainties.

The primary contributors to uncertainty in the heat load calculation are: infiltration, diffuse and direct radiation, slab perimeter coefficient, thermal conductivity of the insulation layer and shading coefficient. The uncertainties of these individual inputs lead to heat load calculation uncertainties greater than or equal to 10%.

In descending order of impact to the cooling load uncertainty are: diffuse radiation, shading coefficient, ground reflectance, direct radiation, total radiation, window area, infiltration and the floor thermal mass. As above, these inputs led to load uncertainties greater than or equal to 10%.

To provide a rough estimate of the overall input-related uncertainty associated with the calculated loads, an error-propagation technique designed for linear, multi-variable functions was used [6]. This was done despite the fact that the constraint of the specified allowable zone temperature range introduces non-linearities into the calculation of node temperatures.

$$\text{Overall Uncertainty} = \left\{ \sum_{\text{model inputs}} \left(\text{Load Uncertainty}_{\text{model input}} \right)^2 \right\}^{0.5} \qquad (115)$$

The variable within the summation is what is shown in **Table 8**: the load uncertainty introduced by an individual model input. Equation (115) yields:

$$\text{Overall Heat Load Uncertainty} = \pm 32\%$$
$$\text{Overall Cooling Load Uncertainty} = \pm 41\% \qquad (116)$$

It should be pointed out that in **Table 8**, the same source of uncertainty can be accounted for more than once. For example, neighboring buildings and vegetation motivate the reduction of total radiation by 50% in **Figure 28**. Neighboring buildings and vegetation also motivate reduction of the shading coefficient to 0.5 in **Figure 40**. It is unreasonable to consider simultaneous

reduction of both factors. For this reason, the direct and diffuse radiation[55] and the shading coefficient are removed from the set of "uncertainty-inducing" inputs used to determine the overall uncertainties shown in (116).

For the "extreme" case, the heat and cooling load uncertainties are ±53% and ±95%, respectively.[56]

To summarize the results of this sub-section, rough estimates of the overall load uncertainties associated with input uncertainties are approximately ±30% and ±40% for the sensible heat and cooling loads, respectively.

[55] Direct and diffuse radiation are excluded because they cannot be considered independently of total radiation.

[56] Again, removing the direct and diffuse radiation and shading coefficient from the set of inputs.

V. Impact Study of Building Model and Weather Data Simplifications

In the last chapter, it was found that the overall heat and cooling load uncertainties were approximately ±30% and ±40% respectively. As will be shown in this chapter, it is possible to accelerate the program dramatically while introducing additional error of less than 11%. In fact, it will be shown that an "exact" heat load calculation time of about 400 seconds for the massive building can be reduced to about 12 seconds while introducing only 3% error.

The chapter is divided into two sections. The first discusses the ramifications of reducing the number of nodes used to describe the exterior wall and floor. For the heat load calculation for the massive building, the calculation time is reduced to about 48 seconds by the strategies presented in this section. The corresponding error introduced is less than 1%.

The second section reveals how it is possible to pare the calculation time down to 8 and 12 seconds for the lightweight and massive buildings, respectively, by using average monthly weather data.

A. Layer Simplification and Node Reduction

A more refined building model is introduced as a standard for comparison in this chapter. All characteristics of the base-case buildings described before remain the same with the exception of the number of nodes used in the floor and exterior wall. These new base-case buildings have 5 nodes in the floor and 5 nodes in each wall layer.[57] Due to the large number of nodes used, solutions with this new standard will be called the "exact" solutions. Again, the buildings will be studied in the Boston location. All calculation times shown in the tables in section A of this chapter reflect the simulation of all 8760 hours of the year.

---

[57] Recall that, up to this point, the floor has been described by a single node and each wall layer by two nodes. The lightweight wall has 3 wall layers and the massive wall has 4.

	Annual Heat Load	Annual Cooling Load	Calculation Time
	GJ	GJ	seconds
Lightweight Building	33.913	7.595	296
Massive Building	32.549	6.686	401

Table 9. "Exact" load calculation data

Table 10 shows the effect of reducing the number of nodes in the floor from 5 to 1, while keeping all else constant.

Lightweight Building	Ann. Heat Load	Deviation from	Ann. Cool Load	Deviation from	Calc. Time	Percent Time
Number of floor nodes	GJ	"Exact"	GJ	"Exact"	seconds	Reduction
5 ("Exact")	33.913	0.00%	7.595	0.00%	296	0%
4	33.913	0.00%	7.594	0.00%	271	-8%
3	33.914	0.00%	7.594	-0.01%	248	-16%
2	33.911	0.00%	7.592	-0.03%	226	-24%
1	33.860	-0.15%	7.557	-0.49%	204	-31%
Massive Building						
Number of floor nodes						
5 ("Exact")	32.549	0.00%	6.686	0.00%	401	0%
4	32.549	0.00%	6.686	0.00%	372	-7%
3	32.548	-0.01%	6.684	-0.03%	343	-14%
2	32.525	-0.08%	6.661	-0.38%	316	-21%
1	32.400	-0.46%	6.533	-2.29%	290	-28%

Table 10. Effect of changing number of floor nodes

Using just one node to describe the floor introduces minimal error relative to the "exact" case and reduces calculation times by 31% and 28% for the lightweight and massive buildings, respectively. Judging from the fact that an insignificant difference exists between the 4-node and 5-node calculations, the nomenclature of "exact" for the 5-node case appears reasonable.

The following table demonstrates the effect of changing the number of nodes used to describe each wall layer, while keeping the number of floor nodes fixed at 5.

Lightweight Building	Ann. Heat Load	Deviation from	Ann. Cool Load	Deviation from	Calc. Time	Percent Time
Number of wall nodes	GJ	"Exact"	GJ	"Exact"	seconds	Reduction
5 ("Exact")	33.913	0.00%	7.595	0.00%	296	0%
4	33.914	0.00%	7.596	0.01%	226	-23%
3	33.917	0.01%	7.599	0.06%	166	-44%
2	33.924	0.03%	7.612	0.23%	117	-60%
Massive Building						
Number of wall nodes						
5 ("Exact")	32.549	0.00%	6.686	0.00%	401	0%
4	32.547	-0.01%	6.684	-0.04%	293	-27%
3	32.538	-0.03%	6.676	-0.16%	202	-50%
2	32.496	-0.16%	6.636	-0.76%	131	-67%

Table 11. Effect of changing number of nodes in each wall layer

Reducing the number of nodes in each wall layer from 5 to 2 has a negligible impact on the outcome of the annual load calculations. This change provides as much as a two-thirds reduction in calculation times. Again, the use of the term "exact" appears justified for the model with 5 nodes per wall layer.

The "base case" building model used in Chapters III and IV uses a single node for the floor and two nodes for each wall layer. Relative to the "exact" case, this simplification introduces heat load errors of -0.1% and -0.6% for the lightweight and massive buildings, respectively, and -0.3% and -2.8% cooling load errors for the two buildings. As mentioned above, calculation times for the two base-case buildings are about 67 and 76 seconds, which correspond to calculation time reductions of approximately 80% relative to the "exact" case calculations. As expected, the error introduced by the node reduction is greatest for the massive building, although it is significantly lower than the input-related uncertainty described in the last section.

A very important distinction must be made at this stage. As mentioned in the preceding paragraph, the *annual* heat loads depend little on the choice of node number in the floor and wall layers. However, the calculated loads and surface temperatures *at any particular hour* are strongly dependent on the number of nodes used. To illustrate this point, the surface temperature of the floor of the massive building is examined throughout the first four days of the year.

In the base-case model, the entire floor is comprised of a single thermal mass, which has a uniform temperature. In the "exact" model, the surface node is associated with one-eighth of the entire thermal mass of the floor (see the floor model description in Chapter II). As can be seen in **Figure 50**, the floor surface temperature of the "exact" model experiences more substantial

temperature swings than that of the base case. This behavior results from the smaller thermal mass associated with the "exact" floor surface node. At times, the "exact" surface temperature exceeds that of the base case by approximately 2°C (*e.g.*, hour 12).

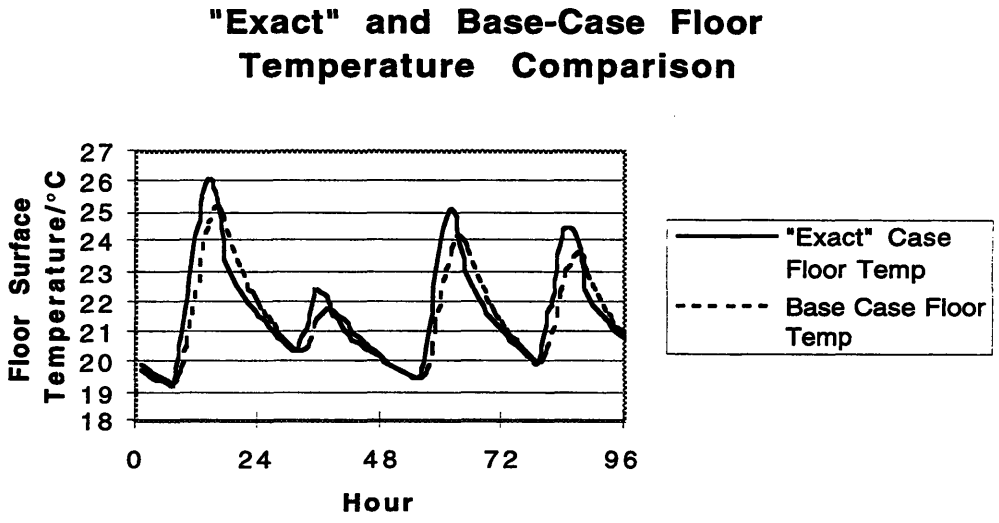

Figure 50. "Exact" and base-case floor temperature comparison

Since the base-case floor is considered to be a single lumped capacitance eight times larger than the "exact" capacitance associated with the surface node, its thermal storage ability is exaggerated.[58] Hence the damping and phase shift of the temperature swings shown in **Figure 50** and the slightly lower annual load predictions recorded above.

The consequences of the temperature discrepancies evident in **Figure 50** are very serious if detailed temperature and heat flow information at a particular time are important. For example, the peak cooling loads for the south-facing sub-zone are found to be 1,474 W and 1,591 W using the base-case and the "exact" models, respectively. In fact, this program should not be used for such purposes unless a large number of nodes are used to describe

[58] The Biot number for the 6-inch concrete floor in the massive building is roughly 0.8, an indication of the inappropriateness of the lumped-capacitance model. Judging from its Biot number (≈0.1), even the "exact" floor surface sub-layer should not be treated as a single lumped capacitance.

the various building materials.[59] Fortunately, for the intended purpose of this program–calculation of annual loads–the discrepancies are of little consequence.

One additional simplification (which, after the preceding paragraphs, may appear foolhardy) is to collapse the wall layers into a single, composite layer, described by a variable number of nodes. As discussed in Chapter II, the minimum number of nodes in the composite wall layer is 2, and the minimum number used in the floor is 1. The following table illustrates the effect of this simplification on the annual loads. A single floor node was used in the calculations.

Lightweight Building	Ann. Heat Load	Deviation from	Ann. Cool Load	Deviation from	Calc. Time	Percent Time
Number of wall nodes	GJ	"Exact"	GJ	"Exact"	seconds	Reduction
4	33.965	0.15%	7.612	0.23%	67	-77%
3	33.983	0.21%	7.628	0.44%	58	-81%
2	34.005	0.27%	7.664	0.91%	49	-83%
Massive Building						
Number of wall nodes						
4	32.617	0.21%	6.669	-0.25%	66	-84%
3	32.548	-0.01%	6.609	-1.16%	57	-86%
2	32.405	-0.45%	6.513	-2.60%	48	-88%

Table 12. Effect of collapsing wall layers into a single composite layer with a variable number of nodes

As evidenced by the data in **Table 12**, the additional time savings relative to the base case calculations (67 reduced to 49 seconds for the lightweight building and 76 reduced to 48 seconds for the massive building) are accompanied by little deterioration of accuracy. If just two nodes are used to describe the exterior wall, deviations from the "exact" calculations are all below 1%, with the exception of the cooling load for the massive building. In fact, the load calculations for the massive building are closer to the "exact" result using this method than they are using the base-case method.

[59] Five floor nodes probably provide an adequate description of the floor in the massive building. Comparison of the hourly floor surface temperatures using 5 and 10 floor nodes shows maximum differences on the order of 0.1°C, well within the input-related uncertainties.

B. Weather Data Simplification

The first section of this chapter demonstrated one technique for reducing calculation times by simplifying the model of the building components. In this section, a different acceleration technique will be explored, namely the acceleration via simplification of boundary conditions– the weather data. The essence of this method, which is described in detail in Chapter II, is the reduction of the full year of hourly weather data to hourly data for twelve average days, one for each month. The number of average days that must be simulated each month is then determined automatically by the program. In this section, the time-reduction benefits will be weighed against the error costs introduced by the simplification.

At first, the base-case building models (for the lightweight and massive buildings in Boston) will be used to explore the effects of this method. Then, this method will be combined with the final technique described in the preceding section wherein the wall layers are reduced to a single composite layer described by two nodes and the floor is described by a single node.

The following table contains the loads calculated for the two buildings using different tolerances. As described in Chapter II, the tolerance represents the degree to which load calculations for a given month have stabilized. If the load calculated on day 3 of the month differs from that on day 2 by less than a certain percentage (the tolerance), then the program advances to the next month.[60] Also shown in the table are the ranges of days required to reach "steady-state" for each choice of tolerance. The average number of days required to reach "steady-state" is also presented for each tolerance.

[60] Note that the weather data for day 2 and day 3 are identical. The weather data used for each day of the month are the weather data for that month's average day.

Lightweight Building Tolerance	Range of Days Required for Stabilization	Average Number of Days Required for Stabilization	Annual Heat Load GJ	Deviation from "Exact"	Annual Cool Load GJ	Deviation from "Exact"	Calc. Time seconds	Percent Time Reduction
0.5%	3-8	3.9	32.334	-4.7%	6.904	-9.1%	12	-96%
1.5%	3-7	3.7	32.335	-4.7%	6.906	-9.1%	11	-96%
2.5%	2-6	3.5	32.337	-4.6%	6.906	-9.1%	11	-96%
3.5%	2-6	3.3	32.337	-4.6%	6.912	-9.0%	10	-97%
4.5%	2-6	2.9	32.331	-4.7%	6.913	-9.0%	10	-97%
5.5%	2-6	2.9	32.331	-4.7%	6.913	-9.0%	10	-97%
6.5%	2-6	2.9	32.331	-4.7%	6.913	-9.0%	10	-97%
7.5%	2-6	2.9	32.331	-4.7%	6.913	-9.0%	10	-97%
8.5%	2-5	2.8	32.331	-4.7%	6.913	-9.0%	9	-97%
9.5%	2-5	2.8	32.331	-4.7%	6.902	-9.1%	9	-97%
10.0%	2-5	2.8	32.331	-4.7%	6.902	-9.1%	9	-97%
20.0%	2-5	2.6	32.345	-4.6%	6.933	-8.7%	9	-97%
30.0%	2-5	2.5	32.324	-4.7%	6.933	-8.7%	9	-97%
40.0%	2-4	2.4	32.324	-4.7%	6.933	-8.7%	8	-97%
50.0%	2-4	2.3	32.295	-4.8%	6.933	-8.7%	8	-97%
Massive	**Building**							
Tolerance								
0.5%	2-31	8.8	31.800	-2.3%	6.024	-9.9%	26	-94%
1.5%	2-31	7.7	31.812	-2.3%	6.029	-9.8%	23	-94%
2.5%	2-31	7.0	31.764	-2.4%	6.022	-9.9%	21	-95%
3.5%	2-16	5.5	31.787	-2.3%	6.013	-10.1%	17	-96%
4.5%	2-16	5.3	31.862	-2.1%	6.049	-9.5%	17	-96%
5.5%	2-16	5.0	31.765	-2.4%	6.011	-10.1%	16	-96%
6.5%	2-13	4.6	31.738	-2.5%	6.009	-10.1%	15	-96%
7.5%	2-9	4.1	31.798	-2.3%	6.001	-10.2%	14	-97%
8.5%	2-9	3.9	31.797	-2.3%	5.980	-10.6%	13	-97%
9.5%	2-9	3.9	31.797	-2.3%	5.980	-10.6%	13	-97%
10.0%	2-8	3.8	31.760	-2.4%	5.980	-10.6%	13	-97%
20.0%	2-13	3.8	31.605	-2.9%	5.800	-13.3%	13	-97%
30.0%	2-13	3.5	31.473	-3.3%	5.708	-14.6%	12	-97%
40.0%	2-13	3.5	31.473	-3.3%	5.708	-14.6%	12	-97%
50.0%	2-13	3.4	30.862	-5.2%	5.708	-14.6%	12	-97%

Table 13. The effect of tolerance on annual loads

As can be seen in the preceding table, choice of a 10% tolerance level leads to a dramatic reduction of calculation times, while introducing minimal error. For the lightweight building, the deviation from the "exact" heat and cooling loads are about -5% and -9%, respectively. For the massive building, the respective deviations are -2% and -11%.

An effect of averaging the monthly weather data is to reduce the temperature and insolation extrema observed in that month. The consequence of this averaging is that heat loads and cooling loads are decreased for both building types relative to the loads obtained when all 8760 hours of the year are simulated. Since thermal mass also acts to smooth out the effects of temperature and insolation extrema, averaging the weather

data influences the massive building loads less than the lightweight building loads. Note that the massive building's deviation from the "exact" heat load is indeed lower than that for the lightweight building. The absolute deviation of the cooling load is also lower for the massive building, but due to the massive building's lower overall cooling load, its percentage deviation from the "exact" load exceeds that of the lightweight building.

Note also that the maximum number of days required to reach steady-state conditions is not a monotonic function of the tolerance level. See, for example, the change from 10-20% tolerance for the massive building. An explanation for this behavior follows: increasing the tolerance level from 10 to 20% may allow the heat load to stabilize for February on the second average day of that month rather than on the third day. However, the new starting building node temperatures for the March calculation may be farther from the March "steady-state" conditions than they were when it took 3 days to stabilize in February. Consequently, the March calculations could be lengthened as a result–it may now take thirteen days rather than eight days to stabilize.

When the monthly averaging of the weather data is combined with the method of collapsing wall layers into a single layer, the results are remarkable. Shown in the next table are the annual loads for the lightweight and massive buildings calculated using the combined simplifications with a tolerance of 10%.

	Range of Days Required for Stabilization	Average Number of Days Required for Stabilization	Annual Heat Load GJ	Deviation from "Exact"	Annual Cool Load GJ	Deviation from "Exact"	Calc. Time seconds	Percent Time Reduction
Lightweight								
Building	2-5	2.75	32.418	-4.4%	6.993	-7.9%	8	-97%
Massive								
Building	2-27	5.25	31.575	-3.0%	5.973	-10.7%	12	-97%

Table 14. Combination of wall description and weather data simplifications

Comparison of **Table 13** and **Table 14** reveals that for the lightweight building, deviations from the "exact" calculations are actually reduced when the combined simplification technique is used. The calculation time remains the same. For the massive building, deviations from the "exact" calculations increase slightly, and calculation time is reduced slightly from 13 seconds to 12 seconds.

The techniques demonstrated in this chapter provide powerful means of reducing annual load calculation times while introducing little error. In fact, the amount of error associated with use of these techniques is marginal when compared with the input-related uncertainties in the calculated annual heat and cooling loads.

VI. Validation of Model: Comparison with Energy-10

The purpose of this chapter is to ensure that the building loads calculated by this new program are consistent with those calculated by other building energy analysis software. The program selected for comparison, Energy-10, is widely used and has itself been validated by comparison with other, more detailed programs. It should be stressed that this sort of validation does not imply accuracy. Accuracy is a quality that must be assessed by comparison with experimental measurements on actual buildings.

It will become evident later in this chapter that the results of the program developed in this thesis (hereafter, the new program) generally agree quite well with those of Energy-10. In that sense, the performance of the new program is shown to be validated. However, in particular instances, real differences do exist between the predictions of the two programs. No attempt is made here to determine "who is right," but rather to point out some possible causes of the observed discrepancies.

A. Description of Energy-10

Energy-10[61] is a software package developed by the National Renewable Energy Laboratory in conjunction with the Lawrence Berkeley National Laboratory and the Berkeley Solar Group. Its purpose is to aid in the design of low-energy buildings under 10,000 square feet (hence the name). The software is relatively "user-friendly" and simple to use: a two-day workshop provided ample training in the use of the primary features of the package.

The level of detail of building inputs is variable. For example, the user may enter building location, type, floor area, HVAC system and local energy costs and have two buildings automatically constructed using default values for the wall material properties, number and type of windows, *etc.* One building is a "basic" building, the other includes a number of suggested

[61] Version 1.2.

energy-conserving modifications. At the other extreme, the user can change details such as the thermal conductivity of each wall layer, the solar absorptivity of each wall surface, and the infiltration rate. These changes can be made to both buildings. For the most part, all building description inputs are fully adjustable by the user. Although not considered in this study, the Energy-10 program allows investigation of energy savings made possible through the use of daylighting.

When the features of the two buildings have been selected, an hourly simulation for an entire year is performed using hourly TMY2 weather data. On a 200 MHz Pentium computer, the joint simulation of the two buildings requires about 25 seconds.

B. Input of Base-Case Buildings into Energy-10

While it has not been possible to obtain information about many of the details of the assumptions made in creating the Energy-10 simulation code, the on-line help files and the technical support[62] have provided numerous clues into how the program operates. Given the information available at this time, an attempt was made to recreate faithfully within the Energy-10 framework the base-case buildings studied in this work.

This section provides some of the details for how the building descriptions of the base-case lightweight and massive buildings were entered into Energy-10. Where known, modeling differences between the two programs are highlighted.

Walls of identical composition to the ones described in Chapter III were input into Energy-10. In the lightweight building, Energy-10 considers the inside and outside surfaces of the wall to be isothermal planes, rather than the inside and outside surfaces of the insulation/stud layer. For this reason, the (clear) wall R-values used in the two programs differ slightly. For Energy-10, the wall R-value is 3.22 m°C/W while that used in the new program is 3.15 m°C/W.[63]

---

[62] Kristine Anstead, at KMAnstead@aol.com, was very helpful in finding anwers to questions about Energy-10.

[63] Excluding film coefficients on both sides of the wall.

Energy-10 uses combined convection/radiation heat transfer coefficients on all internal and external building surfaces. To allow comparison, combined coefficients were formed using the distinct convection and radiation coefficients utilized by the new program.[64] The combined coefficients are shown in **Table 15.**

Surface	New Program	Energy-10
	W/m^2°C	W/m^2°C
Exterior of Exterior Wall	34.00	33.90
Interior of Exterior Wall	8.35	8.35
Interior Walls	7.96	8.35
Floor	9.47	7.49
Ceiling	6.33	7.49

Table 15. Comparison of the combined heat transfer coefficients used by Energy-10 with the corresponding coefficients from the new program

Note that the discrepancies between the coefficients do not lead to significant error in annual load predictions. For example, see **Figure 49.** If the floor convection coefficient used by the new program is 2.0 rather than 4.0 $W/m^2°C$, then the combined coefficients for the two programs are roughly equal. As can be seen in **Figure 49**, this change leads to a decrease in the annual heat load of less than 1% and a decrease in cooling load of about 3-4%.

As modeled in Energy-10, the floor slab has an adiabatic surface at the base of the slab and a perimeter heat transfer coefficient. These conditions are also built into the model used by the new program. It is not known how many nodes are used to describe the floor in Energy-10 (if a nodal model is used).

The identical ceiling/roof used in the new program can be input into Energy-10. The capacitance of the ceiling/roof materials was set to zero, and the overall R-value was set to 4, in order to match the ceiling R-value used by the new program (including the inside and outside film resistances).

---

[64] This was done by assuming that the sub-zone air and all internal sub-zone surfaces (with the exception of the surface of interest) were isothermal. For these conditions, the sum of the radiative and convective heat transfer coefficients yields the combined coefficients.

It was not possible to input identical glazing systems into the two programs. In the new program, the entire glazed area is transparent and is described by a single U-value. In Energy-10, allowance is made for the influence of the window edge on the overall window U-value and for the frame's role in reducing the amount of light transmitted through the window. To minimize the differences between the two programs, the center glass U-value was set to 2.60 W/m^2°C, as was that of the frame/edge of glass. Therefore, the overall Energy-10 window U-value is 2.60 W/m^2°C, identical to that used in the new program. The opaque thickness of the frame was set to 1 mm. The main difference between the glazing models, the method of determining the amount of transmitted solar energy, will be discussed in a later section.

Of the solar energy that is transmitted through the windows in Energy-10, 50% is absorbed by the floor, 20% by the air and lightweight objects (see following paragraph), 20% by the walls and 10% by the ceiling.

Lightweight objects and the air form a combined thermal capacitance in Energy-10 that is ignored in the new program. In addition to the capacitance of the air, lightweight objects are assumed to contribute 0.5 BTU/°F for every square foot of floor area. The effect of ignoring this combined thermal capacitance in the new program will be addressed below.

Energy-10 allows the user to specify thermal mass in addition to that contained in the building floor and envelope. This mass is entered in the form of internal partitions. No additional mass was specified for this work.

Infiltration can be determined via the building's "estimated leakage area" (following the Sherman-Grimsrud method mentioned in Chapter II), or by specifying a constant air change rate.[65] A constant air change rate of 0.5 ACH was used.

The internal gains originating from sources such as lighting and occupants were set to zero in Energy-10 since internal gains are not included in the base-case buildings.

The HVAC system is another component of the building model that cannot be modeled identically by both programs. The new program calculates

[65] The two sources of infiltration may also be combined.

the annual heat and cooling loads for the building based on the prescribed temperature range, 20-27°C, and the humidity ratio setpoint, 0.008 kg vapor/kg dry air. The cooling load is broken into two independent parts: the sensible and the latent load. It is assumed that these loads can be met exactly by whatever HVAC system is used in the building. No prediction is made of the energy required to satisfy the loads.

In Energy-10, the user selects equipment for heating and cooling. In this case, electric baseboard heating with 100% efficiency and packaged terminal air conditioning were chosen. The COP of the air conditioner was set to 1.0, so that the electricity used would correspond directly to the cooling load. A sensible ratio of 0.75 is defaulted for the air conditioner. It is not clear how this ratio is used by Energy-10. The fan efficiency of the air conditioner was set to 100%. Based on the selection of HVAC equipment, Energy-10 sizes the equipment to meet heating and cooling requirements on winter and summer design days.

It is not clear how Energy-10 converts the building's heating and cooling requirements into figures representing annual electricity usage. It seems fair to assume that the electrical energy used for baseboard heating is identical to the building's annual heat load. The conversion for cooling, however, does not appear to be so straightforward. This issue will be discussed below.

C. Description of the Building Variants

A set of ten building variants was formed using the base-case lightweight and massive buildings as starting points. In other words, ten buildings, all identical to the lightweight base-case building with the exception of several features, were simulated by both programs. The same features were altered on the base-case massive building, forming ten additional massive variants that were simulated by both programs.

A summary of the building variants follows in **Table 16.**

Variant 1	Infiltration=0, Percent Glazed = 0%, Solar Radiation = 0
Variant 2	Infiltration=0, Percent Glazed = 0%
Variant 3	Percent Glazed = 0%
Variant 4	Percent Glazed = 10%, Solar Radiation = 0
Variant 5	Percent Glazed = 20%, Solar Radiation = 0
Variant 6	Percent Glazed = 10%
Variant 7	Percent Glazed = 20% (This is the base-case)
Variant 8	Percent Glazed on North = 10% (Glazing percentage on other sides = 0%)
Variant 9	Percent Glazed on South = 10% (Glazing percentage on other sides = 0%)
Variant 10	Percent Glazed on South = 20% (Glazing percentage on other sides = 0%)

Table 16. Definition of the building variants

For variants 1,4, and 5, the solar radiation was eliminated in Energy-10 by setting all solar absorptivities to zero and by setting the window shading coefficients to zero. In the new program, the solar radiation was eliminated directly. All other changes involve simple parameter alterations.

D. Comparison of Calculated Variant Loads

All ten variants were simulated for both lightweight and massive buildings in the Boston and Phoenix locations. Before presenting the simulation results, a few points must be made.

A heat load occurs in Energy-10 regardless of season. For example, if the indoor temperature falls below the minimum setpoint in June, the baseboard heaters turn on. To facilitate comparisons, year-round heat and cooling loads were also calculated in the new program. The total heat load is the sum of the heating season heat load and the cooling season exhaust load. The total cooling load is the sum of the cooling season cooling load and the heating season exhaust load.

The methods in which the latent cooling loads are calculated by the two programs are very different. In the new program, the latent and sensible loads are independent. In Energy-10, a latent load arises only when the thermostat-controlled air conditioner turns on. For this reason, only sensible cooling loads predicted by the two programs will be compared.

The results of the simulations are presented below in two formats. In **Figure 51**, the heat load and sensible cooling load calculated for each variant

in each location by Energy-10 is plotted against the corresponding load calculated by the new program. As shown in the figure, the agreement between the two programs is excellent on an absolute scale.[66] Viewed from this perspective, the programs agree to within approximately ±5 GJ, regardless of the load calculated. The cooling loads in the abscissa are the sensible loads calculated by the new program.

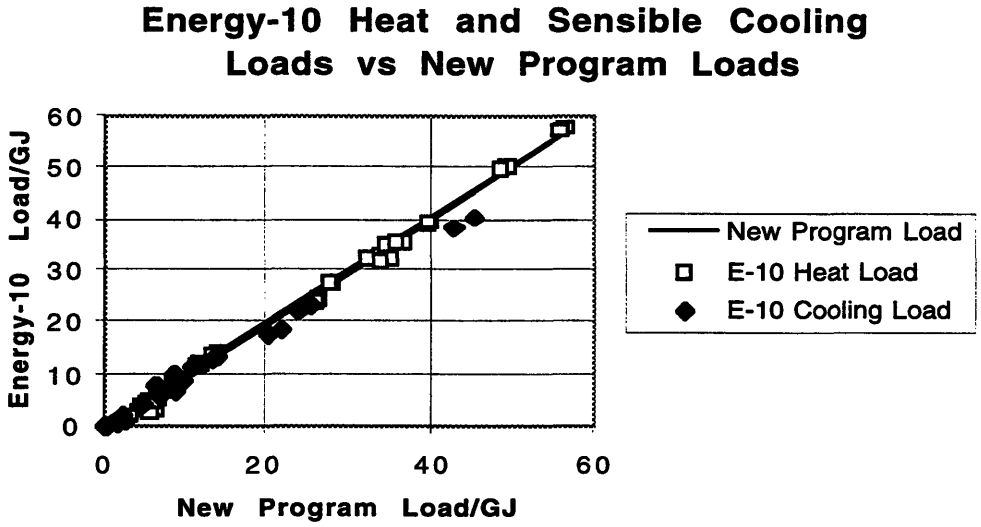

Figure 51. Energy-10 heat and cooling loads plotted against the corresponding loads predicted by the new program (The solid line represents exact agreement)

Tabulated below are the same calculation results that are plotted in **Figure 51**. Also shown are the percentages by which the Energy-10 loads deviate from those of the new program. Highlighted in both tables are the results for the base-case buildings. For reference purposes, the Boston buildings have annual latent cooling loads of 1.033 GJ, while the Phoenix annual latent cooling loads are 0.163 GJ. Note that since the latent load occurs only in the presence of infiltration, variants 1 and 2 have no latent loads associated with them. In the tables below, the cooling loads associated with the new program are sensible loads only.

---

[66] By this is meant that the deviations between the calculated loads expressed in GJ are small. Deviations expressed in terms of percentages portray a different picture, especially for the loads of small magnitude.

It should be noted that the data for the Energy-10 sensible and latent cooling loads came from the "Air Handler Report" portion of the Energy-10 output file. The total cooling load was taken from the "Summary Page." It is not clear why the sum of the latent and sensible loads is not equal to the total cooling load.

Lightweight Building				Program CL	E-10 CL	Sensible CL	E-10 CL	E-10 CL
Boston	Program HL	E-10 HL	% Deviation	Sensible	Sensible	% Deviation	Latent	Total
1	28.132	27.925	-0.7%	0.000	0.000	0.0%	0.000	0.000
2	26.504	24.492	-7.6%	0.008	0.086	1029.4%	0.000	0.086
3	40.208	39.097	-2.8%	0.015	0.062	303.6%	0.013	0.073
4	49.286	49.931	1.3%	0.004	0.001	-77.3%	0.000	0.001
5	56.558	57.227	1.2%	0.009	0.006	-37.7%	0.001	0.007
6	35.325	34.998	-0.9%	2.542	2.380	-6.4%	0.295	2.483
7	33.921	33.011	-2.7%	8.749	7.090	-19.0%	0.551	6.941
8	40.237	39.549	-1.7%	0.240	0.206	-14.1%	0.044	0.239
9	36.848	35.369	-4.0%	0.636	0.349	-45.1%	0.071	0.399
10	35.343	32.267	-8.7%	2.721	1.040	-61.8%	0.160	1.129
Massive Building				Program CL	E-10 CL	Sensible CL	E-10 CL	E-10 CL
Boston	Program HL	E-10 HL	% Deviation	Sensible	Sensible	% Deviation	Latent	Total
1	27.834	27.838	0.0%	0.000	0.000	0.0%	0.000	0.000
2	26.194	24.407	-6.8%	0.000	0.003	0.0%	0.000	0.003
3	39.719	38.82	-2.3%	0.000	0.001	0.0%	0.000	0.001
4	48.764	49.629	1.8%	0.000	0.000	0.0%	0.000	0.000
5	55.977	56.862	1.6%	0.000	0.000	0.0%	0.000	0.000
6	34.639	34.589	-0.1%	1.576	1.551	-1.6%	0.226	1.648
7	32.362	32.059	-0.9%	6.835	5.880	-14.0%	0.541	5.828
8	39.756	39.28	-1.2%	0.075	0.038	-48.9%	0.006	0.049
9	36.162	35.052	-3.1%	0.290	0.082	-71.7%	0.013	0.105
10	34.058	31.718	-6.9%	1.674	0.493	-70.5%	0.090	0.546

Table 17. Comparison of loads for the Boston variants (loads expressed in GJ)

Lightweight Building				Program CL	E-10 CL	Sensible CL	E-10 CL	E-10 CL
Phoenix	Program HL	E-10 HL	% Deviation	Sensible	Sensible	% Deviation	Latent	Total
1	6.794	6.749	-0.7%	4.829	4.554	-5.7%	0.000	5.293
2	5.888	4.905	-16.7%	6.400	8.143	27.2%	0.000	9.337
3	9.311	8.266	-11.2%	8.811	10.130	15.0%	0.416	11.904
4	12.142	12.113	-0.2%	8.576	7.902	-7.9%	0.347	9.401
5	14.009	14.013	0.0%	9.878	9.158	-7.3%	0.372	10.877
6	5.457	4.65	-14.8%	25.353	23.740	-6.4%	0.578	26.715
7	4.507	3.114	-30.9%	45.325	40.100	-11.5%	0.661	43.824
8	8.992	8.195	-8.9%	11.436	12.050	5.4%	0.455	14.065
9	6.974	5.363	-23.1%	14.107	13.660	-3.2%	0.465	15.760
10	6.535	3.486	-46.7%	21.804	18.500	-15.2%	0.506	20.859
Massive Building				Program CL	E-10 CL	Sensible CL	E-10 CL	E-10 CL
Phoenix	Program HL	E-10 HL	% Deviation	Sensible	Sensible	% Deviation	Latent	Total
1	6.580	6.567	-0.2%	4.672	4.444	-4.9%	0.000	5.790
2	5.725	4.764	-16.8%	6.231	7.965	27.8%	0.000	9.021
3	8.970	7.981	-11.0%	8.568	9.883	15.3%	0.455	11.561
4	11.712	11.724	0.1%	8.318	7.702	-7.4%	0.374	9.137
5	13.513	13.572	0.4%	9.591	8.937	-6.8%	0.393	10.586
6	4.743	3.898	-17.8%	24.147	22.870	-5.3%	0.639	25.632
7	3.395	2.013	-40.7%	43.011	38.350	-10.8%	0.736	41.820
8	8.639	7.892	-8.6%	11.084	11.740	5.9%	0.496	13.636
9	6.414	4.8	-25.2%	13.243	13.080	-1.2%	0.509	15.044
10	5.726	2.594	-54.7%	20.078	17.480	-12.9%	0.559	19.690

Table 18. Comparison of loads for the Phoenix variants (loads expressed in GJ)

A few general comments will be made about the results, then some individual features will be examined more carefully.

Study of **Table 17** shows that the programs' agreement for the Boston heat load calculations is excellent. In no case is the discrepancy between the loads calculated by Energy-10 and by the new program greater than 9%.

With a few exceptions, Energy-10 tends to underpredict both heat loads and cooling loads in both Boston and Phoenix.

E. Discussion of Variant Loads

Short of removing all the thermal mass from the building, variant 1 illustrates the simplest building scenario that can be modeled. The effects of solar radiation are removed, infiltration is ignored and no windows are used.

A degree-day calculation is easily performed to double-check the loads. Using the building data provided in **Table 4** and **Table 5**, along with the degree-day values shown in **Table 3**, the following UA values were determined for the lightweight and massive buildings:[67]

$$(UA)_{walls} = 32.71\ W/°C$$
$$(UA)_{slab\ perimeter} = 33.83\ W/°C$$
$$(UA)_{ceiling} = 23.23\ W/°C$$
$$(UA)_{tot} = 89.77\ W/°C$$

(117)

The annual loads in Boston were found to be:

$$\text{Annual Heat Load (Degree - Day)} = 29.36\ GJ$$
$$\text{Annual Cooling Load (Degree - Day)} = 0.17\ GJ$$

(118)

and the annual loads in Phoenix were found to be:

$$\text{Annual Heat Load (Degree - Day)} = 8.48\ GJ$$
$$\text{Annual Cooling Load (Degree - Day)} = 6.24\ GJ$$

(119)

Using UA values that Energy-10 generated for the same lightweight and massive buildings, 88.3 and 88.9 W/°C,[68] respectively, annual loads calculated using the degree-day method for variant 1 are found to be:

---

[67] Recall that the building materials were selected so that U-values for all portions of the building envelopes were identical for the massive and lightweight buildings.

[68] Material properties were input to Energy-10 to match those in the new program. In the new program, the lightweight wall R-value matches that of the massive wall. However, in Energy-10, since the wall R-value is calculated assuming that the wall surfaces are isothermal rather than the surfaces of the stud/insulation layer, the UA values for the two constructions differ.

	Degree-Day Heat Load	Degree-Day Cooling Load
Boston	GJ	GJ
Lightweight Building	28.88	0.17
Massive Building	29.08	0.17
Phoenix		
Lightweight Building	8.34	6.13
Massive Building	8.40	6.18

Table 19. Degree-day loads for the Energy-10 variant 1 buildings

The difference between the Energy-10 UA values and those of the new program are thought to arise from rounding and conversion errors in Energy-10. Energy-10 stores all its material properties in I-P units, then converts the numbers to SI units for display. The discrepancy, which is of the order of a couple percentage points, should not detract from the comparisons presented in this chapter.

Comparison of the predicted degree-day loads with the actual loads calculated for variant 1 (**Table 17** and **Table 18**) shows that degree-day load estimates consistently exceed the actual loads. Two factors contribute to this behavior: the presence of thermal mass in the variant 1 buildings and the range through which the temperature is allowed to float. Evidence of the importance of thermal mass can be seen by comparing the loads for the lightweight and massive buildings.[69]

Finally, with the exception of the Phoenix cooling loads, the Energy-10 calculations for variant 1 agree with those of the new program to within 1%. The deviations between the sensible cooling loads predicted by the new program and by Energy-10 are approximately 5%.

Variant 2 is formed by adding to variant 1 the effects of sunlight striking the roof and exterior walls. Examination of **Table 17** and **Table 18** shows that the impact of the sun on the Energy-10 loads is considerably stronger than on the loads of the new program. The reduction of heat loads

[69] One anomaly exists in the cooling loads for the variant 1 Phoenix buildings. It appears that the total cooling load is larger for the massive building. This problem is related to the automatic sizing of the air-conditioner in Energy-10. If both buildings are given the same a.c. system, the massive total building load is lower than that of the lightweight building. This anomaly does not appear for the sensible cooling loads.

and the increase in cooling loads calculated by Energy-10 significantly exceed the corresponding reduction and increase predicted by the new program. In effect, the Energy-10 insolation appears stronger than that in the new program. The observed difference may arise from the use of a different correlation relating the diffuse radiation striking a horizontal surface to that striking a vertical surface. In fact, use of the equation (25) presented in Chapter II that allows for an anisotropic distribution of diffuse sky radiation could lead to diffuse sky radiation more than double that used in the new program. The observed difference may also arise from the model used by Energy-10 to incorporate the solar flux into the overall heat transfer through the envelope.

Infiltration is added to generate the variant 3 buildings. Using a constant air density of 1.2 kg/m^3, an infiltration rate of 0.5 ACH and the number of degree days for the two sites, the infiltration is predicted to increase heat loads by 13.89 and 4.01 GJ in Boston and Phoenix. The cooling loads are predicted to increase in the two sites by 0.08 and 2.95 GJ. Actual heat load increases are damped by the presence of thermal mass in the buildings. With an allowance for the damping, the effect of infiltration on the heat loads is as expected for both programs.[70] The impact of infiltration on the Phoenix cooling loads is as expected (slightly lower than 2.95 GJ), while in Boston, the impact is mixed. Due to the uncertainty of the calculation output, it is not clear whether the infiltration changes the cooling loads significantly in Boston. It should be mentioned that the storage of coolness from the night air by the thermal mass could allow the addition of infiltration to decrease rather than increase the cooling load.

Variants 4 through 7 will be discussed as a group. Variants 6 and 7 are identical to variants 4 and 5, except for the fact that the sun is "turned off" in variants 4 and 5. Several points bear mentioning.

By removing the solar radiation, variants 4 and 5 isolate the impact of the window conduction model described in Chapter II. Agreement with Energy-10 loads is excellent for these variants, especially for the heat loads.

---

[70] Except for the heat loads calculated for the Boston buildings by Energy-10. The impact of the infiltration exceeds the degree-day estimate. A possible explanation is the use of a different air density.

The effect of transmitted sunlight may be isolated by comparing variants 4 and 6 and variants 5 and 7.[71] Several trends are apparent:

As expected, "turning on" the solar radiation reduces the heat loads of the massive buildings more than it does the heat loads of the lightweight buildings. Conversely, the cooling loads for the massive buildings are increased to a lesser extent than those of the lightweight buildings.

The effect of adding solar radiation on building heat loads is always greater for the Energy-10 calculations than for those of the new program. This finding is consistent with the behavior observed when changing from variant 1 to 2. A similar trend is not found for the cooling loads.

Variant 8 is included so that the role of diffuse radiation on heat loads can be examined. During the heating season, all radiation transmitted through the north window is diffuse. Note that in Boston, where the winter is more severe, the north-facing window loses more energy than it admits (compare variants 3 and 8). However, in Phoenix, the north-facing window reduces heat loads slightly. In both locations, the presence of the north-facing window increases cooling loads.

Interesting behavior occurs when the south glazing percentage changes from 10 to 20% (variants 9 and 10). The heat loads predicted by the new program decrease less than those predicted by Energy-10, while the cooling loads increase more than those predicted by Energy-10. A convincing explanation for this behavior has not been found.

F. Additional Comparisons

In the course of attempting to understand the differences between the predictions of the two programs, several model components were examined in more detail. The first is the thermal capacitance of the air (or lack thereof) and the second is the transmission of solar energy through the glazing.

---

[71] Isolation is not complete since the inclusion of sunlight in variants 6 and 7 affects heat transfer through the opaque walls and roof.

1. Thermal Capacitance of Air

In order to determine whether the omission of the thermal capacitance of the air (and lightweight objects) might seriously impact the results of the new program, a modified version of the program ("modified program A") was created that incorporated the combined capacitance of the air and other lightweight objects in the same manner as Energy-10. Heat and cooling loads for this modified massive base-case building in Boston differed from the original loads by less than 0.5%. The heat load for the modified lightweight building was 0.2% lower than the original load, and the cooling load was 2% lower than the original cooling load. Consistent with all calculations performed so far, these calculations were performed under the assumption that all heat gains to the air (and now lightweight objects) occurred via convection.

As mentioned earlier in this chapter, the thermal model in Energy-10 distributes 20% of all incoming sunlight to the air and lightweight objects. The effect of this modeling approach was investigated by adding this feature to modified program A (to form "modified program B"). 20% of incoming solar radiation was allotted to the thermal capacitance representing the air and lightweight objects. The remaining 80% was apportioned between the floor, interior walls, ceiling and exterior wall as before.[72] The principal effect of this change was to increase the importance of solar energy in calculating the cooling load. The cooling load of the lightweight Boston building increased by more than 50% as a result of this change. The heat load was minimally affected.

At first glance, it appears that inclusion of the air capacitance in the modified program B necessarily worsens agreement between the two programs. In the absence of other modeling changes, this conclusion is certainly valid. However, the next subsection of this chapter shows that the quantity of glazing-transmitted insolation predicted by the Energy-10 model can be significantly lower than that predicted by the model in the new program. "Modified program C" is defined by reducing the amount of solar energy transmitted through the glazing in the modified program B by changing the shading coefficient from 0.9 to 0.72. This change yields a heat load roughly 4% higher than the base-case heat load for the lightweight

[72] 50% of the 80% strikes the floor first and the other 50% strikes the interior walls first.

Boston building and a cooling load roughly 6% lower than the base-case cooling load.

In effect, the two modeling strategies employed by Energy-10 cancel each other out. Directing 20% of the incoming solar energy to the air capacitance increases the cooling load, while reducing the amount of incoming solar energy reduces the load. The behavior just described permits the two programs, with distinctly different strategies for treating incoming solar radiation, to reach very similar predictions of heat and cooling loads.

2. Transmission of Solar Energy Through Glazing

As mentioned in the preceding subsection, the model used in Energy-10 nearly always underpredicts the quantity of solar energy transmitted through glazing, as compared with the model used in the new program. It is beyond the scope of this research to make a detailed study of the discrepancies and to determine the "correct" modeling approach. However, it is clear that predictions of annual loads are very sensitive to the model used to calculate solar energy transmission. For this reason, a detailed study of this topic should be performed before the next version of this software is created.

To motivate future research, the preliminary results obtained thus far regarding the transmission of solar energy through glazing will be presented.

In Energy-10, the total solar energy transmitted though glazing at any time of the year is available in graphical form. Eight days were selected for study: January 1, February 2 and 28, April 1, May 2, May 31, June 1 and July 2. Daily maximum levels of total solar flux through glazing on the north and south faces of the building were obtained. It was found that, on cloudy days, the north window transmitted the same amount of solar energy as the south window.[73] It was therefore concluded that the north window flux could serve as a surrogate measure of the diffuse radiation passing through the south window.

[73] This is consistent with use of model that assumes all vertical surfaces receive identical amounts of diffuse radiation. The new program incorporates this same assumption.

Using the total solar flux from the Energy-10 output and the estimate of the diffuse radiation, the transmitted direct solar radiation was calculated for each day studied. The particular glazing system studied was a double-glazed clear window with a shading coefficient of 0.90. These data were then compared with the predictions of the SHGF (used in the new program) and SHGC methods for the transmitted solar energy at the same times. Comparison was facilitated by the fact that both Energy-10 and the new program use TMY2 weather data.

One minor detail of the new program should be mentioned before any comparisons are given. Solar radiation data given in the TMY2 format for 2 p.m. represents the integrated incident solar energy for the hour between 1 and 2 p.m. The question arises as to when the angle of incidence for direct radiation should be calculated. It was decided to use the 1:30 p.m. sun position to determine the angle of incidence for use for the entire hour between 1 and 2 p.m. This subtlety should be kept in mind when repeating the study--incident angles associated with the 12 noon solar flux impinging on the south-facing window represent 11:30 a.m. incident angles.

For each time when the Energy-10 transmitted flux was sampled, the total incident direct and diffuse/reflected radiation and the angle of incidence (θ) were calculated using the equations presented in Chapter II in concert with the TMY2 weather data. Given this information, the total radiation transmitted through the same clear, double-glazed window was calculated. The transmitted solar heat gain was calculated using the shading coefficient and the TSHGF described in Chapter II.[74] It was also calculated using the SHGC method using Table 11 in Chapter 29 of the ASHRAE Fundamentals Handbook. All details of window 5a given in that table were used, despite the slight discrepancy in the shading coefficients (0.87 versus 0.90).

Shown in the next three figures are the predicted solar fluxes through a south-facing window according to the TSHGF, SHGC and Energy-10 models. It is clear that the model used by Energy-10 is different from both the TSHGF and the SHGC models. In general, the TSHGF method produces the largest estimate of transmitted diffuse radiation, followed by the SHGC method, then the Energy-10 method. A simple trend is not apparent for the transmitted direct radiation. The Energy-10 method at times exceeds and at

[74] The shading coefficient used was 0.9, to match that used by Energy-10.

other times falls below the ASHRAE methods. Viewed in terms of total radiation transmitted, the winter points (through February 28) appear to show the best agreement among the models, while the points corresponding to later dates reveal significant disparities among the models.

Recall that in the previous subsection, when the modified program C was formed by reducing the shading coefficient from 0.90 to 0.72, the heat load exceeded and the cooling load fell below the respective loads of the base-case buildings by 4 and 6%. It appears that improved agreement between Energy-10 and the modified program C could be achieved if the shading coefficient were reduced during summer months alone. This conclusion was reached in light of the reasonable agreement among the three different total solar flux transmission models during the winter months. This change would preserve the good agreement already existing between the heat loads predicted by the modified program B and Energy-10 and would improve the agreement between the programs' cooling load predictions.

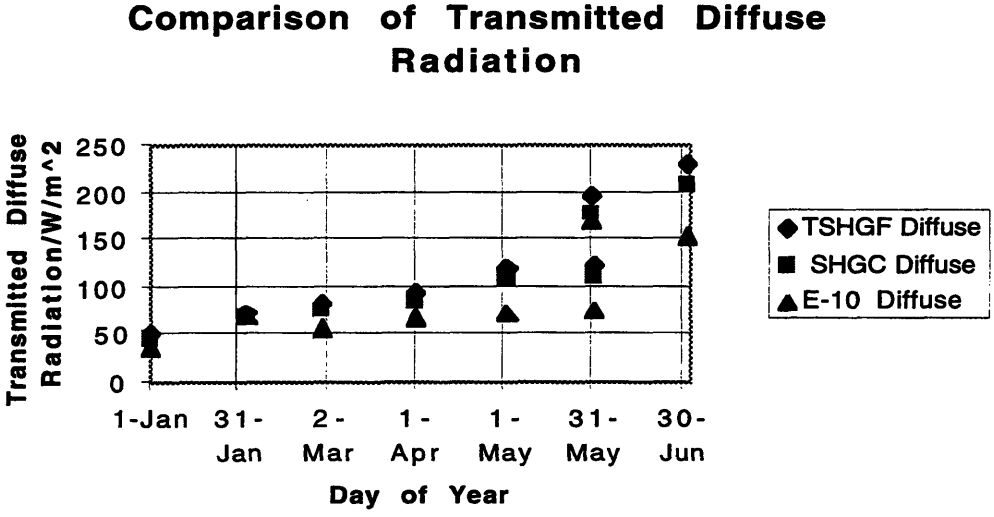

Figure 52. Comparison of Transmitted Diffuse Radiation

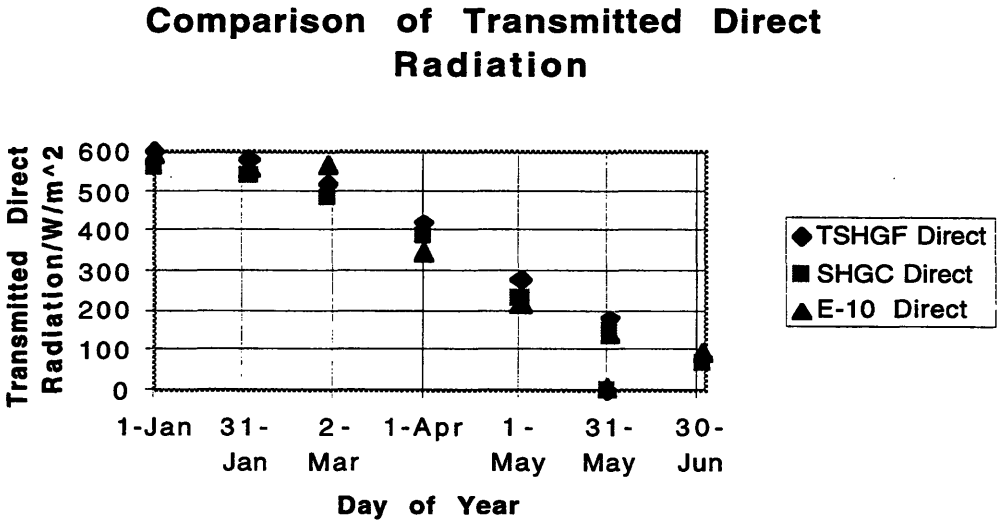

Figure 53. Comparison of Transmitted Direct Radiation

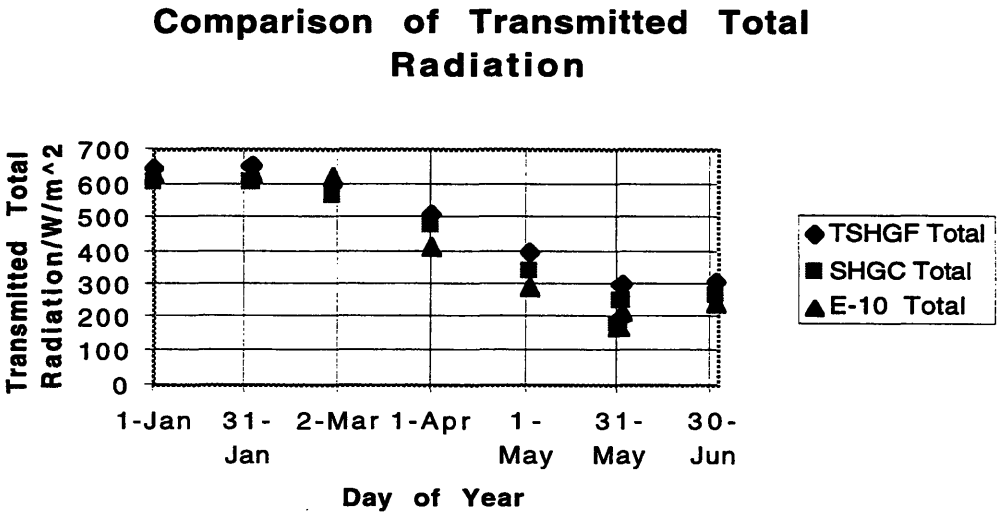

Figure 54. Comparison of Transmitted Total Radiation

G. Summary of Comparison With Energy-10

The results presented in this chapter demonstrate that the (unmodified) model developed in this thesis is in reasonable agreement with the model built into Energy-10 software. For the most part, percentage differences between the two programs' load predictions are lower than the uncertainties associated with the loads. While discrepancies do exist between individual portions of the models (*e.g.*, the transmission of solar radiation through glazing), and annual load predictions may differ by large percentages for particular building variants, the programs produce, on balance, very similar predictions of annual loads (**Figure 51**).

The most important ramification of this chapter is that the conclusions made about uncertainty levels in Chapters IV and V were obtained using a well-functioning building thermal model. Consequently, the overall uncertainty estimates for the annual loads should be applicable to at least other simplified energy analysis programs, and perhaps to more detailed programs as well.

VII. Conclusion and Suggestions for Future Study

Two principal goals were set forth at the outset of this work. The first goal was to create a simplified building energy simulation program that could be used as a tool for designing energy-efficient residential buildings. The second goal was to use this program to investigate the effects of model input uncertainties on the overall uncertainty of the buildings' predicted heat and cooling loads.

In order to accomplish the first goal, the primary factors influencing a residential building's energy consumption were modeled individually and then linked together to form a thermal model of the entire building. Measured weather data, including temperature and solar radiation data, were used as boundary conditions for the interconnected thermal elements of the building.

Given these boundary conditions, heat transfer through the building walls was modeled by accounting for the effects of both the thermal storage capacity and the thermal resistance of the walls. Independent models for convection and long-wave radiation were implemented to govern surface-surface and surface-air heat transfer inside the building. Solar radiation passing through glazing was distributed partly to a thermally massive floor and partly to the other interior surfaces of the building. Also incorporated into the model were such important factors as infiltration, heat transfer through the ceiling and attic, and heat transfer through the perimeter of slab-on-grade floors.

Using an implicit method, the equations describing heat transfer among and through the many components of the building were solved simultaneously. The results of these calculations were used to determine hourly and annual heat and cooling load contributions of the individual building components. Individual contributions were then combined to obtain overall building loads.

In order to accomplish the second goal of this work, estimates were made of the uncertainties associated with model input parameters. Using these estimates and the program described above, studies were performed on two base-case buildings (one lightweight, one massive) to determine the sensitivity of overall building loads to the uncertainties in the input

parameters. The outcome of this series of studies was the conservative estimates[75] of overall uncertainties associated with the sensible heat and cooling loads: ±30% and ±40% for heat and cooling loads, respectively.

Although these overall uncertainty estimates were obtained using two particular buildings located in Boston, the implications of these results are more far-reaching. Specifically, even building loads predicted by detailed building energy analysis programs are likely to have wide uncertainty bands--perhaps not as great as 30%, but significant nonetheless.

Since large uncertainty bands appeared to be inevitable for the load predictions of even detailed programs, it became apparent that certain additional modeling simplifications could safely be made. It was shown that annual load calculations could be dramatically accelerated without significantly augmenting the overall uncertainty associated with the predicted loads. Joint simplification of the weather data and the wall and floor models made it possible to obtain annual heat and cooling load predictions in about 8 and 12 seconds, respectively, on a 180 MHz computer. (Standard load calculations required more than a minute on the same computer.) The errors associated with these simplifications were approximately 4% and 10% for the sensible heat and cooling loads, respectively. In light of the annual load uncertainties arising from input parameter uncertainties, 4 and 10% errors are insignificant penalties to pay for almost real-time feedback about the building's annual thermal performance.

Two program validation studies were performed to ensure that the program was operating properly. A series of buildings were simulated using this program and the software package Energy-10. On the whole, agreement between the two programs' predictions was very good. Nevertheless, the different modeling approaches taken by the two programs led to some discrepancies in the annual load predictions. The second validation study, shown in Appendix 1, demonstrated that the finite difference algorithm used in the program showed excellent agreement with the exact solution describing periodic conduction in an infinite slab.

---

[75] It is the estimate of the uncertainty that is conservative, not the level of certainty. See Chapter II, section J.

It is hoped that the work presented in this thesis will serve as a solid starting point for those assembling the integrated building design tool described in the introduction. Before incorporating this program into such a tool, several recommendations should be considered. These include: careful assessment of the accuracy of the available models for predicting solar heat gain through windows, and incorporation of additional models for heat transfer in different basement configurations. Further work is also required to allow simulation of multi-story buildings. Additional refinements, such as the introduction of shading devices, may be desired. Care should be taken, however, to weigh the importance of these model refinements against the cost of increased calculation times. Finally, special attention should be granted to the development of the user interface for this program.

VIII. References

[1] *ASHRAE Handbook, Fundamentals Volume*, American Society of Heating, Refrigerating and Air-Conditioning Engineers, Inc., Atlanta, GA, 1997.

[2] Athienitis, A.K., and M. Stylianou, "Method and Global Relationship for Estimation of Transmitted Solar Energy Distribution in Passive Solar Rooms," *Energy Sources*, **13**, pg. 319, 1991.

[3] Athienitis, A.K., *Application of Network Methods to Thermal Analysis of Passive Solar Buildings in the Frequency Domain*, Doctoral Thesis, University of Waterloo, Ontario, 1985.

[4] Athienitis, A.K., *Building Thermal Analysis*, MathCad Electronic Book, Ch. 7, 1993.

[5] Bauman, F., A. Gadgil, R. Kammerud, E. Altmayer, M. Nansteel, "Convective Heat Transfer in Buildings: Recent Research Results," *ASHRAE Transactions*, **89**:1a, pg. 215, 1983.

[6] Bragg, G.M., *Principles of Experimentation and Measurement*, Prentice-Hall, Inc., New Jersey, 1974.

[7] Busch, R.D., "Characterization of Energy Processes in Buildings," *Fundamentals of Building Energy Dynamics*, Hunn, B.D., Editor, MIT Press, Cambridge, pg. 141, 1996.

[8] Carslaw, H.S., and J.C. Jaeger, *Conduction of Heat in Solids*, 2nd Ed., Oxford University Press, London, pg. 105, 1959.

[9] Christian, J.E., and J. Kosny, "Thermal Performance and Wall Ratings," *ASHRAE Journal*, pg. 56, March 1996.

[10] Claesson, J., and C.-E. Hagentoft, "Heat Loss to the Ground from a Building–I. General Theory," *Building and Environment*, **26**:2, pg. 195, 1991.

[11] Coblentz, C.W., and P.R. Achenbach, "Field Measurements of Air Infiltration in Ten Electrically-heated Houses," *ASHRAE Journal*, **5**, pg. 69, 1963.

[12] Elkins, R.H., and C.E. Wensman, "Natural Ventilation of Modern Tightly Constructed Homes." Paper presented at the American Gas Association – Institute of Gas Technology, Conference on Natural Gas Research and Technology, Chicago, February 28–March 3, 1971.

[13] Galanis, N. and R. Chatigny, "A Critical Review of the ASHRAE Solar Radiation Model," *ASHRAE Transactions*, **92**:1a, pg. 410, 1986.

[14] Hottel, H.C., "A Simple Model for Estimating the Transmittance of Direct Solar Radiation Through Clear Atmospheres," *Solar Energy*, **18**, pg. 129, 1976.

[15] http://rredc.nrel.gov/solar/old_data/nsrdb/tmy2/

[16] http://www.eren.doe.gov/building/tools_directory/

[17] Incropera, F.P., and D.P. DeWitt, *Fundamentals of Heat and Mass Transfer*, 4th Ed., John Wiley & Sons, New York, 1996.

[18] Iqbal, M., *An Introduction to Solar Radiation*, Academic Press, Toronto, 1983.

[19] Khalifa, A.J.N., and R.H. Marshall, "Validation of Heat Transfer Coefficients on Interior Building Surfaces Using a Real-Sized Indoor Test Cell," *International Journal of Heat and Mass Transfer*, **33**:10, pg. 2219, 1990.

[20] Krarti, M., and S. Choi, "Simplified Method for Foundation Heat Loss Calculation," *ASHRAE Transactions*, **102**:1, pg. 140, 1996.

[21] Krarti, M., D.E. Claridge, J.F. Kreider, "A Foundation Heat Transfer Algorithm for Detailed Building Energy Programs," *ASHRAE Transactions*, **100**:2, pg. 843, 1994.

[22] Kuehn, T.H., "Field Heat-Transfer Measurements and Life-Cycle Cost Analysis of Four Wood Frame Wall Constructions," *ASHRAE Transactions*, **88**:1, pg. 651, 1982.

[23] Kuehn, T.H., and E.A.B. Maldonado, "Two-dimensional Transient Heat Transfer through Composite Wood Frame Walls–Field Measurements and Modeling," *Energy and Buildings*, **6**, pg. 55, 1984.

[24] Liu, B. and R. Jordan, "The Interrelationship and Characteristic Distribution of Direct, Diffuse, and Total Solar Radiation," *Solar Energy*, 4, pg. 1, 1960.

[25] McQuiston, F.C., and J.D. Parker, *Heating, Ventilating and Air Conditioning: Analysis and Design*, 4th Ed., John Wiley & Sons, New York, Ch. 6, 1994.

[26] Mitalas, G.P., "Calculation of Below-Grade Residential Heat Loss: Low-Rise Residential Building," *ASHRAE Transactions*, **93**:1, pg. 743, 1987.

[27] Özisik, M.N., *Heat Conduction*, 2nd Edition, John Wiley & Sons, New York, Chapter 8, 1993.

[28] Peterson, J.E., "Estimating Air Infiltration into Houses," *ASHRAE Journal*, **21**:1, pg. 60, 1979.

[29] Press, W., S. Teukolsky, W. Vetterling, B. Flannery, *Numerical Recipes in C: The Art of Scientific Computing*, 2nd Ed., Cambridge University Press, 1995.

[30] Reeves, G., M.F. McBride, and C.F. Sepsy, "Air Infiltration Model for Residences," *ASHRAE Transactions*, **85**:1, pg. 667, 1979.

[31] Reilly, M.S., F.C. Winkelmann, D.K. Arasteh, and W.L. Carroll, "Modeling Windows in DOE-2.1E," *Energy and Buildings*, **22**, pg. 59, 1992.

[32] Richards, P.G., and E.H. Mathews, "A Thermal Design Tool for Buildings in Ground Contact," *Building and Environment*, **29**:1, pg. 73, 1994.

[33] Sherman, M.H., and D.T. Grimsrud, "Infiltration-Pressurization Correlation: Simplified Physical Modeling," *ASHRAE Transactions*, **86**:2, pg. 778, 1980.

[34] Sobotka, P.S., H. Yoshino and S. Matsumoto, "The Analysis of Deep Basement Heat Loss by Measurements and Calculations," *ASHRAE Transactions*, **101**:2, 1995.

[35] Sowell, E.F., "The Use and Limitations of ASHRAE Solar Algorithms in Solar Energy Utilization Studies," *ASHRAE Transactions*, **84**:2, pg. 77, 1978.

[36] Sparrow, E.M., and R.D. Cess, *Radiation Heat Transfer*, Brooks/Cole Publishing Co., Belmont, CA, pg. 301, 1966.

[37] Threlkeld, J.L. and R.C. Jordan, "Direct Solar Radiation Available on Clear Days," *ASHRAE Transactions*, **64**, pg. 45, 1958.

[38] Threlkeld, J.L., *Thermal Environmental Engineering*, 2nd Ed., Prentice Hall, New Jersey, 1970.

[39] *User's Manual for TMY2s*, Analytic Studies Division, National Renewable Energy Laboratory, June 1995.

[40] Weber, D.D., and R.J. Kearney, "Natural Convective Heat Transfer Through an Aperture in Passive Solar Heated Buildings," *Proceedings, 5th National Passive Solar Conference*, Amherst, MA, pg. 1037, Oct. 19-26, 1980.

IX. Nomenclature

Terms are dimensionless unless otherwise noted.

A	altitude for Hottel/Liu-Jordan clear-sky model (km)
A	ASHRAE clear-sky parameter: direct normal solar radiation outside atmosphere (W/m^2)
A	parameter for determining infiltration rate (hr^{-1})
A	used in Appendix 1 for calculating temperature distribution in a slab
$\hat{\mathbf{A}}$	coefficient matrix multiplying the vector of node temperatures at time $t+\Delta t$
ACH	air changes per hour (hr^{-1})
$A_{ceiling}$	surface area of ceiling (m^2)
$A_{Exterior\ Wall}$	surface area of exterior wall (m^2)
A_{floor}	surface area of floor (m^2)
A_{ins}	fraction of wall surface area comprised of insulation
$A_{opening\ size}$	size of opening between sub-zones (m^2)
ASHGF	absorbed solar heat gain factor ($W/m^{2\circ}C$)
A_{stud}	fraction of wall surface area comprised of studs
A_{wall}	surface area of exterior wall (m^2)
A_{walls}	surface area of interior walls (m^2)
A_{window}	surface area of window (m^2)
a_o	Hottel/Liu-Jordan clear-sky parameter
a_1	Hottel/Liu-Jordan clear-sky parameter
B	ASHRAE clear-sky parameter: atmospheric extinction coefficient
B	parameter for determining infiltration rate ($1/hr^{\circ}C$)
$\hat{\mathbf{B}}$	coefficient matrix multiplying the vector of node temperatures at time t
C	ASHRAE clear-sky parameter: ratio of diffuse horizontal radiation to direct normal radiation
C	constant for determining h_{iz} ($W/m^{2.5\circ}C^{1.5}$)
C	heat capacity (or thermal mass) per unit area ($J/m^{2\circ}C$)
C	boundary condition vector
C_x	heat capacity per unit area associated with an internal floor or wall node in material x ($J/m^{2\circ}C$)

C_{equiv}	total heat capacity of wall or floor per unit area ($J/m^2°C$)
C_n	clearness number
c_p	specific heat ($J/kg°C$)
$c_{p,eff}$	effective specific heat of a composite stud/insulation layer ($J/kg°C$)
D	parameter for determining infiltration rate (s/mhr)
D	vector used in LU decomposition
F	perimeter heat transfer coefficient for floor slab ($W/m°C$)
$F_{x->y}$	view factor from surface x to surface y
front	front wall (exterior wall)
H_A	height of opening between sub-zones (m)
h_{above}	convection heat transfer coefficient for the upper surface of the ceiling (or roof, in which case it equals h_{out})
h_{below}	convection coefficient between lower surface of the floor and the T_{below} ($W/m^2°C$) (defined in terms of floor surface area)
$h_{ceiling}$	ceiling convection coefficient ($W/m^2°C$)
$\Delta h_{evaporation}$	enthalpy of evaporation (J/kg)
h_{in}	inside vertical surface convection coefficient ($W/m^2°C$)
$h_{in(conv+rad)}$	sum of all convection and radiation heat transfer coefficients at the interior surface of the window ($W/m^2°C$)
$h_{in,\ eff}$	convection heat transfer coefficient between the window temperature node and the inside air temperature that accounts for part of the thermal resistance of the window ($W/m^2°C$) (defined in terms of window area)
$h_{infiltration}$	heat transfer coefficient used for calculating infiltration losses ($Whr/°C$)
h_{iz}	inter-zonal convection coefficient ($W/m^2°C$)
h_{out}	combined convection/radiation heat transfer coefficient for exterior surfaces of the building ($W/m^2°C$)
$h_{out,\ eff}$	combined convection/radiation heat transfer coefficient between the window temperature node and the outside air temperature that accounts for part of

	the thermal resistance of the window ($W/m^2°C$) (defined in terms of window area)
$h_{r,window->y,\ eff}$	radiation heat transfer coefficient between the window temperature node and surface y that accounts for part of the thermal resistance of the window ($W/m^2°C$) (defined in terms of window area)
$h_{r,x->window,eff}$	radiation heat transfer coefficient between surface x and the window temperature node that accounts for part of the thermal resistance of the window ($W/m^2°C$) (defined in terms of the surface area of surface x)
$h_{r,x->y}$	radiation heat transfer coefficient between surface x and surface y ($W/m^2°C$) (defined in terms of the surface area of surface x)
I_{DN}	direct normal solar radiation at the earth's surface (W/m^2)
I_D	direct solar radiation striking a surface (W/m^2)
$I_{DN,out}$	direct normal solar radiation outside the atmosphere (W/m^2)
$I_{d,ground->surface}$	ground-reflected diffuse radiation striking a surface (W/m^2)
$I_{d,horiz}$	diffuse solar radiation striking a horizontal surface (W/m^2)
$I_{d,sky->surface}$	diffuse sky radiation striking a surface (W/m^2)
$I_{d,total}$	total diffuse and reflected solar radiation striking a surface (W/m^2)
$I_{global,\ horiz}$	total solar radiation striking a horizontal surface (W/m^2)
I_o	solar constant (1367 W/m^2)
$I_{tot,surface}$	total solar radiation striking a surface (W/m^2)
k	Hottel/Liu-Jordan clear-sky parameter
k	thermal conductivity ($W/m°C$)
K	used in Appendix 1 for calculating temperature distribution in a slab (m^{-1})
k_{eff}	effective thermal conductivity of a composite stud/insulation layer ($W/m°C$)
L	slab thickness (m)
left	left interior wall (as seen looking into the sub-zone through a window in the exterior wall)

n	counter representing day of year (January 1: n = 1)
n_x	number of nodes in material x (in wall or floor layer)
P	perimeter length of floor slab (m)
p	atmospheric pressure (Pa)
$p_{v,s}$	vapor pressure at saturation (Pa)
$q_{slab,perim}$	rate of heat transfer through the perimeter of a floor slab (defined as flowing from inside air to outside air) (W)
$q_{internal}$	internal heat gain due to electricity usage and occupants (W)
q_{sun}	total solar radiation absorbed by a surface (W/m^2)
$q_{sun,\ absorbed}$	see q_{sun}
$q_{sun,reflected}$	total solar radiation absorbed on an internal surface of the sub-zone after reflection off other surfaces ($W/m^2°C$)
R	thermal resistance of a material ($m^2°C/W$)
$R_{ceiling}$	thermal resistance of ceiling (or ceiling plus attic) ($m^2°C/W$)
R_{equiv}	total thermal resistance of all layers in wall or floor ($m^2°C/W$)
$R_{glazing}$	thermal resistance of window in the absence of film resistances ($m^2°C/W$)
RH	percent relative humidity
right	right interior wall (as seen looking into the sub-zone through a window in the exterior wall)
r_k	Hottel/Liu-Jordan clear-sky parameter
R_x	thermal resistance of material between two nodes in material x ($m^2°C/W$)
r_o	Hottel/Liu-Jordan clear-sky parameter
r_1	Hottel/Liu-Jordan clear-sky parameter
SC	shading coefficient of glazing
SHGC	solar heat gain coefficient
SHGF	solar heat gain factor (W/m^2)
t	time (s)
T	temperature (°C or K)
T_{ab}	temperature at the interfacial node between material a and b
T_{above}	temperature of the air above the ceiling or above the roof (=T_{out}, in this case) (°C)

T_{below}	dry-bulb temperature of air below the floor
$T_{ceiling}$	ceiling surface temperature (°C)
$T_{dew\ point}$	dew point temperature (°C)
$T_{exterior\ wall}$	inside surface temperature of exterior wall
$T_{ext\ wall}$	inside surface temperature of exterior wall (°C)
T_{floor}	floor surface temperature (°C)
T_{glass}	temperature of window node (°C)
T_{in}	dry-bulb inside air temperature (°C)
$T_{interior\ walls}$	interior partition walls surface temperature (°C)
T_l	temperature (in wall) at node to the left (°C)
$T_{left\ sub\text{-}zone}$	temperature in the adjacent sub-zone on other side of left interior wall. (°C)
T_m	mean temperature of surfaces in radiative contact (K)
$T_{neighbor}$	$T_{right\ sub\text{-}zone}$ or $T_{left\ sub\text{-}zone}$ (°C)
T_{out}	dry-bulb outside air temperature (°C)
T_r	temperature (in wall) at node to the right (°C)
$T_{right\ sub\text{-}zone}$	temperature in the adjacent sub-zone on other side of right interior wall. (°C)
TSHGF	transmitted solar heat gain factor (W/m^2°C)
T_{wall}	inside surface temperature of exterior wall (°C)
T_{window}	temperature of window node (°C)
ΔT_{iz}	temperature difference between neighboring sub-zones (°C)
U	overall heat transfer coefficient of whole window (W/m^2°C)
$(UA)_{wall\ to\ left\ sub\text{-}zone}$	heat transfer coefficient used for calculating the rate of heat transfer between a sub-zone and the adjacent sub-zone on the left (W/°C)
$(UA)_{wall\ to\ right\ sub\text{-}zone}$	heat transfer coefficient used for calculating the rate of heat transfer between a sub-zone and the adjacent sub-zone on the right (W/°C)
$(UA)_x$	overall heat transfer coefficient representing heat transfer between the inside air and the outside air via x (W/°C)
V_{wind}	local wind speed (m/s)
W	humidity ratio (kg vapor/kg dry air)
Weight Factor	parameter used for estimating T_{below}
wall	exterior wall
walls	interior walls (left and right)

x	distance (m)
Δx	separation between nodes (m)
Y	ratio of diffuse radiation striking a vertical surface to that striking a horizontal surface.

Symbols

'	signifies that variable is evaluated at time $t+\Delta t$
α	solar altitude angle (°)
α	thermal diffusivity (m^2/s)
α_{solar}	solar absorptivity of outside surface of exterior wall
$\alpha_{solar,floor}$	solar absorptivity of floor
$\alpha_{solar,roof}$	solar absorptivity of roof
$\alpha_{solar,walls}$	solar absorptivity of interior walls
β	surface tilt angle (°)
γ	surface solar azimuth angle (°)
$\varepsilon_{IR,\ floor}$	IR emissivity of floor
$\varepsilon_{IR,\ walls\ and\ ceiling}$	IR emissivity of interior walls and ceiling
$\varepsilon_{IR,\ window}$	IR emissivity of window glass
θ	angle at which incident solar radiation strikes surface (°)
ρ	density (kg/m^3)
ρ_{eff}	effective density of a composite stud/insulation layer (kg/m^3)
ρ_{ground}	ground reflectance
σ	Stefan-Boltzmann constant, 5.67×10^{-8} W/m^2K^{-4}
τ_b	atmosphere direct solar transmittance
τ_d	atmosphere diffuse solar transmittance
ϕ	solar azimuth angle (°)
ϕ	used in Appendix 1 for calculating temperature distribution in a slab (radians)
Φ_{back}	angle between the two interior walls of the sub-zone (radians)
Φ_{left}	angle between exterior wall and interior wall to the left (as seen looking into the sub-zone through a window in the exterior wall) (radians)

Φ_{right}	angle between exterior wall and interior wall to the right (as seen looking into the sub-zone through a window in the exterior wall) (radians)
ψ	surface azimuth angle (°)
ω	frequency of oscillation of slab surface temperature (radian/sec)
$\%_{glazed}$	percentage of exterior wall area devoted to glazing
$\%_{sun->floor}$	percentage of incoming sunlight striking the floor first
$\%_{sun->walls}$	percentage of incoming sunlight striking the interior walls first

X. Appendix 1. Validation of Finite-Difference Method

In order to ensure that the Crank-Nicolson implicit finite difference algorithms were properly implemented in the program, a simple comparison study was performed. The temperature distribution as a function of time was determined within an infinite slab using both the finite difference model and the exact solution. The test conditions were as follows:

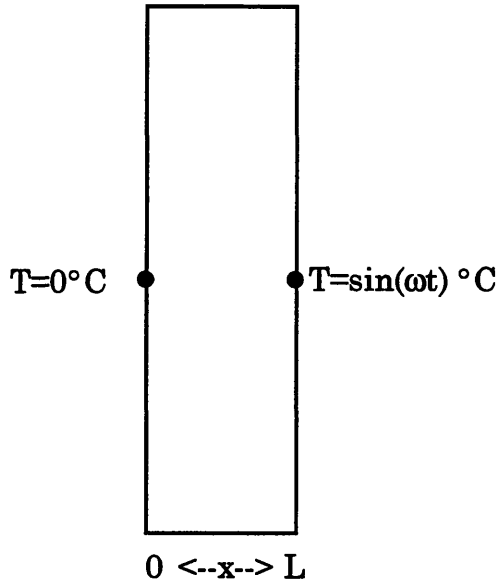

Figure 55. Infinite slab with surfaces x=0 and x=L subject to constant and sinusoidally varying temperatures, respectively

The thermal diffusivity of the concrete slab, α, was 5.27×10^{-7} m^2/s and the frequency of temperature oscillation, ω, was 4.36×10^{-4} rad/s, corresponding to a period of oscillation of 4 hours. The thickness of the slab, L, was set to 0.1 m. The initial conditions were T(x,0) = 0°C. The goal was to determine the temperature distribution within the slab as a function of time.

The exact solution to this conduction problem is given by [8]:

$$T(x,t) = A\sin(\omega t + \phi) + 2\pi\alpha\sum_{n=1}^{\infty}\frac{n(-1)^n(-\omega L^2)}{\alpha^2 n^4\pi^4 + \omega^2 L^4}\sin\left(\frac{n\pi x}{L}\right)\exp\left(\frac{-\alpha n^2\pi^2 t}{L^2}\right), \quad (120)$$

where

$$A = \left|\frac{\sinh\{Kx(1+i)\}}{\sinh\{KL(1+i)\}}\right|, \quad (121)$$

$$\phi = \angle\left(\frac{\sinh\{Kx(1+i)\}}{\sinh\{KL(1+i)\}}\right), \quad (122)$$

and

$$K = \left(\frac{\omega}{2\alpha}\right)^{0.5} \quad (123)$$

A total of 21 equally-spaced nodes were assigned to the slab between (and including) x=0 and x=L. Two finite difference calculations were performed, the first using time steps of 15 minutes, and the second using time steps of 1 minute. The results of the finite difference calculations and the exact calculation are compared below.

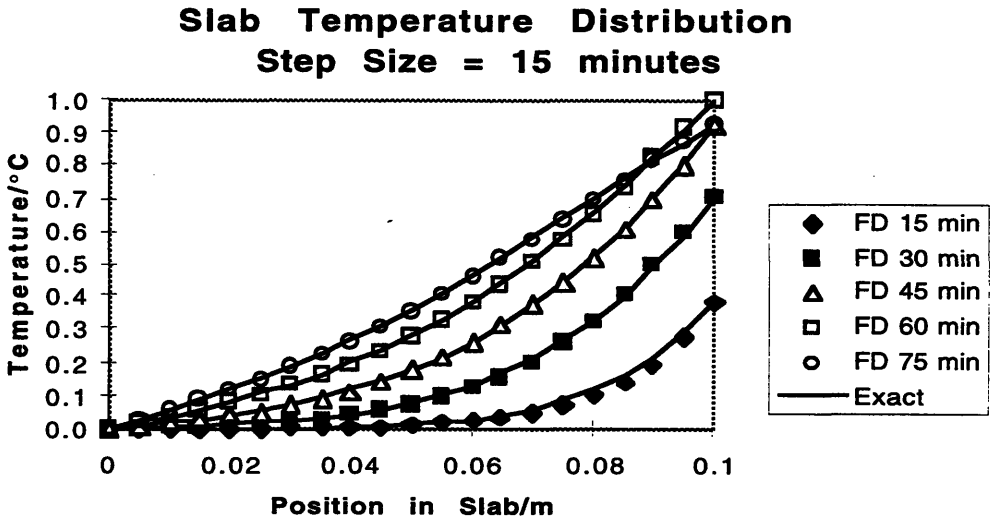

Figure 56. Slab temperature distribution: comparison of exact and finite-difference results at 15-minute intervals. Time step size: 15 minutes (FD = Finite Difference)

Examination of **Figure 56** shows that the finite-difference method used by the program is indeed functioning properly. For the most part, agreement is excellent between the exact and model-predicted temperatures. Note, however, the slight discrepancies near x=L for the temperature distribution at 15 minutes. Since significant discrepancies are not apparent at later times, start-up transients are likely the origin of the errors observed at 15 minutes. For the purposes of the annual load calculations, initial transients are probably of little importance.

A comparison of **Figure 56** and **Figure 57**, which was created using 1 minute time steps for the finite difference calculation, shows that failure of the finite difference method to accurately track the initial transients can be minimized by reducing the time step size. Note that the temperature distributions shown in **Figure 57** are limited to those at 15 minute intervals even though the node temperatures were calculated every minute.

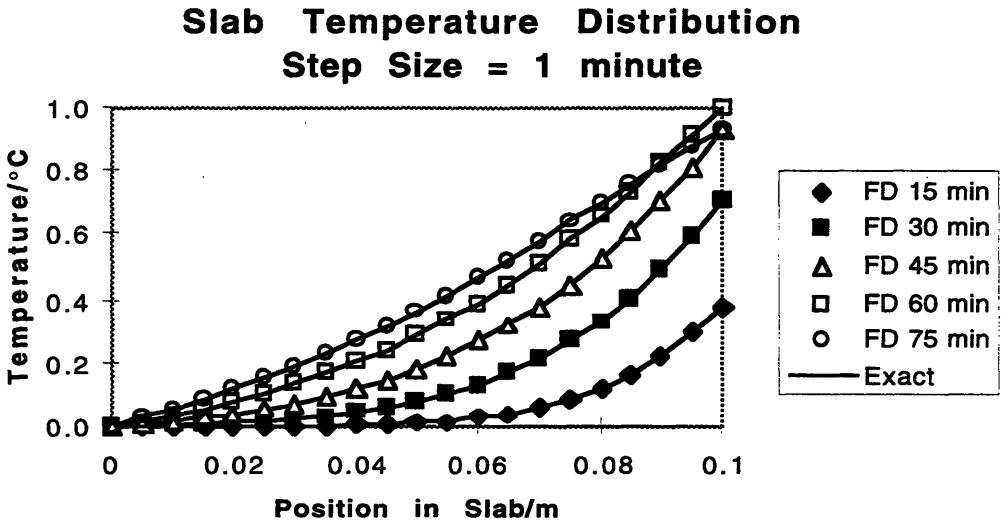

Figure 57. Slab temperature distribution: comparison of exact and finite-difference results at 15-minute intervals. Time step size: 1 minute (FD = Finite Difference)

As a final check, a scenario closer to that used in the load calculations is investigated. In **Figure 58**, the temperature distribution in the slab is plotted once again, this time using 3 nodes for the finite-difference calculation. The temperatures at the midpoint of the slab calculated by the finite difference method differ from the exact temperatures by less than 0.026°C.

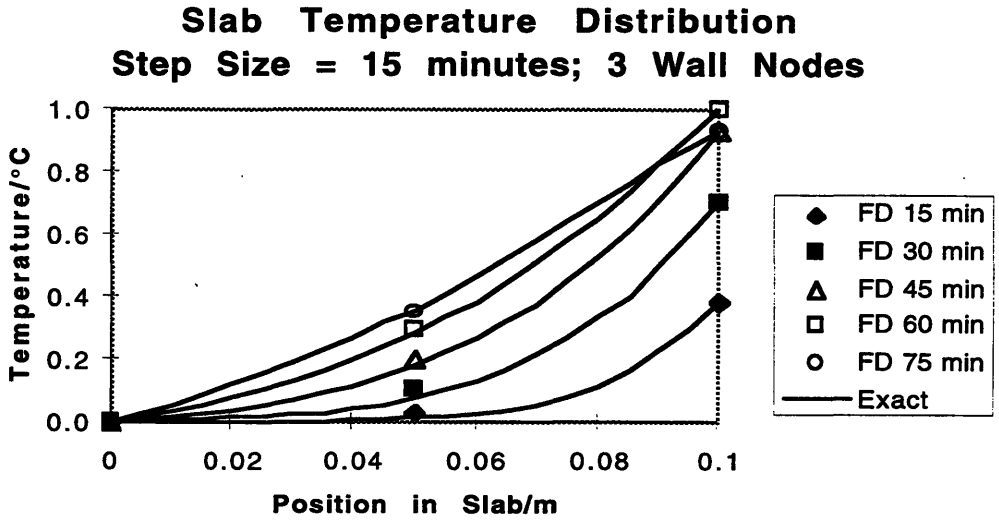

Figure 58. Slab temperature distribution: comparison of exact and finite-difference results at 15-minute intervals. 3 nodes in wall. Time step size: 15 minutes (FD = Finite Difference)

The conclusion of this brief study is that the Crank-Nicolson implicit finite difference method was correctly implemented into the program.

XI. Appendix 2. The Computer Program

This appendix contains three sub-sections. The first section gives a short tutorial describing how the program is used. The second contains a flowchart of the principal program steps. The third is a printout of the main portion of the program, which is set up for simulating the lightweight building. This main program file controls all the other program files and serves as a more detailed summary of program steps than the flowchart. The enclosed diskette contains the complete set of program files and weather data for Boston and Phoenix.

A. Using the Program

Two sample program setups are included in this package: one configured to run the simulation for the lightweight base-case building, and the other to run the simulation for the massive building. Using the lightweight building setup as an example, this chapter will show the user how to enter building properties and make simple changes.

The computer program was written using Symantec C++ for Macintosh, version 7.0. If this particular compiler is not available, the files should work with another compiler. In that case, some of the descriptions below may not be applicable.

To begin, discard the existing Main.cp, make a copy of Main.cp LW and rename the copy Main.cp. Later, if you want to examine and run the simulation of the massive building, copy Main.cp HW (HW=heavyweight and LW=lightweight) and rename the copy Main.cp. Then, double-click on the file Building Energy.π.

In the window that appears, the user can see the different component files of the program. These can be examined immediately, or after this introduction to the program. Double-click on the name of a component file to view its contents.

Open the file Main.cp. At the top of the file is a reminder that this is the lightweight building.

The first entry to be made is below the line marked "INITIALIZATION." The double slash (//) appearing before any typing on a line signifies that the remainder of the line is not read by the program. By adding and removing double slashes, the user can tailor the program as desired.

Select TMY2 for the weather data type and NORMAL for the type of calculation. NORMAL means that every hour of every day is simulated. AVERAGE uses average days for each month.

Select NORMAL for layer simplification. MAJOR puts all of the wall layers into a single composite layer and all floor layers into another composite layer. NORMAL leaves the layers exactly the way they are entered.

If you use TMY2 weather data, the first SITE VARIABLES do not have to be set--they are automatically read in from the TMY2 file.

If your first run is for Boston, make sure the lines for the Boston heating and cooling season start dates are uncommented (*i.e.*, the //'s are removed). If desired, comment them and uncomment those for Phoenix.

In the SET ZONE VARIABLES section, the number of sub-zones is set to 4. Unless substantial (but straightforward) changes are made to the program, this number should not be changed.

Shown immediately below is where air density and specific heat are entered (in SI units). The humidity ratio setpoint (in kg vapor/kg dry air) and $\Delta h_{evaporation}$ are also input here.

base_ach is the standard air change rate (in ACH), and alt_ach is the rate used during times when natural ventilation is appropriate. For now, these variables are both set to 0.5 ACH.

Sensible internal heat gains for the entire building may be entered here by inputting an estimate of monthly electricity usage and the average number of people in the building over a 24-hour period.

The evening setback time is entered as well as the morning resume time. (No setback was used for the base-case building studies.) Below the setback times, the user can enter the maximum and minimum temperature setpoints for occupied and unoccupied times in both winter and summer. Temperatures are in °C.

In the INITIALIZE SITE_INFO CLASS section, select the appropriate command according to the location in which the building is to be simulated.

The CALCULATE DEGREE DAYS IF DESIRED section is currently commented out by the surrounding symbols, /* */. If the degree day numbers are desired, uncomment this section. Note how the reference temperature is chosen for the degree-day calculation.

Skip to the ENTER PROPERTIES FOR DIFFERENT SURFACES section. The base-case building has four faces. The widths of the South and North faces are 11.8 m and are 7.87 m for the East and West faces. The overall floor area is computed and divided into four equal floor areas for the four sub-zones: 23.26 m^2. Refer to Chapter II (sections A and L) for more information about how the sub-zones are configured. Enter the appropriate angles in radians. In this case, right_length and left_length are identical for all sub-zones: half the diagonal lengths of the rectangular building. These lengths are the lengths of the interior walls. height is the floor-to-ceiling distance measured in meters.

In the ENTER CONVECTION COEFFICIENTS section, the heat transfer coefficients are entered in SI units and are defined as in the text. For example, ho is the combined radiation/convection heat transfer coefficient for the outside surface of the exterior wall.

Solar absorptivities and IR emissivities are entered in the section entitled ENTER WALL-FLOOR SURFACE PROPERTIES. Also, the fraction of sunlight passing through the window that strikes the floor first is entered here: 0.5.

The ENTER GLAZING INFO section is where the fraction of the exterior wall area devoted to glazing (perc_glazed) is set. The IR emissivity of glass, the whole-window R value (in SI units) and the shading coefficient are set here.

Since the walls of the base-case building are vertical, beta is set to 90 degrees in the ENTER SURFACE TILT ANGLE section.

The line at the base of the INITIALIZE SURFACE_INFO CLASS section is important to notice. Here, the user must specify how many layers are used to describe the exterior wall (3) and the floor (1). In the Main.cp HW, there are 4, rather than 3 layers in the exterior wall. This function must be set twice in the program: once here and then again in the main loop of the program (the for loop using q as an index).

In the next section, ENTER Lightweight Building LAYER PROPERTIES, the number of nodes used for each layer as well as the layer thermophysical properties and thicknesses are set. All variables are entered in SI units.

Skip down to the SOLAR ANGLES OUTPUT section. This optional section has been commented out. To use this, synthetic weather data (clear-sky radiation models) must be selected, and the first 5 lines in the SET SITE VARIABLES section must be set. (The SET SITE VARIABLES section appears near the top of Main.cp.)

The routine Determine_Angles_for_a_Specific_Time can be used to print to the screen information about solar angles and energy for a particular building surface at a particular time of day and year. Note the "S_Wall." used as a prefix to the routine call. Any wall of the building can be used here.

The routine SI.Output_Angles_for_a_Specific_Day prints to a file ("Site Angles One Day") the solar altitude, azimuth and total horizontal radiation (W/m^2) for the sunlit hours of the specified day. The prefix, "SI." refers to the Site Information class, which holds information that is universally true about the site. Preceded by "S_Wall.", the same routine produces an output file ("Angles One Day South Wall") containing solar information specific to that wall: wall solar azimuth, θ, and incident direct and diffuse/reflected solar energy. Again, these data are calculated for the sunlit hours of the specified day.

The same prefixes can be used with the routine Output_Angles_for_a_Specific_Time. The same information about solar

angles and energy is output to the files: "Site Angles One Time" and "Angles One Time South Wall." This time, however, the data are calculated at the same standard time each day (currently at noon) and the output includes data for all 365 days of the year.

The next section is BEGINNING OF LOAD CALCULATIONS. This section is heavily commented and changes should be relatively straightforward. The for loop involving the variable q contains the main portion of the program. Currently, the loop will run only once, using q=0. However, if a parametric study is to be performed, this loop can be run multiple times. See the comments next to the line "variable=0.1*q;". Each time through the loop, the annual heat loads are calculated and written to a file called "General Output File."

Notice again the occurrence of the routine call: Set_Num_Wall_Floor_Layers(3,1). Make sure the numbers entered here match the numbers entered above.

At this point, everything is entered that must be entered for the program to run. Before running the program, however, ensure that a TMY2 weather data file is inside the folder containing the program files. For Boston, the file is called 14739.txt. If the file does not exist, the weather data files may be downloaded from the web or obtained from a TMY2 CD-ROM (request one from the TMY2 web page) [15]. Expand the Boston file and change the suffix to .txt. It may be necessary to open the file using Word and save it again as a text file. Finally, select Run under the project menu and the simulation begins. Some load information appears on the screen. Details are recorded in the output file, "General Output File."

To obtain an additional potentially interesting output, the user must open the Heat Load Calc.cp file. This output file ("Heat Load South Wall", or "Heat Load North Wall", *etc.*) contains the temperatures of each node at every time step in the simulation. It also contains instantaneous heat and cooling loads and solar radiation information at each hour. Generating this file slows the simulation down greatly, so this option is usually turned off. The relevant lines occur near the base of the code for the routine Determine_Surface_Loads in a section called OUTPUT HOURLY INFO ABOUT NODE TEMPS AND LOADS. If the output information is desired, uncomment this entire section.

B. Program Flowchart

To aid the user in following the main steps of the program, a flowchart has been created. The first line of each "box" in the flowchart is either exactly the same as, or very similar to an actual routine call within the program. This labeling should help the user to locate where the charted steps occur.

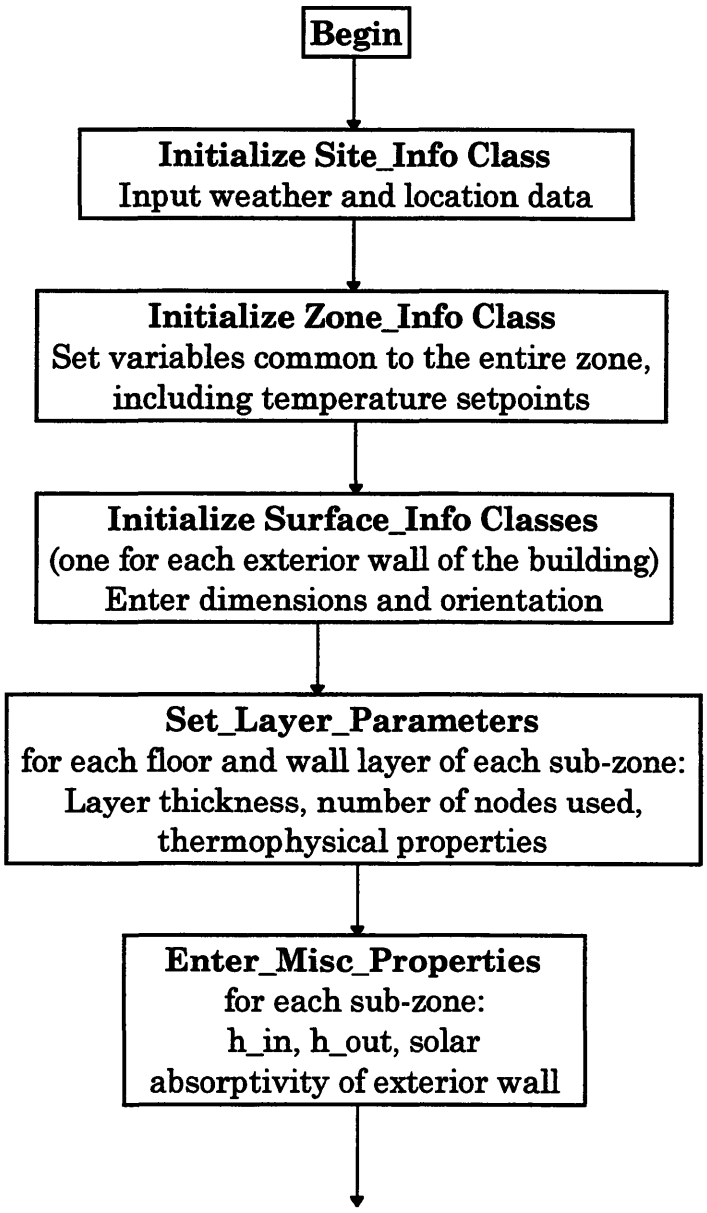

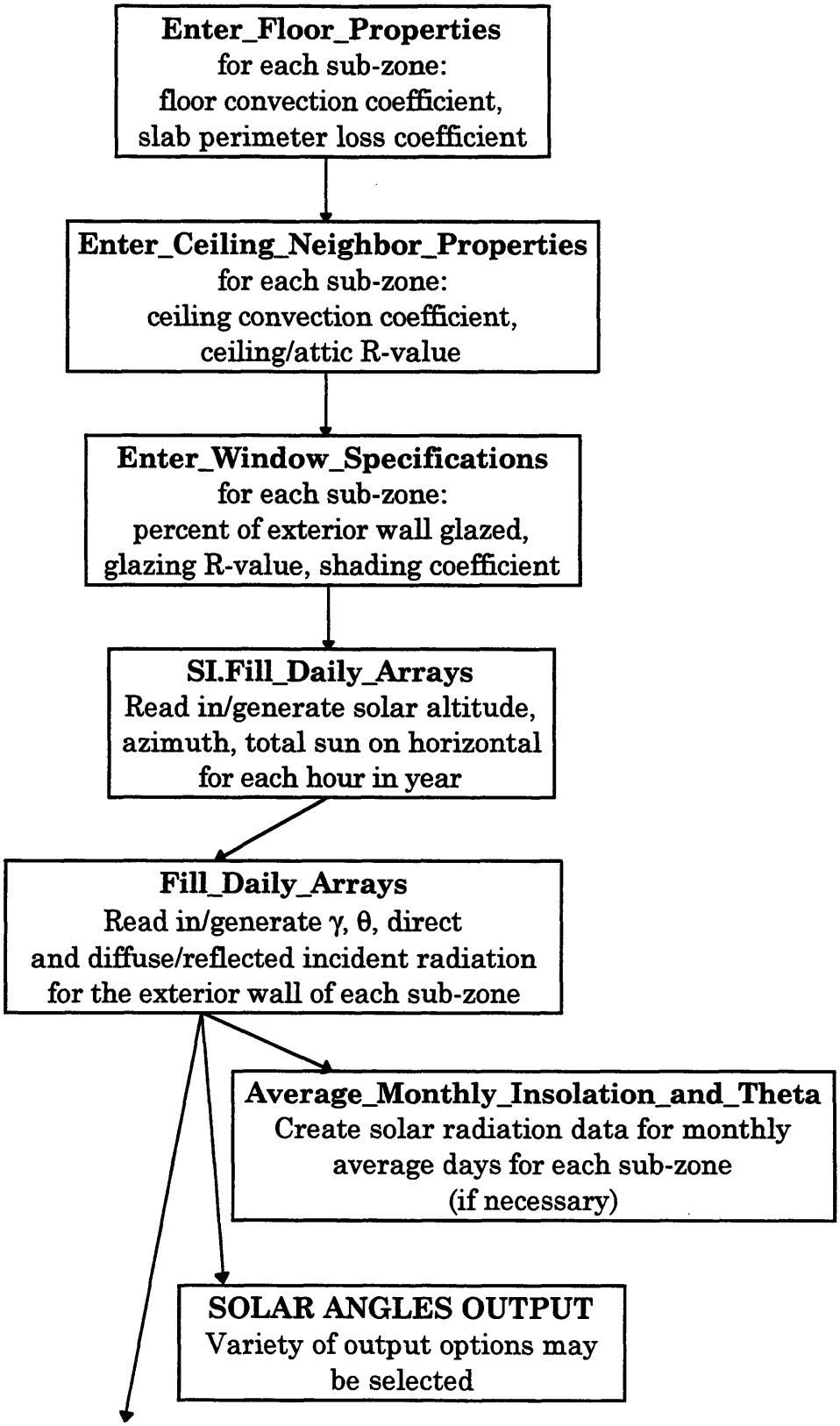
Enter_Floor_Properties
for each sub-zone:
floor convection coefficient,
slab perimeter loss coefficient
Enter_Ceiling_Neighbor_Properties
for each sub-zone:
ceiling convection coefficient,
ceiling/attic R-value
Enter_Window_Specifications
for each sub-zone:
percent of exterior wall glazed,
glazing R-value, shading coefficient
SI.Fill_Daily_Arrays
Read in/generate solar altitude,
azimuth, total sun on horizontal
for each hour in year
Fill_Daily_Arrays
Read in/generate γ, θ, direct
and diffuse/reflected incident radiation
for the exterior wall of each sub-zone
Average_Monthly_Insolation_and_Theta
Create solar radiation data for monthly
average days for each sub-zone
(if necessary)
SOLAR ANGLES OUTPUT
Variety of output options may
be selected

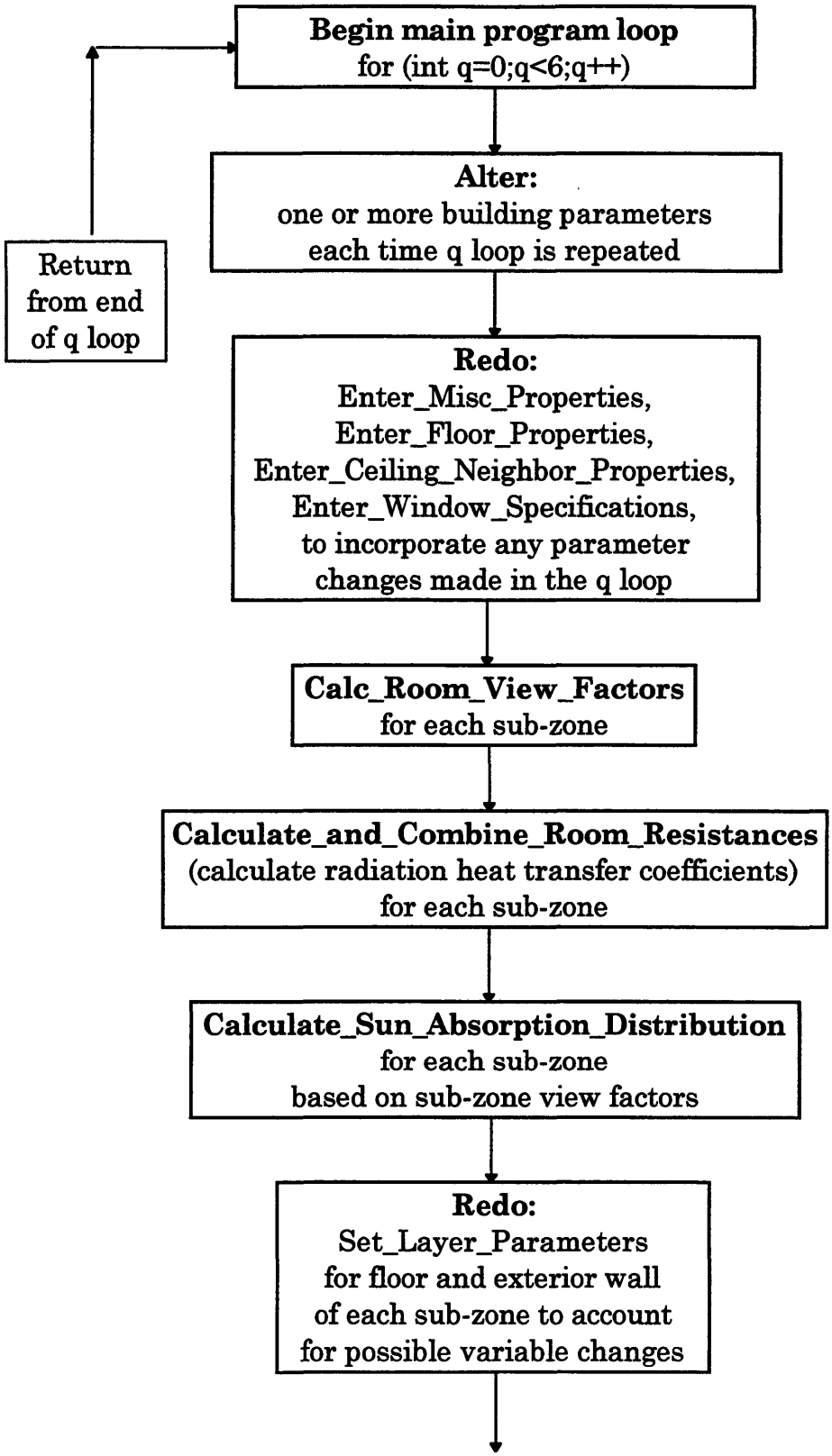
Begin main program loop
for (int q=0;q<6;q++)
Alter:
one or more building parameters
each time q loop is repeated
Return
from end
of q loop
Redo:
Enter_Misc_Properties,
Enter_Floor_Properties,
Enter_Ceiling_Neighbor_Properties,
Enter_Window_Specifications,
to incorporate any parameter
changes made in the q loop
Calc_Room_View_Factors
for each sub-zone
Calculate_and_Combine_Room_Resistances
(calculate radiation heat transfer coefficients)
for each sub-zone
Calculate_Sun_Absorption_Distribution
for each sub-zone
based on sub-zone view factors
Redo:
Set_Layer_Parameters
for floor and exterior wall
of each sub-zone to account
for possible variable changes

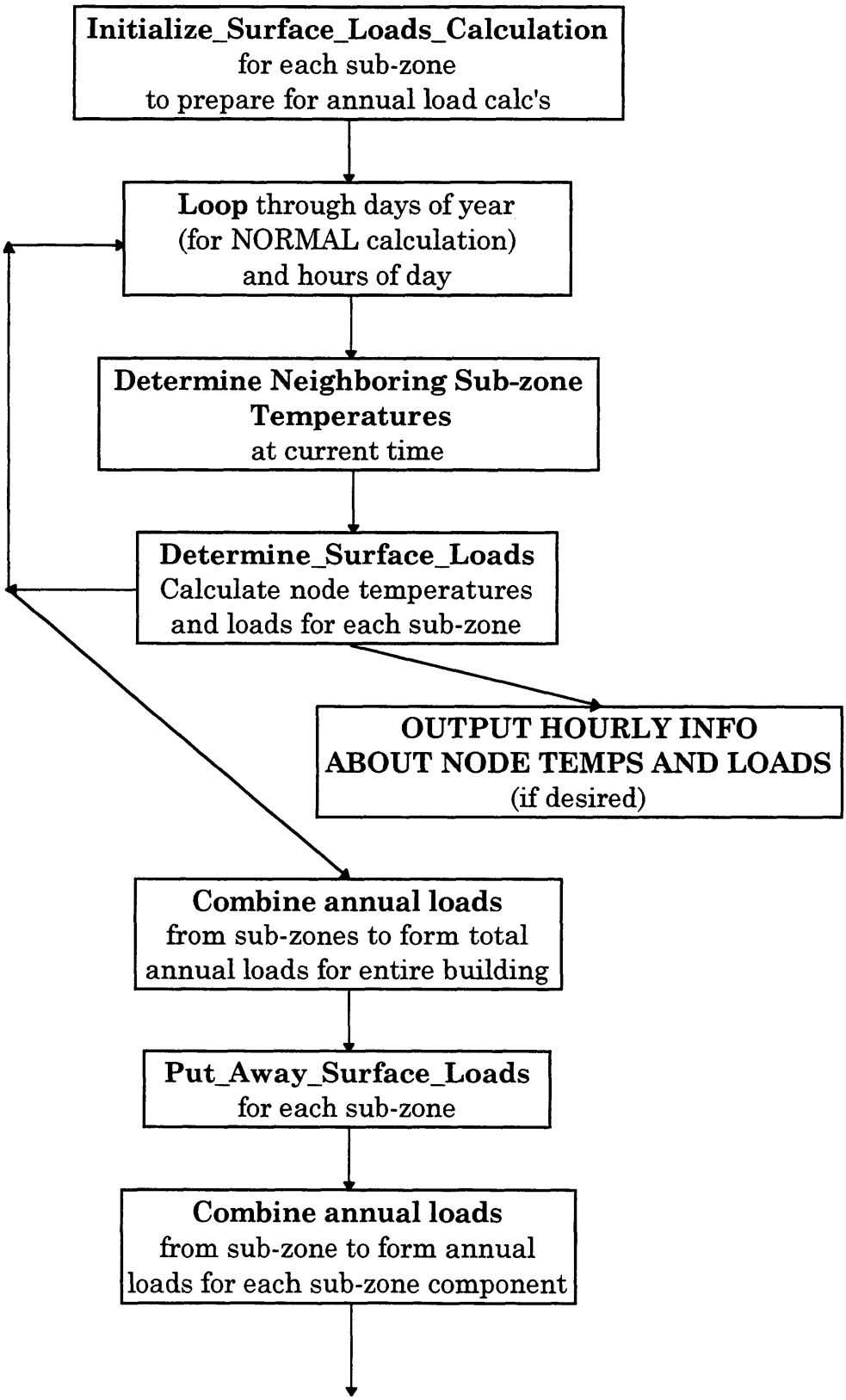
Initialize_Surface_Loads_Calculation
for each sub-zone
to prepare for annual load calc's
Loop through days of year
(for NORMAL calculation)
and hours of day
Determine Neighboring Sub-zone Temperatures
at current time
Determine_Surface_Loads
Calculate node temperatures
and loads for each sub-zone
OUTPUT HOURLY INFO
ABOUT NODE TEMPS AND LOADS
(if desired)
Combine annual loads
from sub-zones to form total
annual loads for entire building
Put_Away_Surface_Loads
for each sub-zone
Combine annual loads
from sub-zone to form annual
loads for each sub-zone component

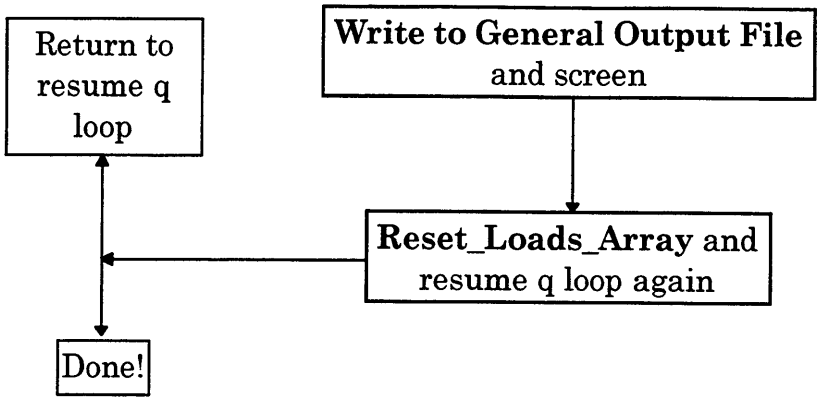

C. Main.cp for the Lightweight Building

The source code is printed out beginning on the next page.

```
//-----------------------------------------------LIGHTWEIGHT Building

#include "Globals.h"
#include "Zone Info.h"
#include "Surface_Info.h"
#include "Site Information.h"
#include "Matrix Functions.h"


void Reset_Load_Contrib();          //this one routine is included in this file


void main()
{
cout<<"Starting..."<<endl;


ofstream General_output_file;              //This output file contains total building annual loads
General_output_file.open("General Output File");//One can vary a single parameter and generate a table
                                           //of annual loads vs this parameter in this file.


Parameter_file.open("Parameter File");     //This output file contains the values of the selected
                                           // parameters, such as the convection coefficients, the
                                           // layer thicknesses...
                                           //This is a global variable accessible to all routines.

//----------------------
clock_t starttime1,starttime2;
float sec;                                 //timing variables
starttime1=clock();
//----------------------
```

```
int recalculate_counter=0;                  //counts the number of times the temperature changes from
                                            //fixed_T to float_T in the Heat Load Calc routine

float variable;                             //this variable can be used for the parametric studies.

//=============================================INITIALIZATION=========================================

//----------------------                    //Choose from several types of program runs
int data_type=TMY2_DATA;                    //use TMY2 weather data
//int data_type=SYNTHETIC_DATA;             //use Hottel/Liu-Jordan clear sky radiation data

//int calc_type=AVERAGE;            //NORMAL calculates loads using all available data.  AVERAGE calculates
int calc_type=NORMAL;               //monthly average values for insolation and temperatures and uses these
                                    //averages for calcs.
float tolerance=.1;                 //tolerance (for AVERAGE program) determines how well the program must
                                    //achieve steady state before proceeding to the next month.  See "if
                                    //calc_type==AVERAGE" below.
                                    //The latent cooling load cannot yet be calculated using the AVERAGE
                                    //calculations.

int max_num_of_days_calc_in_month=40;       //keep at 40 to disable; works as low as 2
                                            //limits the number of days calc'd each month


int layer_simplification_type=NORMAL; //Choosing a MAJOR simplification lumps all the wall parameters
//int layer_simplification_type=MAJOR;//into one single layer with the total wall resistance and
                                      //capacitance.  This layer has the same number of temperature
                                      //nodes as the original first (inner) layer.
//----------------------
```

```
if (INTERVALS_PER_DAY!=24 && data_type==TMY2_DATA)     //hourly data needed for TMY2 data
      {
      cout<<"Using TMY2 data requires you to set the INTERVALS_PER_DAY to 24!"<<endl;
      cin>>sec;
      }


int h=(int)((24.0/INTERVALS_PER_DAY)*3600);      //number of seconds per time step used in calculations


//----------------------SET SITE VARIABLES----------------
int time_zone=EST;                          //these 5 lines are used for synthetic data
float latitude=42+22./60.;          //enter latitude North of equator as positive
float longitude=71+2./60.;          //enter longitude West of Greenwich as positive
float altitude=0.005;               //enter altitude in kilometers
int climate=MID_LATITUDES;          //see Defines.h for climate choices

int year_length=365;                //number of days in year

//Use these lines for Boston
int first_summer_day=151;     //jun 1                After this date, only cooling loads calculated
int first_winter_day=273;     //oct 1                After this date, only heating loads calc'd

//Use these lines for Phoenix
//int first_summer_day=59;    //mar 1                After this date, only cooling loads calculated
//int first_winter_day=334;   //dec 1                After this date, only heating loads calc'd

int num_angle_intervals=90*Num_Points_per_Degree;     //used to calculate an array for TSHGF/ASHGF
                                                      // variables at diff. angles of incidence
```

```
//----------------------SET ZONE VARIABLES----------------
//----------------------
int Num_Room_Subzones=4;                    //number of sub-zones
int n;                                      //sub-zone index
float *Subzone_Temp;
float *Next_Subzone_Temp;                   //current and next temperatures in a given sub-zone
float Air_Temp;
float t_left,t_right,t_below, t_above;      //temps in neighboring sub-zones
//----------------------

float air_density=1.2;  //kg/m^3
float air_Cp=1000;              //J/kg
float humidity_setpt=0.008;    //kg water/kg dry air (humidity ratio)
float evap_enthalpy=2445.2e3; //enthalpy of evaporation J/kg water

float monthly_elec_usage=0;                                          //kilowatt-hours
float number_of_people_in_building=0;                                //on average over the 24 hour day
float internal_load=monthly_elec_usage*1000/(24*31)
                        +70*number_of_people_in_building;    //estimate of internal heat gain in Watts

float base_ach=0.5;      //reasonably tight infiltration
float alt_ach=0.5;       //used when outside temp is warm (cool) enough to blow inside in winter
                         //(in summer)

float wake_up_time=6;    //from night setback (enter integer)
float setback_time=22;   //set back for night (enter integer)

float win_min=20.0;      //heating season temperature setpoints
float win_max=27.0;
float win_sb_min=20.0;   //setback temps
float win_sb_max=27.0;
```

```
float sum_min=20.0;     //cooling season temperature setpoints
float sum_max=27.0;
float sum_sb_min=20.0;  //setback temps
float sum_sb_max=27.0;

//----------------------INITIALIZE SITE_INFO CLASS----------------

//Boston WBAN = 14739
//Phoenix WBAN = 23183

//If location is changed, check first_summer(winter)_day_setting above!!!

Site_Info SI("14739",data_type,latitude,longitude,time_zone,year_length,
                  INTERVALS_PER_DAY,altitude,climate,win_min,
                  num_angle_intervals, calc_type,tolerance,first_summer_day,first_winter_day);
//Site_Info SI("23183",data_type,latitude,longitude,time_zone,year_length,
//                  INTERVALS_PER_DAY,altitude,climate,win_min,
//                  num_angle_intervals, calc_type,tolerance,first_summer_day,first_winter_day);

//-------------------------------------------------------------
//                                        CALCULATE DEGREE DAYS IF DESIRED
/*
cout<<"Degree Days = "<<SI.Calculate_Heating_Degree_Hours(win_min)/24<<endl;   //Calculate heating
Degree
                                                                               //Days based on the
win_min
                                                                               //temperature setpoint
cout<<"Degree Days = "<<SI.Calculate_Cooling_Degree_Hours(sum_max)/24;         //Calculate cooling
Degree
cin>>sec;                                                                      //Days based on the
sum_max
*/                                                                             //temperature setpoint
```

```
//-----------------------------------------------------------------

SI.Fill_TSHG_ASHG_Array();          //calculates SHGF's for DSA window for different angles of
incidence

//----------------------INITIALIZE ZONE_INFO CLASS----------------

Zone_Info Zone1(year_length, INTERVALS_PER_DAY, air_density, air_Cp,humidity_setpt,evap_enthalpy,
                        base_ach,alt_ach);

Zone1.Set_Temp_Array(SI,setback_time,wake_up_time,
                        win_min,win_max,win_sb_min,win_sb_max,
                        sum_min,sum_max,sum_sb_min,sum_sb_max);

Surface_Info **Surface;
Surface = new Surface_Info *[Num_Room_Subzones];
Subzone_Temp=new float [Num_Room_Subzones];
Next_Subzone_Temp=new float [Num_Room_Subzones];
//-------------------------------------------------------------------------------


//----------------------ENTER PROPERTIES FOR DIFFERENT SURFACES----------------------

//for variable def'ns, see the Radiation Heat Transfer section of Chapter 2

float S_width,S_floor_area, S_phi_left, S_phi_right, S_left_length,S_right_length;
float N_width,N_floor_area, N_phi_left, N_phi_right, N_left_length,N_right_length;
float E_width,E_floor_area, E_phi_left, E_phi_right, E_left_length,E_right_length;
float W_width,W_floor_area, W_phi_left, W_phi_right, W_left_length,W_right_length;

S_width=11.8;                   //enter dimensions in meters
S_floor_area=23.26;             //square meters
S_phi_left=.5882;               //enter angles in radians
```

```
S_phi_right=.5882;
S_left_length=7.09;
S_right_length=7.09;

N_width=11.8;
N_floor_area=23.26;
N_phi_left=.5882;
N_phi_right=.5882;
N_left_length=7.09;
N_right_length=7.09;

E_width=7.87;
E_floor_area=23.26;
E_phi_left=.9826;
E_phi_right=.9826;
E_left_length=7.09;
E_right_length=7.09;

W_width=7.87;
W_floor_area=23.26;
W_phi_left=.9826;
W_phi_right=.9826;
W_left_length=7.09;
W_right_length=7.09;


float height=2.743;      //meters


//-----------declare floor and wall layer property variables
float thickness_floor_1,rho_floor_1,k_floor_1,c_floor_1;
float thickness_floor_2,rho_floor_2,k_floor_2,c_floor_2;
int nodes_floor_1, nodes_floor_2;
```

```
float thickness_1,rho_1,k_1,c_1;
int nodes_1;
float thickness_2,rho_2,k_2,c_2;
int nodes_2;
float thickness_3,rho_3,k_3,c_3;
int nodes_3;

int layer_0,layer_1,layer_2,layer_3,layer_4,layer_5;
//----------

//ENTER CONVECTION COEFFICIENTS (and Attic insulation value)

float ho=34;                        //outside combined convection/radiation coefficient
float hi=3.08;                      //inside convection coefficient
float floor_h=4.04;                 //floor convection coefficient
float ceiling_h=0.95;               //ceiling convection coefficient
float ceiling_attic_R=3.81;         //attic insulation value      (without inside/outside films)
float f_slab=0.86;                  //W/mºC slab perimeter loss coeff.

float h_above_ceil=34;        //outside combined convection/radiation coefficient (or
                              //value for fully ventilated attic
float h_below_floor=0;        //adiabatic surface under floor

float h_lt=0.55;              //heat transfer coefficients to neighboring sub-zones
float h_rt=0.55;              //W/m^2ºC


//ENTER WALL-FLOOR SURFACE PROPERTIES

float alpha_wall_solar=0.26;        //solar absorptivity of exterior surface of exterior wall

float inner_walls_eps_IR=0.9;       //IR emissivity of interior walls/ceiling: paint
float inner_walls_alpha_solar=.26;  //solar absorptivity of interior surfaces of sub-zone
```

```
                                        //(except floor)
float floor_eps_IR=.94;                 //IR emissivity of floor
float floor_alpha_solar=.7;             //solar absorptivity of floor
float alpha_solar_roof=0.5;             //solar absorptivity of roof

float perc_sun_on_floor=.5;


//ENTER GLAZING INFO

float perc_glazed=0.2;          //this variable can be changed below.  Each exterior surface
                                //can have a diff. value
float glass_eps_IR=0.93;        //IR emissivity of window
float r_glaze=1/(2.6);          //1/U-value (whole-window) of window in SI units
float sc=0.90;                  //glazing shading coeff.  Can be changed below.

//ENTER SURFACE TILT ANGLE
float beta=90;                  //angle wall forms with the horizontal

//----------------------INITIALIZE SURFACE_INFO CLASS----------------
//0 = North, 90 = West, 180 = South, 270 = East

Surface_Info S_Wall("South Wall",SI,180,beta,height,S_width,S_floor_area,S_phi_left,S_phi_right,
                        S_left_length,S_right_length,Rho_Gen,data_type);
Surface_Info N_Wall("North Wall",SI,0,beta,height,N_width,N_floor_area,N_phi_left,N_phi_right,
                        N_left_length,N_right_length,Rho_Gen,data_type);
Surface_Info E_Wall("East Wall",SI,270,beta,height,E_width,E_floor_area,E_phi_left,E_phi_right,
                        E_left_length,E_right_length,Rho_Gen,data_type);
Surface_Info W_Wall("West Wall",SI,90,beta,height,W_width,W_floor_area,W_phi_left,W_phi_right,
                        W_left_length,W_right_length,Rho_Gen,data_type);
```

```
Surface[0]= &S_Wall;                        //Assign Surface Array
Surface[1]= &N_Wall;
Surface[2]= &E_Wall;
Surface[3]= &W_Wall;


for (n=0;n<Num_Room_Subzones;n++)           //this loop should not be used if the room Subzones have
      {                                                    //walls with different numbers of layers!!!!!!
      Surface[n]->Set_Num_Wall_Floor_Layers(3,1);      //1st number=#wall layers,2nd=#floor layers
      }
//-------------------------------------------------------------------


//--------------------- ENTER Lightweight Building LAYER PROPERTIES (floor and wall)--------------------

//FLOOR bottom layer
thickness_floor_1=0.0762;
rho_floor_1=2242.52;
k_floor_1=1.731;              //these are the data from "Concrete" from E10
c_floor_1=837.4;
nodes_floor_1=1;
layer_0=0;

//FLOOR top layer
thickness_floor_2=0.05; //this floor layer is not currently used in calculations
rho_floor_2=2000;       //if desired, change the 1 to 2 in the call to Set_Num_Wall_Floor_Layers above
k_floor_2=1.37016;      //and in the same call in the calculation loop below
c_floor_2=878.64;       //Also, the wall layers should be re-indexed: layer_2=2, layer_3=3, etc.
nodes_floor_2=2;
layer_1=1;
```

```
//WALL 1                        gypsum board
thickness_1=0.0127;
rho_1=1249.4;
k_1=.1601;
c_1=1088.6;
nodes_1=2;
layer_2=1;

//WALL 2                        composite stud/insulation layer
thickness_2=.1397;
float k_2a,k_2b,rho_2a,rho_2b,c_2a,c_2b,perc_a;       //a represents the stud, b represents insulation

float stud_spacing = 14;  //in inches distance on center.  Enter the spacing dimensions as shown, OR,
float width_of_studs = 1.5; //in inches          //enter the framing percentage below (currently 0.20)
perc_a=width_of_studs/stud_spacing;

perc_a=.20;        //this overrides previous lines

k_2a= .10903;
k_2b= .0433;
rho_2a= 432.5;
rho_2b= 32.04;
c_2a= 2386.5;
c_2b= 837.4;

rho_2 = perc_a*rho_2a + (1-perc_a)*rho_2b;
c_2 = perc_a*c_2a + (1-perc_a)*c_2b;
k_2 = k_2a*perc_a+ k_2b*(1-perc_a);
nodes_2=2;
layer_3=2;
```

```
//WALL 3                                sheathing
thickness_3=0.033;
rho_3=160.18;
k_3=.0554;
c_3=837.4;
nodes_3=2;
layer_4=3;
//--------------------- End Lightweight Building LAYER PROPERTIES-----------------------


//--------------------SET LAYER PROPERTIES-----------------------

S_Wall.Set_Layer_Parameters(layer_0,thickness_floor_1,rho_floor_1,k_floor_1,c_floor_1,nodes_floor_1,
                            PRINT);
N_Wall.Set_Layer_Parameters(layer_0,thickness_floor_1,rho_floor_1,k_floor_1,c_floor_1,nodes_floor_1,
                            PRINT);
E_Wall.Set_Layer_Parameters(layer_0,thickness_floor_1,rho_floor_1,k_floor_1,c_floor_1,nodes_floor_1,
                            PRINT);
W_Wall.Set_Layer_Parameters(layer_0,thickness_floor_1,rho_floor_1,k_floor_1,c_floor_1,nodes_floor_1,
                            PRINT);

/* These lines are for the unused floor layer
S_Wall.Set_Layer_Parameters(layer_1,thickness_floor_2,rho_floor_2,k_floor_2,c_floor_2,nodes_floor_2,
                            PRINT);
N_Wall.Set_Layer_Parameters(layer_1,thickness_floor_2,rho_floor_2,k_floor_2,c_floor_2,nodes_floor_2,
                            PRINT);
E_Wall.Set_Layer_Parameters(layer_1,thickness_floor_2,rho_floor_2,k_floor_2,c_floor_2,nodes_floor_2,
                            PRINT);
W_Wall.Set_Layer_Parameters(layer_1,thickness_floor_2,rho_floor_2,k_floor_2,c_floor_2,nodes_floor_2,
                            PRINT);
*/
```

```
S_Wall.Set_Layer_Parameters(layer_2,thickness_1,rho_1,k_1,c_1,nodes_1,PRINT);
N_Wall.Set_Layer_Parameters(layer_2,thickness_1,rho_1,k_1,c_1,nodes_1,PRINT);
E_Wall.Set_Layer_Parameters(layer_2,thickness_1,rho_1,k_1,c_1,nodes_1,PRINT);
W_Wall.Set_Layer_Parameters(layer_2,thickness_1,rho_1,k_1,c_1,nodes_1,PRINT);


S_Wall.Set_Layer_Parameters(layer_3,thickness_2,rho_2,k_2,c_2,nodes_2,PRINT);
N_Wall.Set_Layer_Parameters(layer_3,thickness_2,rho_2,k_2,c_2,nodes_2,PRINT);
E_Wall.Set_Layer_Parameters(layer_3,thickness_2,rho_2,k_2,c_2,nodes_2,PRINT);
W_Wall.Set_Layer_Parameters(layer_3,thickness_2,rho_2,k_2,c_2,nodes_2,PRINT);

S_Wall.Set_Layer_Parameters(layer_4,thickness_3,rho_3,k_3,c_3,nodes_3,PRINT);
N_Wall.Set_Layer_Parameters(layer_4,thickness_3,rho_3,k_3,c_3,nodes_3,PRINT);
E_Wall.Set_Layer_Parameters(layer_4,thickness_3,rho_3,k_3,c_3,nodes_3,PRINT);
W_Wall.Set_Layer_Parameters(layer_4,thickness_3,rho_3,k_3,c_3,nodes_3,PRINT);


for (n=0;n<Num_Room_Subzones;n++)
      {
      Surface[n]->Enter_Misc_Properties( hi, ho,alpha_wall_solar,inner_walls_eps_IR,perc_sun_on_floor,
                                  inner_walls_alpha_solar,internal_load/Num_Room_Subzones,PRINT);
      Surface[n]->Enter_Floor_Properties(floor_h, f_slab, floor_eps_IR,
                                        floor_alpha_solar,h_below_floor,PRINT);
      Surface[n]->Enter_Ceiling_Neighbor_Properties(ceiling_h,ceiling_attic_R,
                                        h_above_ceil,alpha_solar_roof,h_lt,h_rt,PRINT);
      }

S_Wall.Enter_Window_Specifications(perc_glazed, r_glaze,sc,glass_eps_IR,PRINT);
N_Wall.Enter_Window_Specifications(perc_glazed, r_glaze,sc,glass_eps_IR,PRINT);
E_Wall.Enter_Window_Specifications(perc_glazed, r_glaze,sc,glass_eps_IR,PRINT);
W_Wall.Enter_Window_Specifications(perc_glazed, r_glaze,sc,glass_eps_IR,PRINT);

//-----------------------------------------------------------------
```

```
if (data_type==SYNTHETIC_DATA)
      {
      SI.Fill_Daily_Arrays();       //read in/create temperatures and solar altitude/azimuth info
      for (n=0;n<Num_Room_Subzones;n++)
            Surface[n]->Fill_Daily_Arrays(SI);  //read in/create solar angle info for all surfaces

      if (calc_type==AVERAGE)
            {
            for (n=0;n<Num_Room_Subzones;n++)
                  Surface[n]->Average_Monthly_Insolation_and_Theta();    //form averages of the weather
            }// end if AVERAGE                                          //data
      }//end if synthetic data

else if (data_type==TMY2_DATA)
      {
      SI.Fill_Daily_Arrays_TMY2();        //read in weather data and solar altitude/azimuth info
      for (n=0;n<Num_Room_Subzones;n++)
            Surface[n]->Fill_Daily_Arrays_TMY2(SI);    //read in/create solar angle info for all
                                                       //surfaces
if (calc_type==AVERAGE)
            {
            for (n=0;n<Num_Room_Subzones;n++)
                  Surface[n]->Average_Monthly_Insolation_and_Theta();    //form averages of the weather
            }// end if AVG                                              //data
      }//end if TMY2 data
//=========================================END INITIALIZATION=====================================
```

```
//=========================================SOLAR ANGLES OUTPUT (if desired)=======================
/*
//Use only with synthetic (clear-sky) data!!     (otherwise angles are not correct)


int Time_Interval_Number=INTERVALS_PER_DAY/2;          //this is the noon interval in standard time
int mon=12;
int day=21;


S_Wall.Determine_Angles_for_a_Specific_Time(SI,900,mon,day);       //this routine will show solar info
                                                                   //on the screen for a particular day
                                                                   //of the year and time of day


SI.Output_Angles_for_a_Specific_Day(mon,day);          //these routines output (to files) solar angles
S_Wall.Output_Angles_for_a_Specific_Day(SI,mon,day);   //and energy on a particular day from sunrise
N_Wall.Output_Angles_for_a_Specific_Day(SI,mon,day);   //to sunset
E_Wall.Output_Angles_for_a_Specific_Day(SI,mon,day);
W_Wall.Output_Angles_for_a_Specific_Day(SI,mon,day);

//SI.Output_Angles_for_a_Specific_Time(Time_Interval_Number);           //these routines output solar
//S_Wall.Output_Angles_for_a_Specific_Time(SI,Time_Interval_Number);    //info at a given time of day
                                                                        //for every day of the year

cin>>mon;          //prevents remainder of program from running
*/
```

```
//=============================================================================================
//=====================================BEGINNING OF LOAD CALCULATIONS=========================
//=============================================================================================

float annual_heat_load, annual_cool_load, annual_latent_load;

float heat_load_today;        //these 8 variables used for "quick" calculation using monthly avg's
float heat_load_yesterday;
float cool_load_today;
float cool_load_yesterday;
float unzeroed_heat_load_today;
float unzeroed_heat_load_yesterday;
float unzeroed_cool_load_today;
float unzeroed_cool_load_yesterday;

int num_days_required_to_stabilize;             //variable used in AVG calculation below
int Refining;                                   //variable used in AVG calculation below


for (int q=0;q<1;q++)    //This MAIN loop can be run multiple times to test different parameter values
      {
      starttime2=clock();
      Reset_Load_Contrib();

      SI.Set_Tolerance(tolerance);  //change the tolerance for the avg calculation here, if desired

      Zone1.Set_ACHs(base_ach,alt_ach);         //change the air change rates here, if desired

      Zone1.Set_T_Below_Weight_Factor(.5);      //enter # between 0 and 1
                                          //this number is used to estimate the basement temperature
                                          //see the Floor sub-section of Chapter 2 in the thesis
```

```
        variable=0.1*q;          //set this to anything desired, then replace a variable below with it
                                 //For example, set variable=0.21+.05*q
                                 //replace alpha_wall_solar below with this variable
                                 //set the maximum q to 4 in the q loop (q=0;q<5;q++)
                                 //this runs the program 5 times, with
                                 //alpha_wall_solar={0.21, 0.26...0.41}
        for (n=0;n<Num_Room_Subzones;n++)    //this loop should not be used if the room Subzones
                                             //have different properties
              {
//            Surface[n]->Set_Multipurpose_Param(variable);    //sends a variable into the heat load
                                                               //calculation routine for
                                                               //parametric studies.  eg, change solar
                                                               //radiation by factors of 0.5,0.6,...1.0


              Surface[n]->Enter_Misc_Properties( hi, ho,alpha_wall_solar,inner_walls_eps_IR,
                                                 perc_sun_on_floor,inner_walls_alpha_solar,
                                                 internal_load/Num_Room_Subzones,PRINT);
              Surface[n]->Enter_Floor_Properties(floor_h, f_slab, floor_eps_IR,
                                                 floor_alpha_solar,h_below_floor,DONT_PRINT);
              Surface[n]->Enter_Ceiling_Neighbor_Properties(ceiling_h,ceiling_attic_R,
                                                 h_above_ceil,alpha_solar_roof,h_lt,h_rt,DONT_PRINT);
              }

        S_Wall.Enter_Window_Specifications(perc_glazed, r_glaze,sc,glass_eps_IR,DONT_PRINT);
        N_Wall.Enter_Window_Specifications(perc_glazed, r_glaze,sc,glass_eps_IR,DONT_PRINT);
        E_Wall.Enter_Window_Specifications(perc_glazed, r_glaze,sc,glass_eps_IR,DONT_PRINT);
        W_Wall.Enter_Window_Specifications(perc_glazed, r_glaze,sc,glass_eps_IR,DONT_PRINT);
```

```
//========
      Calc_Room_View_Factors(S_Wall);
      S_Wall.Calculate_and_Combine_Room_Resistances(Zone1,.5,1);  //The 0.5 represents the location of
      S_Wall.Calculate_Sun_Absorption_Distribution();             //the window node within the
                                                    //window's thermal resistance.  The 1 is  a
                                                    //factor by which all radiation coefficients are
      Calc_Room_View_Factors(N_Wall);               //multiplied. Set to 0 to remove all radiation.
      N_Wall.Calculate_and_Combine_Room_Resistances(Zone1,.5,1);
      N_Wall.Calculate_Sun_Absorption_Distribution();

      Calc_Room_View_Factors(E_Wall);
      E_Wall.Calculate_and_Combine_Room_Resistances(Zone1,.5,1);
      E_Wall.Calculate_Sun_Absorption_Distribution();

      Calc_Room_View_Factors(W_Wall);
      W_Wall.Calculate_and_Combine_Room_Resistances(Zone1,.5,1);
      W_Wall.Calculate_Sun_Absorption_Distribution();
//========

for (n=0;n<Num_Room_Subzones;n++)          //this loop should not be used if the room Subzones have
      {                                    //walls with different numbers of layers!!!!!!
      Surface[n]->Set_Num_Wall_Floor_Layers(3,1);     //3 wall layers, 1 floor layer (this routine
                                                      //called above as well)
      }

      S_Wall.Set_Layer_Parameters(layer_0,thickness_floor_1,rho_floor_1,k_floor_1,
                                  c_floor_1,nodes_floor_1,DONT_PRINT);
//    unused floor layer:S_Wall.Set_Layer_Parameters(layer_1,thickness_floor_2,rho_floor_2,k_floor_2,
//                                  c_floor_2,nodes_floor_2,DONT_PRINT);
      S_Wall.Set_Layer_Parameters(layer_2,thickness_1,rho_1,k_1,c_1,nodes_1,DONT_PRINT);
      S_Wall.Set_Layer_Parameters(layer_3,thickness_2,rho_2,k_2,c_2,nodes_2,DONT_PRINT);
      S_Wall.Set_Layer_Parameters(layer_4,thickness_3,rho_3,k_3,c_3,nodes_3,DONT_PRINT);
      S_Wall.Simplify_Layer_Parameters(layer_simplification_type);
```

```
      N_Wall.Set_Layer_Parameters(layer_0,thickness_floor_1,rho_floor_1,k_floor_1,
                                  c_floor_1,nodes_floor_1,DONT_PRINT);
//    unused floor layer:N_Wall.Set_Layer_Parameters(layer_1,thickness_floor_2,rho_floor_2,k_floor_2,
//                                  c_floor_2,nodes_floor_2,DONT_PRINT);
      N_Wall.Set_Layer_Parameters(layer_2,thickness_1,rho_1,k_1,c_1,nodes_1,DONT_PRINT);
      N_Wall.Set_Layer_Parameters(layer_3,thickness_2,rho_2,k_2,c_2,nodes_2,DONT_PRINT);
      N_Wall.Set_Layer_Parameters(layer_4,thickness_3,rho_3,k_3,c_3,nodes_3,DONT_PRINT);
      N_Wall.Simplify_Layer_Parameters(layer_simplification_type);

      E_Wall.Set_Layer_Parameters(layer_0,thickness_floor_1,rho_floor_1,k_floor_1,
                                  c_floor_1,nodes_floor_1,DONT_PRINT);
//    unused floor layer:E_Wall.Set_Layer_Parameters(layer_1,thickness_floor_2,rho_floor_2,k_floor_2,
//                                  c_floor_2,nodes_floor_2,DONT_PRINT);
      E_Wall.Set_Layer_Parameters(layer_2,thickness_1,rho_1,k_1,c_1,nodes_1,DONT_PRINT);
      E_Wall.Set_Layer_Parameters(layer_3,thickness_2,rho_2,k_2,c_2,nodes_2,DONT_PRINT);
      E_Wall.Set_Layer_Parameters(layer_4,thickness_3,rho_3,k_3,c_3,nodes_3,DONT_PRINT);
      E_Wall.Simplify_Layer_Parameters(layer_simplification_type);


      W_Wall.Set_Layer_Parameters(layer_0,thickness_floor_1,rho_floor_1,k_floor_1,
                                  c_floor_1,nodes_floor_1,DONT_PRINT);
//    unused floor layer:W_Wall.Set_Layer_Parameters(layer_1,thickness_floor_2,rho_floor_2,k_floor_2,
//                                  c_floor_2,nodes_floor_2,DONT_PRINT);
      W_Wall.Set_Layer_Parameters(layer_2,thickness_1,rho_1,k_1,c_1,nodes_1,DONT_PRINT);
      W_Wall.Set_Layer_Parameters(layer_3,thickness_2,rho_2,k_2,c_2,nodes_2,DONT_PRINT);
      W_Wall.Set_Layer_Parameters(layer_4,thickness_3,rho_3,k_3,c_3,nodes_3,DONT_PRINT);
      W_Wall.Simplify_Layer_Parameters(layer_simplification_type);
```

```
if (calc_type==NORMAL)        //This is the standard calculation (hourly, every day of the year)
      {
      for (n=0;n<Num_Room_Subzones;n++)
      {
      Surface[n]->Initialize_Surface_Loads_Calculation(SI,Zone1,&Air_Temp);
      Next_Subzone_Temp[n]=Air_Temp;
      }
      annual_heat_load=0;
      annual_cool_load=0;
      annual_latent_load=0;

      int season=1;     //start out in the heating season

      for (int i=0;i<year_length;i++)           //both starting day (0=Jan 1) and final day
            {                                   //(year_length-1=Dec 31) can be changed
            if (i%10==0)
                  cout<<".";                    //indicates progress in calculation


            if (i==first_summer_day||i==first_winter_day)    //change season
                  {
                  season=abs(season-1);
                  cout<<i;
                  }

            for (int j=0;j<INTERVALS_PER_DAY;j++)           //step through all hours in a day
                  {
                  copy_vector(Num_Room_Subzones, Next_Subzone_Temp,Subzone_Temp);
                  for (n=0;n<Num_Room_Subzones;n++)
                        {
                        t_above=ATTIC;          //change these lines for a setup
                        t_below=BASEMENT;       //with multiple stories.
```

```
                        switch (n)
                              {
                              case 0:           //south subzone
                                    {
                                    t_left=Subzone_Temp[3]; //temperature in west subzone
                                    t_right=Subzone_Temp[2];//temperature in east subzone
                                    break;
                                    }
                              case 1:           //north subzone
                                    {
                                    t_left=Subzone_Temp[2]; //temperature in east subzone
                                    t_right=Subzone_Temp[3];//temperature in west subzone
                                    break;
                                    }
                              case 2:           //east subzone
                                    {
                                    t_left=Subzone_Temp[0];
                                    t_right=Subzone_Temp[1];
                                    break;
                                    }
                              case 3:           //west subzone
                                    {
                                    t_left=Subzone_Temp[1];
                                    t_right=Subzone_Temp[0];
                                    break;
                                    }
                              }//end switch


//-----------------Calculate the heat load for that hour:

                        while ( !Surface[n]->Determine_Surface_Loads(SI,Zone1,i,j,season,
                                          &Air_Temp,t_left,t_right,t_above,t_below) )
```

```
                        {
                        recalculate_counter++;
                        };
                    Next_Subzone_Temp[n]=Air_Temp;
                    }//end Subzones loop (n)
                }   //end j loop
            }//end of i loop
            cout<<endl;

        for (n=0;n<Num_Room_Subzones;n++)          //calculate annual loads for whole zone
            {
            annual_heat_load+=Surface[n]->Get_Annual_Heat_Load();
            annual_cool_load+=Surface[n]->Get_Annual_Cool_Load();
            annual_latent_load+=Surface[n]->Get_Annual_Latent_Load();
            Surface[n]->Put_Away_Surface_Loads();
            }

        annual_heat_load*=h;    //multiply by the number of seconds per timestep to get Joules
        annual_cool_load*=h;
        annual_latent_load*=h;

        cout<<endl;
        cout<<"Normal calculation results: "<<endl;
        cout<<"Annual Heating Load: "<<annual_heat_load*1e-9<<" GJ"<<endl;
        cout<<"Annual Cooling Load: "<<annual_cool_load*1e-9<<" GJ"<<endl;
        cout<<"Annual Latent Load: "<<annual_latent_load*1e-9<<" GJ"<<endl;
        cout<<endl;

        }
    else if (calc_type==AVERAGE)          //This is the "quick" calculation using monthly averages
        {                                 //of the weather data
        annual_heat_load=0;
        annual_cool_load=0;
```

```
annual_latent_load=0;

for (n=0;n<Num_Room_Subzones;n++)
{
Surface[n]->Initialize_Surface_Loads_Calculation(SI,Zone1,&Air_Temp);
Next_Subzone_Temp[n]=Air_Temp;
}

int season=1;      //start out in the heating season

for (int m=0;m<12;m++)  //this loop steps through the 12 months of the year
      {
      heat_load_today=0;            //reset variables for next month's calculations
      heat_load_yesterday=0;
      cool_load_today=0;
      cool_load_yesterday=0;
      unzeroed_heat_load_today=0;
      unzeroed_heat_load_yesterday=0;
      unzeroed_cool_load_today=0;
      unzeroed_cool_load_yesterday=0;

      num_days_required_to_stabilize=0;
      Refining=1;       //Refining=1 means the program has not found steady state loads
                        //for a particular month

      if (Months[m]>=first_summer_day&&Months[m]<first_winter_day)
            season=0;
      else
            season=1;

      while (Refining)
      {
      heat_load_today=0;
```

```
cool_load_today=0;
unzeroed_heat_load_today=0;
unzeroed_cool_load_today=0;

for (int j=0;j<INTERVALS_PER_DAY;j++) //this loop steps through the hours in the day
      {
      copy_vector(Num_Room_Subzones, Next_Subzone_Temp,Subzone_Temp);
      for (n=0;n<Num_Room_Subzones;n++)
            {
            t_above=ATTIC;     //change these lines for a setup with multiple
            t_below=BASEMENT; //stories.  t_above and t_below shouldn't be
                              //constants in that case

            switch (n)
                  {
                  case 0:           //south subzone
                        {
                        t_left=Subzone_Temp[3]; //temperature in west subzone
                        t_right=Subzone_Temp[2];//temperature in east subzone
                        break;
                        }
                  case 1:           //north subzone
                        {
                        t_left=Subzone_Temp[2]; //temperature in east subzone
                        t_right=Subzone_Temp[3];//temperature in west subzone
                        break;
                        }
                  case 2:           //east subzone
                        {
                        t_left=Subzone_Temp[0];
                        t_right=Subzone_Temp[1];
                        break;
                        }
```

```
                        case 3:           //west subzone
                              {
                              t_left=Subzone_Temp[1];
                              t_right=Subzone_Temp[0];
                              break;
                              }
                        }//end switch

                  while ( !Surface[n]->Determine_Surface_Loads(SI,Zone1,Months[m],j,
                              season,&Air_Temp,t_left,t_right,t_above,t_below) )
                        {};
                  Next_Subzone_Temp[n]=Air_Temp;

                  heat_load_today+=Surface[n]->Get_Instantaneous_Heat_Load(Months[m],j+1);
                  cool_load_today+=Surface[n]->Get_Instantaneous_Cool_Load(Months[m],j+1);

                  unzeroed_heat_load_today+=Surface[n]->Get_Latest_Unzeroed_Heat_Load();
                  unzeroed_cool_load_today+=Surface[n]->Get_Latest_Unzeroed_Cool_Load();

                  }//end of for loop through room Subzones

            }     //end of j loop

            num_days_required_to_stabilize++;

//--------------Determine whether the load calculations have stabilized for this month

            if (max_num_of_days_calc_in_month==num_days_required_to_stabilize||
                  num_days_required_to_stabilize>1&&
                  (unzeroed_heat_load_today==0||( fabs((unzeroed_heat_load_today-
unzeroed_heat_load_yesterday)/unzeroed_heat_load_yesterday)<SI.Get_Tolerance()) )&&
                  (unzeroed_cool_load_today==0||( fabs((unzeroed_cool_load_today-
unzeroed_cool_load_yesterday)/unzeroed_cool_load_yesterday)<SI.Get_Tolerance()) ) )
```

```
                                {
                                Refining=0;
//     cout<<"It took "<<num_days_required_to_stabilize<<" days to stabilize in month "<<m+1<<endl;
                                annual_heat_load+=heat_load_today*h*(Months[m+1]-Months[m]);
                                annual_cool_load+=cool_load_today*h*(Months[m+1]-Months[m]);
                                }

//--------------Or find out if the end of the month has been reached without stabilization

                          else if (num_days_required_to_stabilize==(Months[m+1]-Months[m]))
                                {
                                Refining=0;
                                cout<<"Loads never stabilized in month "<<m+1<<endl;
                                annual_heat_load+=heat_load_today*h*(Months[m+1]-Months[m]);
                                annual_cool_load+=cool_load_today*h*(Months[m+1]-Months[m]);
                                }


                          heat_load_yesterday=heat_load_today;
                          cool_load_yesterday=cool_load_today;
                          unzeroed_heat_load_yesterday=unzeroed_heat_load_today;
                          unzeroed_cool_load_yesterday=unzeroed_cool_load_today;

                          }//end while refining
                    }//end of m loop
                    cout<<endl;
                    cout<<"Quick calculation results: "<<endl;
                    cout<<"Tolerance: "<<SI.Get_Tolerance()<<endl;
                    cout<<"Annual Heating Load: "<<annual_heat_load*1e-9<<" GJ"<<endl;
                    cout<<"Annual Cooling Load: "<<annual_cool_load*1e-9<<" GJ"<<endl;
                    cout<<endl;
```

```
            for (n=0;n<Num_Room_Subzones;n++)
                  Surface[n]->Put_Away_Surface_Loads();
            }     //end of AVERAGE calc


      cout<<q<<", "<<variable<<", "<<annual_heat_load*1e-9<<", "
                        <<annual_cool_load*1e-9<<", "
                        <<annual_latent_load*1e-9<<", "
                        <<float(clock()-starttime2)/float(CLOCKS_PER_SEC)<<endl;


//Update loads for building components
      for (n=0;n<Num_Room_Subzones;n++)
            {
            H_Load_Summary.Window_Load+=Surface[n]->Heat_Load_Summary[0].Window_Load;
            H_Load_Summary.Wall_Load+=Surface[n]->Heat_Load_Summary[0].Wall_Load;
            H_Load_Summary.Floor_Load+=Surface[n]->Heat_Load_Summary[0].Floor_Load;
            H_Load_Summary.Infiltration_Load+=Surface[n]->Heat_Load_Summary[0].Infiltration_Load;
            H_Load_Summary.Slab_Load+=Surface[n]->Heat_Load_Summary[0].Slab_Load;
            H_Load_Summary.Walls_Load+=Surface[n]->Heat_Load_Summary[0].Walls_Load;
            H_Load_Summary.Ceiling_Load+=Surface[n]->Heat_Load_Summary[0].Ceiling_Load;
            H_Load_Summary.Adjacent_Rooms_Load+=Surface[n]->Heat_Load_Summary[0].Adjacent_Rooms_Load;
            H_Load_Summary.Solar_Flux+=Surface[n]->Heat_Load_Summary[0].Solar_Flux;
            H_Load_Summary.Exhaust_Load+=Surface[n]->Heat_Load_Summary[0].Exhaust_Load;


            C_Load_Summary.Window_Load+=Surface[n]->Cool_Load_Summary[0].Window_Load;
            C_Load_Summary.Wall_Load+=Surface[n]->Cool_Load_Summary[0].Wall_Load;
            C_Load_Summary.Floor_Load+=Surface[n]->Cool_Load_Summary[0].Floor_Load;
            C_Load_Summary.Infiltration_Load+=Surface[n]->Cool_Load_Summary[0].Infiltration_Load;
            C_Load_Summary.Slab_Load+=Surface[n]->Cool_Load_Summary[0].Slab_Load;
            C_Load_Summary.Walls_Load+=Surface[n]->Cool_Load_Summary[0].Walls_Load;
            C_Load_Summary.Ceiling_Load+=Surface[n]->Cool_Load_Summary[0].Ceiling_Load;
```

```
            C_Load_Summary.Adjacent_Rooms_Load+=Surface[n]->Cool_Load_Summary[0].Adjacent_Rooms_Load;
            C_Load_Summary.Solar_Flux+=Surface[n]->Cool_Load_Summary[0].Solar_Flux;
            C_Load_Summary.Exhaust_Load+=Surface[n]->Cool_Load_Summary[0].Exhaust_Load;
            }

//-----------------------------------------BEGIN OUTPUT OF RESULTS---------------------------------

      if (q==0)         //print labels for data in output file
      {
      General_output_file<<"q,var.,Ann.HL,Tot HL,Ann.CL,Tot CL,Lat. LD,
                           SouthHL,SouthCL,NorthHL,NorthCL,EastHL,EastCL,WestHL,WestCL,";
      General_output_file<<"WinHGain,WallHGain,FloorHGain,InfHGain,SlabHGain,WallsHGain,
                           CeilingHGain,AdjHGain,ExHGain,SolarHGain,";
      General_output_file<<"WinCGain,WallCGain,FloorCGain,InfCGain,SlabCGain,WallsCGain,
                           CeilingCGain,AdjCGain,ExCGain,SolarCGain,";
      General_output_file<<"Time"<<endl;
      }


//--Put data in output file
      General_output_file<<q<<","
                         <<variable<<","
                         <<annual_heat_load*1e-9<<","
                         <<1e-9*(annual_heat_load+C_Load_Summary.Exhaust_Load*h)<<","//total heat load
                         <<annual_cool_load*1e-9<<","
                         <<1e-9*(annual_cool_load-H_Load_Summary.Exhaust_Load*h)<<","//total cool load
                         <<1e-9*annual_latent_load<<",";

      for (n=0;n<Num_Room_Subzones;n++)
            General_output_file<<h*1e-9*Surface[n]->Get_Annual_Heat_Load()<<","
                                     <<h*1e-9*Surface[n]->Get_Annual_Cool_Load()<<",";
```

```
                General_output_file<<h*1e-9*H_Load_Summary.Window_Load<<","
                                        <<h*1e-9*H_Load_Summary.Wall_Load<<","
                                        <<h*1e-9*H_Load_Summary.Floor_Load<<","
                                        <<h*1e-9*H_Load_Summary.Infiltration_Load<<","
                                        <<h*1e-9*H_Load_Summary.Slab_Load<<","
                                        <<h*1e-9*H_Load_Summary.Walls_Load<<","
                                        <<h*1e-9*H_Load_Summary.Ceiling_Load<<","
                                        <<h*1e-9*H_Load_Summary.Adjacent_Rooms_Load<<","
                                        <<h*1e-9*H_Load_Summary.Exhaust_Load<<","
                                        <<h*1e-9*H_Load_Summary.Solar_Flux<<","

                                        <<h*1e-9*C_Load_Summary.Window_Load<<","
                                        <<h*1e-9*C_Load_Summary.Wall_Load<<","
                                        <<h*1e-9*C_Load_Summary.Floor_Load<<","
                                        <<h*1e-9*C_Load_Summary.Infiltration_Load<<","
                                        <<h*1e-9*C_Load_Summary.Slab_Load<<","
                                        <<h*1e-9*C_Load_Summary.Walls_Load<<","
                                        <<h*1e-9*C_Load_Summary.Ceiling_Load<<","
                                        <<h*1e-9*C_Load_Summary.Adjacent_Rooms_Load<<","
                                        <<h*1e-9*C_Load_Summary.Exhaust_Load<<","
                                        <<h*1e-9*C_Load_Summary.Solar_Flux<<",";

        General_output_file<<float(clock()-starttime2)/float(CLOCKS_PER_SEC)<<endl;


for (n=0;n<Num_Room_Subzones;n++)
                Surface[n]->Reset_Loads_Array();

        }//end of q loop

General_output_file.close();
Parameter_file.close();
//---------------------------------END OUTPUT---------------------------------------
```

```
sec=float(clock()-starttime1)/float(CLOCKS_PER_SEC);
cout<<"This operation lasted "<<(sec)<<" seconds."<<endl;
cout<<"\a\a\a\a\a\a"<<endl;
delete[] Surface;
}
//=============================================================================================
void Reset_Load_Contrib()
{
            H_Load_Summary.Window_Load=0;
            H_Load_Summary.Wall_Load=0;
            H_Load_Summary.Floor_Load=0;
            H_Load_Summary.Infiltration_Load=0;
            H_Load_Summary.Slab_Load=0;
            H_Load_Summary.Walls_Load=0;
            H_Load_Summary.Ceiling_Load=0;
            H_Load_Summary.Adjacent_Rooms_Load=0;
            H_Load_Summary.Exhaust_Load=0;
            H_Load_Summary.Solar_Flux=0;
            H_Load_Summary.Total_Heat_Load=0;
            C_Load_Summary.Window_Load=0;
            C_Load_Summary.Wall_Load=0;
            C_Load_Summary.Floor_Load=0;
            C_Load_Summary.Infiltration_Load=0;
            C_Load_Summary.Slab_Load=0;
            C_Load_Summary.Walls_Load=0;
            C_Load_Summary.Ceiling_Load=0;
            C_Load_Summary.Adjacent_Rooms_Load=0;
            C_Load_Summary.Exhaust_Load=0;
            C_Load_Summary.Solar_Flux=0;
            C_Load_Summary.Total_Cooling_Load=0;
            C_Load_Summary.Latent_Cooling_Load=0;
}
```